UNIVERSITY OF CALIFORNIA, SAN DIEGO

Design and Environmental Force-Induced Moment Analysis of a Shallow Water Oceanographic Mooring Dynamic Antenna

A Thesis submitted in partial satisfaction of the requirements
of the degree Master of Science

in

Engineering Sciences (Applied Ocean Sciences)

by

Nam Huu Nguyen

Committee in Charge:

Professor Sutanu Sarkar, Chair
Professor Uwe Send, Co-Chair
Professor James Rottman

2012

The thesis of Nam Huu Nguyen is approved and it is acceptable in quality and form for publication on microfilm and electronically:

Co-Chair

Chair

University of California, San Diego

2012

Dedication

This thesis is dedicated to the many people, friends and family alike, that have helped me along my path and have given me unending support.

This is dedicated to the members of my research lab that have, through their counsel and kindness, have given me once in a lifetime experiences that will be with me forever.

This is dedicated to Professor Uwe Send, who saw the potential within me to accomplish this thesis and so much more. Without his trust and faith and support, none of this would have come to pass.

This is dedicated to the many professors that pushed me to excel and succeed.

This is dedicated to the friends who provided succor and bastions from which I could rest, recoup, and re-strengthen my resolve.

This is dedicated to the men and women, past, present, and future of the Human-Powered Submarine Project. Through the trials that the watery medium presents, speed can be attained and bonds can be formed that propel naive minds into engineering warriors.

This is dedicated to the laughs and joys of FOOSH, who presented what was best and possible about a university: acceptance, friendship, and kindness during bleak times lacking in healing humor.

This is dedicated to my mother and father, who, through will, grace, and wisdom, helped shape my mind and spirit for exploration and understanding in a wholly mysterious world.

This is dedicated to my sister, a titan of knowledge and champion for science; without her guidance and encouragement, the sea would be merely a wet place, rather than the bountiful frontier I wish to conquer.

Epigraph

"I'm not what is called a civilized man. I have done with society for reasons that seem good to me. Therefore, I do not obey its laws."

-Captain Nemo

Table of Contents

List of Figures

List of Tables

List of Graphs

ABSTRACT OF THE THESIS

Design and Environmental Force-Induced Moment Analysis of a
Shallow Water Oceanographic Mooring Dynamic Antenna

by

Nam Huu Nguyen

Master of Science in Engineering Sciences (Applied Ocean Sciences)

University of California, San Diego, 2012

Professor Sutanu Sarkar, Chair
Professor Uwe Send, Co-Chair

Obtaining real-time, long time-series data physical oceanography in shallow water regimes between five and ten meters continues to be an engineering challenge not only in terms of the process of obtaining and transmitting it, but creating a form that will allow it to operate unimpeded by vandalism. A conceptual design for a Dynamic Antenna utilizes a shifting mass to change the center of gravity, causing the assembly to rotate about a pivot to raise an antenna to pierce the surface and lower it to place it out of view underwater. Utilizing a range of environmental parameters that it is expected to be deployed in, the moments due to hydrodynamic loading as well as its own weight are analyzed and compared to examine an example configuration of the Dynamic Antenna's ability to overcome these forces to provide a suitable platform with enough clearance for antenna to transmit data and rotate said antenna down out below the surface. The specific factors will be the current forces modeled as a uniform flow profile, wave forcing derived from Morison forcing using the

maximum horizontal wave particle velocity, and the static buoyancy and mass force. Understanding the factors that have the greatest impact on the system in terms of moment, further development can be conducted to reduce those factors' total influence on the system to create a more resilient, robust, and reliable mechanism.

Introduction

The ocean is a vast and mysterious realm bearing questions scientists have been seeking to answer, with engineers building the tools to pierce its surface. Around the world, from the placid waters of inshore lagoons to the tempestuous gales of the North Atlantic, scientist and engineers face the many challenges the sea presents for the sake of knowledge. With the environment itself corrosive, materials have to be created that will withstand the degrading effects of salt water. Perpetually subjected to the forces imparted by the ocean, tools, instruments, ships, and men are built to take pressure, beatings, and the elements. From the first forays into oceanography with bucket and shovel, to larger endeavors on sailing ships across a still-flat world, to the latest advances in underwater acoustics and robotics, the tools Man has created are the eyes and ears that allow him to explore a truly inhospitable and alien realm. This pursuit of understanding has sunken ships and broken men. But the pursuit continues on nonetheless, perhaps even stronger because of the hardship interred with ocean science and the benefit it has to Mankind.

The value of understanding the oceans is worth all of this toil and grueling effort. The ocean is a source of food and water, power and communication, and is both lifeblood and gauge of health for the Earth. Learning the patterns of the ocean over time has contributed to the development of human civilization. Just one global case is the mapping of the ocean's currents, used every day by ships to reduce travel time. Another is the simple observation of the tides on shorelines around the world, where the levels are gaged and tracked by captains to determine the most optimum time to embark on their voyages and to return back into port. Such implications of ocean science can be brought further from the water's edge as well. Following the migration of vital food species improves the harvesting capability as well as environmental policy, affecting the quality, quantity, and therefore price, of what appears on store shelves. In the 21st century, the emphasis has been made on improving conservation and examining the process and effects of a global warming trend due to carbon emissions by the modern industrial world creating a greenhouse effect. The implications of global warming has sent the oceanographic world into a frenzy, attempting to investigate habitats and see how the environment's flora and fauna could possibly change due to rising ocean temperatures, as well as observing the possible changes in ocean currents and patterns.

In this thesis, a new potential design for a tool for shallow-water oceanography is analyzed in regards to the environmental forces impacting its proposed operation. The hope is that this new item will create a resilient means of data telemetry for many instrument packages that would be

placed in shallow water regimes as part of an oceanographic mooring deployed for long periods of time. Since this is a completely new system, many considerations were made concerning the current areas of interest to the scientific community, previous solutions presented by other groups, and the requirements of operations by the end users of the system.

Shallow Water Oceanography

Due to the proximity of human populations, gaging the properties and patterns of near-shore waters that impact the development of the local communities is vital. Water temperature, tide levels, nutrient levels, and dissolved chemicals are several values that are important to the local economy and environment (Breitburg, 2002). Collecting this data is also important for observing a habitat over time, with species reacting to these changes throughout a diurnal cycle, a season, or even an entire year. There are several particular areas of interest for both scientists and environmental policy makers. With the development of Marine Protected Areas (MPA) in the United States, *in-situ* marine observation is used to monitor the properties of these regions, with the hope that preserving and protecting these areas will have benefits outside of them (Rashid, et. al., 2000). Another shallow water regime requiring deeper scrutiny has been coral reefs around the world. Since coral reefs are a particularly sensitive environment, ecologists and biologists are keen to have the physical and chemical data to combine with their own observations of the local species. In addition, the potential dangers due to global warming has placed an increased pressure to investigate tropical habitats (Hoegh-Guldberg, et. al., 2007).

However, as vital as it may seem to collect data for shallow regimes, that area creates its own challenges apart from the more commonly presented issues such as extreme pressures at depth and open ocean storms and swells. For depth regimes of ten meters of less, the actions from waves impacts the entire water column, affecting instruments all the way down to the anchor (Sorenson, 2006). This is different than with other systems such as moorings in deeper water that have the majority of their components out of the influence of surface conditions, particularly for completely subsurface moorings (Thorpe, 2009). Another situation that comes from having near-shore instrument installations is the proximity of valuable equipment to human populations. With these coastal communities come the dangers from vessels running into surface elements such as buoys and also direct interaction between persons and the instruments themselves, stealing components such as solar panels, tying boats to oceanographic buoys as anchorages, and cutting lines and wires

because it had snagged their fishing equipment (Teng, et. al., 2009). This issue is compounded even more when the site is located in waters around less-developed countries, as there is more inclination to acquire readily available expensive equipment as well as being farther away from advanced and capable facilities for repairs and refurbishing (Teng, et. al., 2009).

Marine Protected Areas

Spread out along the vast shoreline of the United States are Marine Protected Areas (MPA) that have varying levels of severity in terms of the fishing that one can do. Some have regulations that allow seasonal or specific fishing periods and species. Shown in Figure 1 is the vast network of MPA that are under the auspices of the Unted States and Figure 2 shows the network of MPA along the California Coast in particular. Some are limited to only scientific research collecting. Some, particularly the most sensitive or the most vital habitats for threatened species, have a strict no-take policy that prevents anyone from harvesting species (Rashid, et. al., 2000). There are several reasons stated behind the creation of these areas, the most obvious being marine conservation for sensitive or threatened habitats. Another reason is to improve fishing stocks, wherein Marine Protected Areas will be a safe haven for sensitive, but commercially valued species. With the MPA acting as an incubator for an increasing population, the surrounding areas that are not subject to the same fishing regulations will receive the benefit of healthier, more numerous, and larger catches (Palumbi, 2001).

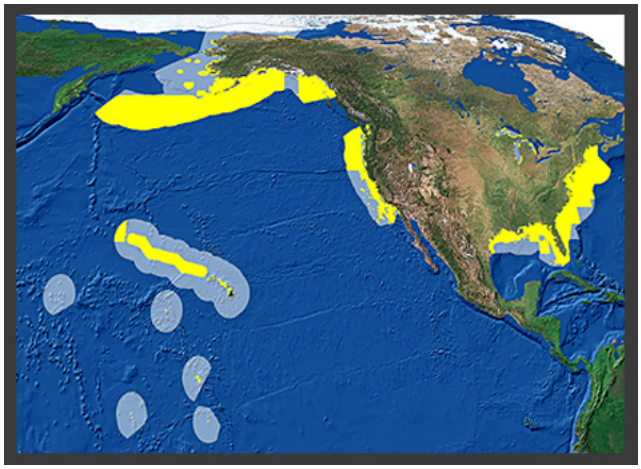

Figure 1: Locations of Assorted Marine Protected Areas around the United States and the Pacific Territories. NOAA.

As such, there is a desire to gather as much information as possible regarding not only

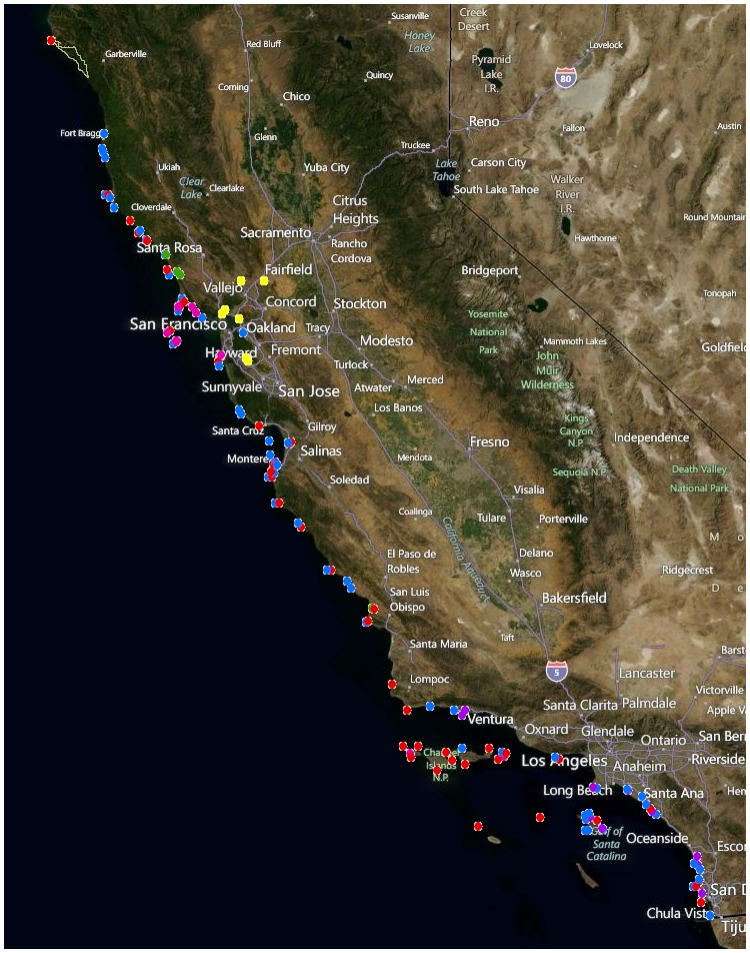

Figure 2: Locations of Assorted Marine Protected Areas in California. California Department of Fish and Game.

biological terms such as population density, but also in terms of chemical and physical oceanographic properties. The composition of chemicals and particles in the water can help determine the changes over time in the MPA as reactions to the conservation efforts as well potentially discovering any interaction between local human communities with any runoff into the waters offshore (Palumbi, 2001). From the perspective of those in charge of fisheries or who depend on them for their livelihood, understanding the physical conditions of a particular environment during biological phenomenon can help illuminate the cycles of species in that environment such as during El Niño and La Niña seasons. Similarly, one can notice the conditions for particularly important milestones in a species lifetime, such as the temperature potentially affecting breeding times.

Coral Reefs

A major area of interest is the waters around coral reefs. The concern is that the coral species could face a problem of reduced productivity stemming from a higher acidity environment that could occur from rising ocean temperatures (Anthony, et. al., 2008). Understanding the changes in the temperature and pH of the tropical, coral reef areas will help provide data towards examining the effects of global warming (Eakin, et. al., 2009). With potentially higher global water temperatures, areas of these warmer waters result in a higher acidity (Anthony, et. a., 2008). The National Ocean and Atmosphere Administration (NOAA) has collected several years worth of data illustrating this connection (Graph 1).This resultant higher acidity then creates conditions where animals create thinner protective calciferous shells. An alarming situation, thinner shells for animals mean that they become more susceptible to predation and protection. For the coral reefs in particular, being actually colonies of animals taking shelter in calcium castles, it is a two-pronged attack on their health, as the acidity creates weaker coral structures and the higher temperatures kill off the sensitive reefs to begin with (Anthony, et. al., 2008). A common reaction to the increased temperatures, as well as pollution, is the death of entire coral reefs, leaving behind only the white calcium skeletal structures. This is what is called "bleaching", as illustrated (Figure 3). The difficulty in investigating the dire situation facing large swaths of coral reefs is only compounded by the difficulty of compiling in-situ data from coral reefs (Sandin, et. al., 2008).

Figure 3: This is an illustration of the coral bleaching that can result from rising water temperatures affecting their sensitive constitution. NOAA.

Graph 1: Graph Showing the Correlations between Carbon Dioxide and decreasing pH levels at Mauna Loa. NOAA.

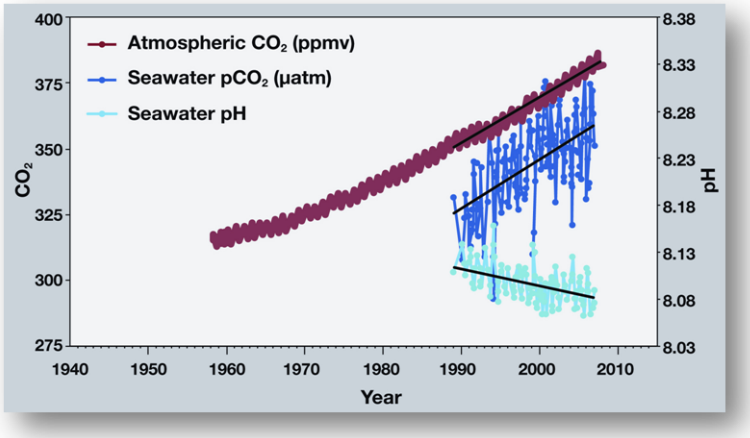

This graph shows the correlation between rising levels of carbon dioxide (CO_2) in the atmosphere at Mauna Loa with rising CO_2 levels in the nearby ocean at Station Aloha. As more CO_2 accumulates in the ocean, the pH of the ocean decreases. (Modified after R.A. Feely, Bulletin of the American Meteorological Society, July 2008)

Frequently, due to the remote locations, moorings and underwater stations are used in conjunction with field surveys and experiments (Thorpe, 2009). However, with the current slate of mooring technologies and techniques, they are usually placed in areas outside the breakwaters and lagoons from coral reefs, preferring to be placed in waters deeper than 100 meters. This means that the mooring's instruments will be able to collect data offshore, but the actual conditions that some of the more shallow coral reef areas go ignored except for field work conducted by scientists. The issue, then, goes back to the remote locations far from established and capable facilities like laboratories and ports where deploying these moorings and servicing them become cost prohibitive, which goes doubly for field technicians, who are limited in their time on station or on site since most work is conducted via diving and controlled tests at a lab onsite (Anthony, et. al., 2008). The unfortunate result is that data collected is either beyond the scope of the desired area or is at widely spaced intervals with no real-time updating and monitoring.

Different organizations have tried different means of taking data from shallow areas. The main methods utilized were oceanographic moorings, instrument stations that lead to a shore station,

and field work by scientists and surveys. Each of these methods have their benefits and means. The primary benefit to wired stations leading to shore is better reliability and direct link between data collection and commands (Howell, 1998). There is subsequently no delay due to conditions out on the water. However, with a direct link to shore, there are complications with the distance from shore for the link. The connection itself becomes more vulnerable as more cable is laid leading from the station to shore from outside interference but also the impedance in the wire itself. While it is possible to not rely on battery power if one can directly hook up a shore-based power source to the instrument site, that then can create its own slew of issues with the danger of power outages that can interrupt the data. Also, having a presence on shore leaves that system vulnerable to vandalism. Others, to monitor shallow areas, have based their instruments either on moorings or on shore stations on piers.

Implemented Designs

Shallow Water Moorings

One of the best means of providing long time-series data for an area is to use a mooring below are two examples of moorings used in oceanography (Figure 4). Suspending instruments below a float, or having the float itself armed with instruments, tethered to an anchor on the ocean floor provide a stable platform for in-situ data. The suite of instruments becomes not only modular but varied. Being a fixed point, it is possible to keep better track of it and have it be a economical option, with the biggest operational cost is the turnaround - recovering and replacing the mooring - to the system. While at times the cost can be prohibitive, the amount of data accumulated over a period from months to years offsets those costs. Compared to other options such as untethered Lagrangian floats that are self-contained pods that follow currents and are considered expendable, the recoverable instruments of a mooring provide the ability to provide maintenance and improve upon capabilities. For shallow water regimes, moorings lend themselves to being even easier to service and maintain, as the usually smaller size means that smaller vessels can be used. Additionally, for the small confines of near-shore environments, moorings, anchored to the sea-floor, give scientists a point of observation in an area of interest without the danger of having an untethered option wash up on an estuary bank or shore (Thorpe, 2009).

Moorings also have the benefit of providing a station for consistent and reliable data telemetry. Whether through satellite link, wireless Internet, or even cellular phone networks, the strength

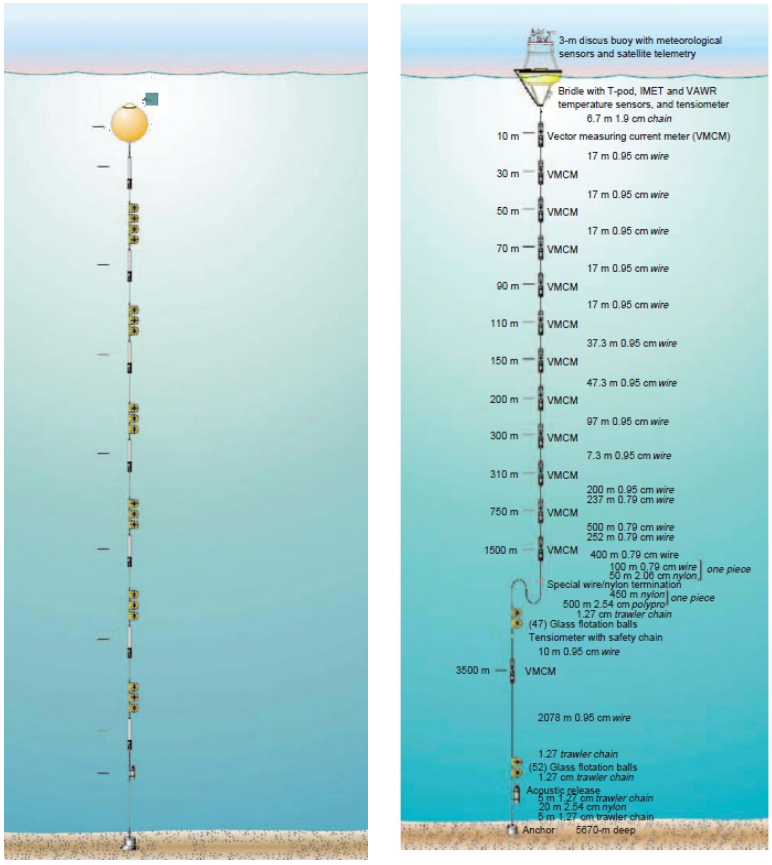

(a) Example of a Subsurface Mooring, Thorpe 2009.

(b) Example of a Surface Mooring, Thorpe 2009.

Figure 4: Examples of a subsurface and a surface mooring illustrating the different aspects. The subsurface mooring provides protection from the surface leements, while the surface mooring provides a platform for data telemetry. Thorpe, 2009.

of mooring hardware allows for a relatively consistent connection when needed for data telemetry as well as receiving commands. This allows for the creation of real-time data sets, where a scientist can observe the changes in the water relatively closely (Thorpe, 2009).

Coastal Data Information Program

The Coastal Data Information Program (CDIP) is a network of American oceanographic moorings and research stations that collect coastal data at sites ranging from Guam to Florida, with an extensive network off the Southern California coast (Figure 5). These moorings collect wave data, meteorological data, as well as physical and chemical data. The moorings nominally consist of a surface float with instruments attached on a mooring wire below (Figure 7). In addition to these moorings, there are stations located on piers, such as one located on at the Scripps Institution of

Oceanography in La Jolla, California. These moorings and stations are able to wirelessly transmit their data and update through satellite links. Finally, complementing these telemetering stations are several underwater stations that record pressure and wave data, to be downloaded upon recovery.

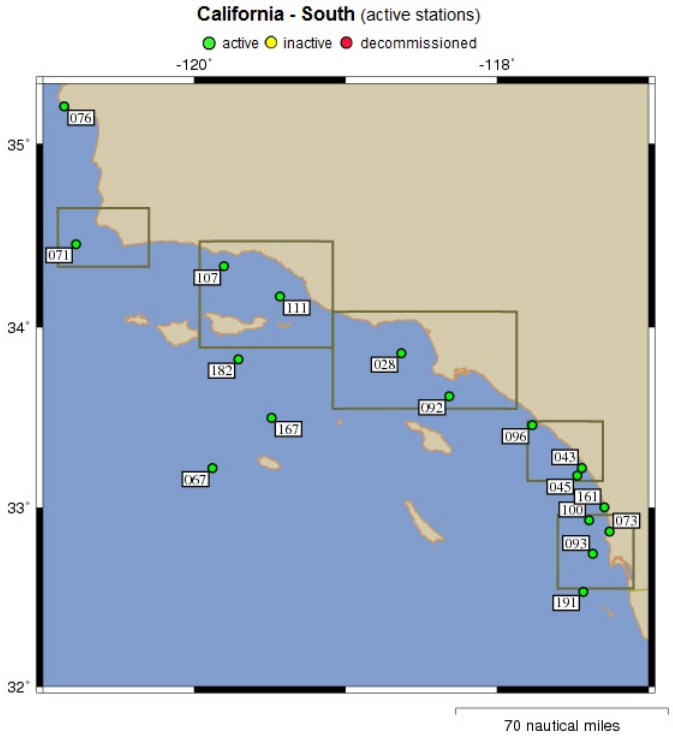

Figure 5: A map of the many oceanographic monitoring stations in Southern California as part of the Coastal Data Information Program (CDIP). CDIP.

Land Ocean Biogeochemical Observatory

The Elkhorn Slough that flows into the Monterey Bay in California is a major estuary that is, itself, a large habitat, but the properties of the flow into the bay is deeply investigated (Adams, et. al., 2007). The Monterey Bay Aquarium Research Institute (MBARI) has a series of moorings and instrument stations in the slough and close to shore through the Land Ocean Biogeochemical Observatory (LOBO) network (Figure 6). This network collects a wide range of data. A typical example of a station is a foam float with data telemetry items connected to an underwater sensor platform (Figure 8). The data is then sent via wireless LAN Internet connection. On these moorings there are instruments such as sensors for turbidity, Acoustic Doppler Current Profilers (ADCP), phosphate, dissolved oxygen, and nitrate. These moorings are part of the larger network that includes several off-shore moorings set in deeper water.

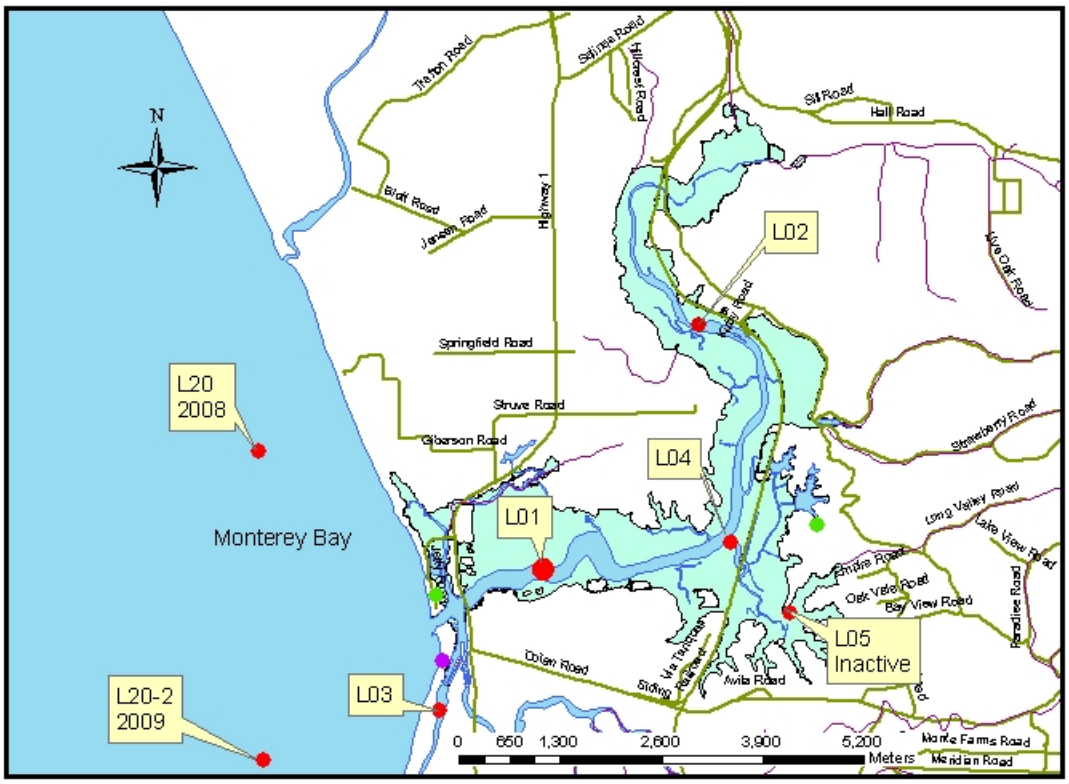

Deployed LOBO Mooring GPS Positions

Table Generated on **Wed 14 Dec 2011 02:45:04 (PST8PDT)**

ing	GPS Timestamp, PST8PDT	GPS Latitude	GPS Longitude	GPS Heading
1	Tue 29 Nov 2011 06:33:20	+36°48'44.75"	-121°46'29.41"	000°
2	Wed 14 Dec 2011 01:29:08	+36°50'27.21"	-121°44'51.99"	149°
4	Wed 14 Dec 2011 02:20:19	+36°48'54.95"	-121°44'43.30"	118°

Figure 6: Map of Monitoring Stations in the Land/Ocean Biogeochemical Observatory (LOBO) Network in the Monterey Bay and Elkhorn Slough. MBARI.

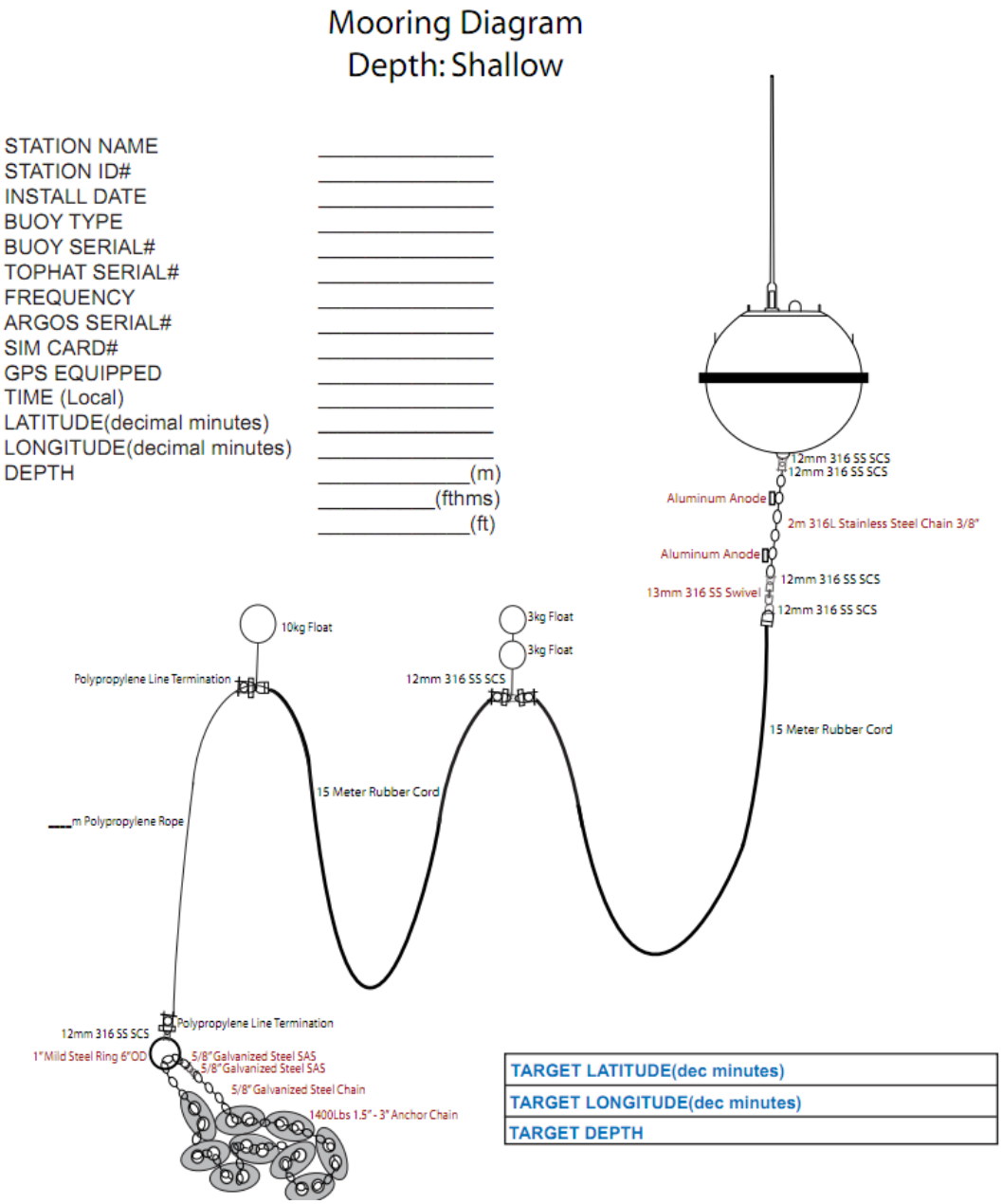

Figure 7: An example of a CDIP mooring designed for depths from 8 to 10 meters depth. As one can see, there are no instruments on the Mooring Wire and 1400 lbs. of anchor cannot be handled without proper equipment. CDIP.

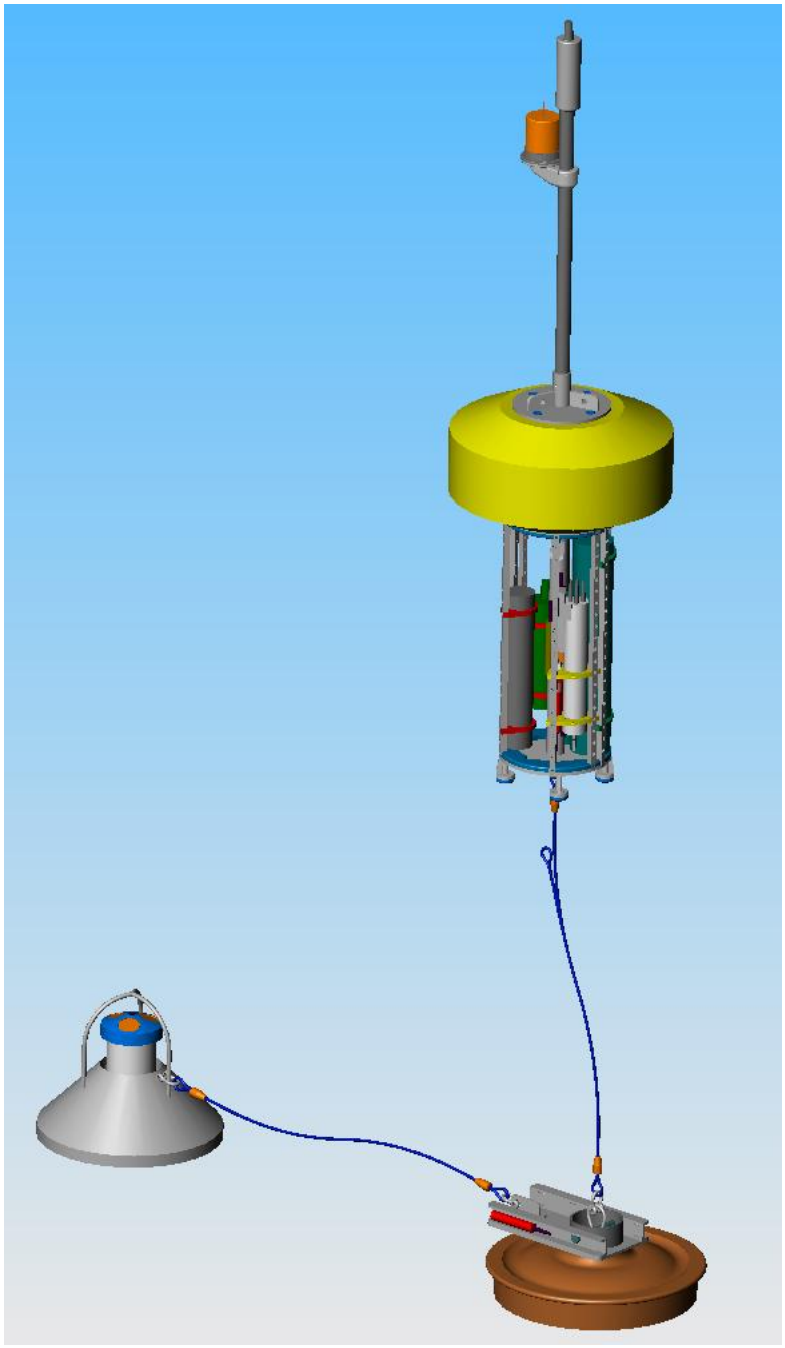

Figure 8: Illustration of a Mooring Used in the Elkhorn Slough, showing the variety of instruments and sensors (including an Acoustic Dopper Current Profiler to the left of the mooring). This also shows the different large elements such as the surface buoy and the anchor, which necessitate equipment to deploy and recover. MBARI.

Deficiencies

The current methods of ocean monitoring in shallow waters have extreme benefits that have been built up over years of experience. Moorings provide a stable point for instrumentation that can be allowed to stand without major maintenance repairs or interaction barring catastrophic damage. Surface moorings also have the benefit of allowing for direct to shore telemetry through different methods such as radio transmission, cellular network, and satellite-based Iridium. However, there are several deficiencies to having a static placement. Also, being subjected to the forces from winds and waves, several cases see wires and cables break under load and, at times, the entire mooring becomes disconnected from its anchor and drifts away from its station, necessitating a rescue and recovery operation. Additionally, being closer to the surface means residing in a more productive habitat, leading to increased biological growth that could hamper the mooring's systems (Figure 9). Several surface moorings used by the Scripps Institution of Oceanography easily accumulate massive amounts of wildlife on the underside of its buoys after a year of operation. A means of countering the stress from environmental factors is to keep the entire mooring below the surface. This brings then another issue which is that it removes the possibility of real-time data telemetry. For subsurface moorings, the only means of collecting data would be to physically recover the instruments and download data directly or through an acoustic modem, which necessitates an operator with a hydrophone on a vessel to establish the link and gather data then.

Outside of the additional environmental factors such as animals biting and weakening mooring lines and cables, there is the added danger imposed by outside persons on mooring equipment. A major issue with surface moorings, particularly those that reside in locations close to remote populated areas, is that the surface buoys can easily become impacted. Boat strikes, being used as a mooring point for boats, and theft and vandalism are just a few of the actions that have disabled oceanographic moorings (Teng, 2009). There have been cases where a buoy's entire suite of electronics were removed, leaving only the float and its frame for scientists to find. This comes from the valuable batteries, electronics, and systems such as weather vanes, GPS tracking, and solar panels that are left out to the elements which may be stolen by those wishing to either use it for themselves or sell them after the fact (Figure 10).

Figure 9: A buoy in the GEOCE project recovered off of Catalina Island shows the amount of growth that can accumulate on a mooring after a deployment of a year, Send Group.

Figure 10: The remnants of theft, the NOAA flotation is all that is left after the main instruments and components have been removed. NOAA.

Dynamic Antenna

A possible arrangement that overcomes a few of the faults of shallow water surface moorings is to create a subsurface mooring that has the ability to create a surface presence for data telemetry and then recover said presence to allow it to continue collecting data hidden from sight. This would allow for the periodic telemetry of data to shore for real-time updates, while providing some measure of protection from interference by outside forces such as the surface weather elements and human activity. This mooring could and should be able to have a scheduled communication link, necessitating a reliable means to create and hide its surface presence.

Environment Regime

The idea of the Dynamic Antenna Mooring is to provide an oceanographic presence in extremely shallow waters. This ranges from five meters to 10 meters in depth. As such, the influences from currents and waves will be much different since waves will be able to influence most of the entire water column. Also, because of the ocean environment, the system must be able to withstand the growth and fouling that occurs from long deployments. Just as importantly, the system needs to be able to tuck itself safely away to avoid interference. As such, the smallest surface presence is desirable as well as the ability to place itself deep enough to avoid the draft of passing boats overhead. An example of the environment that a Dynamic Antenna System can be in place would be close to La Jolla in that conservation area. There, such a mooring would have to contend with assorted wave actions as well as frequent surface traffic due to boats, kayaks, and surfers. An added side benefit to the local area is that with the antenna being hidden from view, the mooring can be then placed in areas valued for its pristine vistas such as nature preserves and parks that advertise themselves to tourists and visitors. It would be beneficial to these parks to have moorings that could monitor the local habitat, but be hidden during park hours so that the scenery isn't obstructed or interrupted by an antenna. While this seems like an innocuous request, people do care about maintaining the character and vision of their local parks and communities.

Operational Requirements

For the purposes of this project, the mooring is supposed to be an easily deployable and recoverable system that can be created relatively inexpensively and operated in a variety of different regimes. This would allow for the capability for forming a wide network of moorings. As such, a

relatively compact structure that wouldn't be too cumbersome in terms of weight would be ideal. An example of what is not appropriate would be the LOBO and CDIP mooring systems, where the main float has a wide diameter as well as consisting of additional heavy components such as the anchor. With the added weight of instruments attached to the float, there is a requirement to use a substantial deployment crew and a vessel with a strong enough davit, crane, or A-frame to place the mooring on site (Figure 11 and 12). This is insufficient for this requirement as the access to such levels of manpower and mechanical might can vary greatly from location to location.

An example of a simple, two-man deployable item would be the autonomous floats frequently used, such as with the ARGO oceanographic monitoring network. Consisting of a one-meter to one and half meter cylindrical housing, it is easily launched over the side of many different types of vessels, from small dinghies to global-range research ships. Therefore, this shallow water mooring system should be a balance between the two designs in terms of maintaining the mooring aspects of the LOBO network, but keeping the simpler operational requirements for the autonomous, untethered floats. An added benefit to this simplified operation is the reduced operational costs. This reduction lends the system to potentially creating a larger network of moorings allowing scientists to track patterns and phenomena across a larger area.

Figure 11: This gives an idea of the size of these CDIP buoys as well as the effort that goes into deploying them. A boat would tow them out to position and then drop the large clumps of chain. This scale and level of equipment is to be unused for the Dynamic Antenna System. CDIP.

Figure 12: The deployment of a LOBO Mooring, as shown, requires a properly outfitted boat, something that the Dynamic Antenna System will be designed to not require. MBARI.

Design Concept

Preliminary Design Concepts

There are a multitude of different means of solving the problem of having an antenna while being able to hide itself when necessary. One possibility is to have a system where the antenna acts similarly to a submarine, where a shift in buoyancy will cause the system to either rise to the surface or sink. Another method is to have a telescoping antenna, akin to that seen on cars. Lastly, one can utilize a basic see-saw mechanism where a shift in the center of mass can rotate the assembly and subsequently raise and lower the antenna.

Tethered Buoyancy-Controlled Float

The buoyancy-controlled system is based on the technology of the common and successful SOLO floats used in the ARGO oceanographic network (Roemmich, 2009). A motor would pump oil into a bladder which would change the displacement of the float, causing it to surface. Inversely, pumping oil out of the bladder subsequently caused the system to sink. This repeated action would allow for vertical profiles of the water column to be recorded and also transmitted back to shore on the surface through its satellite Iridium antenna. Subsequently, the methodology to create a similar system would not be difficult. In fact, it could also be possible to simply adapt one of these floats to be tethered to the rest of the mooring through a connecting cable. The rest of the mooring would consist of a substantial subsurface float with the necessary instruments and anchor. The surfacing and submerging float, then would be freely loose about the mooring itself (Figure 13).

Because a buoyancy driven float would most likely be whipped around by currents and waves in such an extreme area, a more stable means of raising and lowering the antenna would be needed. To be a viable option, the buoyancy control would need to be extremely accurate, as a deviation on the order of one meter can easily cause a submerged antenna float to sink farther than intended and put weight on the element meant to hold up the rest of the mooring. This results precludes the option of merely having the free float be negatively buoyant, since it would create the exact effect of putting undue weight on the main flotation element. Also, as per the design requirements, the entire mooring needs to be submerged some safe distance from the surface to allow the passing of small craft with impunity. This would mean that the float would require a lengthy tether, as one that is too short would begin to pull on the entire mooring when the antenna is on the surface, as the large surface area of the float would create much in the way of wave-induced drag on the surface.

A longer antenna tether, coupled with the lack of accuracy, can create a dangerous situation for the mooring. Should an error or deviation in depth occur, it would be very easy for the tethering cable to allow itself to be caught any number of out-hanging edges, hooks, and hooks present from instruments on the mooring. Also, when the tethered antenna is at the surface, whipping wave action can create a watch circle around the mooring, where the float is circulated by surface forces, causing the cable to either wrap itself around the main flotation or, potentially worse, wear the cable as it rubs on the mooring, weakening the cable, leading to losing the floating antenna. As if losing the antenna from the mooring wouldn't be enough, if that antenna float housed the main controllers for its buoyancy, it could potentially sink as part of its normal operation, possibly losing it to the briny depths. Augmenting all of these arguments is the simple fact that the end user is unable to control the trajectory of the float as it passes through the vertical. While sinking, the antenna float could fall upon the rest of the mooring. While rising, it could embed itself in the rest of the mooring. With the elements of the ocean realm constantly and persistently at odds with the desires of the scientists and engineers, reducing the elements that are unrestricted in movement is ideal.

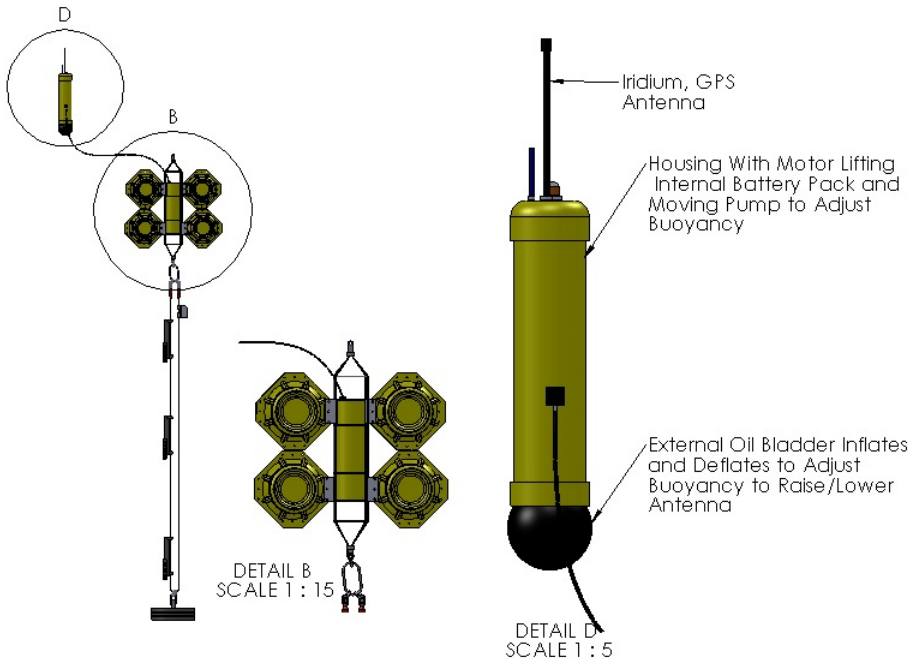

Figure 13: Concept Drawing of an Oceanographic Mooring with a Tethered, Buoyancy-Controlled Float. The black half-globe on the bottom of the antenna housing controls the buoyancy of the system. From the illustration, it is easy to see the potential for the tethered float to be tossed around the mooring.

After examining the dangers of having a loose Dynamic Antenna element, the next step, naturally, is to have a system that effectively anchors the system to the rest of the mooring, while allowing for the antenna to pierce the surface and recover effectively. This system, rather than perhaps having an additional offshoot to the mooring, which would create an additional task for deployments, could be attached to the top of the main mooring. In this vein of design, there are several potential options, one of which to have a large subsurface float with a telescoping antenna.

Telescoping Antenna

For the notion of having a surface-piercing antenna, it would seem that the simplest option would be to utilize a telescoping antenna (Figure 14). Much like that found on cars and in remote controls, a telescoping antenna would consist of concentric and tapering cylinders with the telemetry equipment on the top. A motor or mechanism would extend the antenna to its maximum length, allowing the transmission of data and the reception of commands and requests. The most common method for motorized telescoping antennas is to have a motor drive a rack and pinion system, where a flexible rack would be pushed into the antenna, causing the entire system to extend. Inversely, with the interior tip of the antenna attached to the same rack, the rack can be pulled back down to retract the antenna. The entire assembly would, naturally, have to be encased on its own housing. The potential, here, is to combine the flotation that would normally be necessary to hold up the entire mooring with the housing for the telescoping antenna mechanisms.

While the telescoping antenna would have several attributes that would be useful for the application, the problem of the ocean itself and sealing the concentric tubes can not be overcome since any sealant would suffer greatly from the repeated extension and retraction. Another side effect of the concentric tubing would be that the system would be susceptible to mechanical failure should the antenna, in a raised position, face any extremely large forcing either due to waves, currents, or boat strikes. Since the antenna would be rigidly fixed to the stable flotation of the mooring, it would have less compliance with large forcing. Providing more resistance on a very long antenna, the structure could buckle one of the tubes, rendering the telescoping mechanism unusable. Having that vulnerability in a complex antenna structure, let alone the complexity of the motors and the rack and pinion mechanism within, leads to a situation where there are multiple points of potential failure. What could be considered, then, is a system where the antenna is made of a single component, to maximize strength. Also, since the antenna and the mooring will be subject to such forces, designing in some sort of compliance, where the system does not provide enough resistance

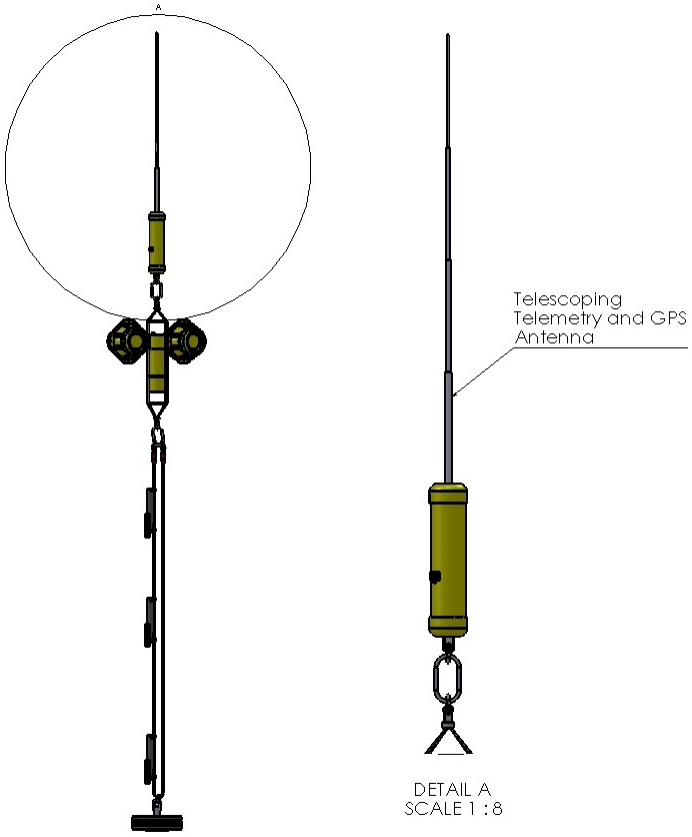

Figure 14: Concept Drawing of an Oceanographic Mooring with a Telescoping Antenna. The efforts to properly seal the concentric tubing as well as minimize the wear on the system through cycles of telescoping point to potential points of failure in a long-deployment system.

that physical damage could result, is essential. Finally, having the simplest mechanism is vital to the longevity of the system and the mooring on site. Where there are more systems exposed to the elements, or more moving pieces, both inside a housing and outside, the likelihood of a fault developing increases.

Tilting Antenna

A possible design is to have the antenna rigidly affixed to a housing that has a shifting weight within. The shifting weight would then change the center of gravity and would then cause the entire assembly to rotate about a pivot, enabling the raising and lowering of the antenna depending on the position of the shifting weight (Figure 15). The internal weight would most likely consist of a combination of batteries and additional lead for the necessary mass within the confined volume. The

antenna would consist of a single, solid piece. Within the main housing would be the counterweight and a method to shift it, either a lead screw or a modified gearing system (Figure 16). To connect the antenna to the rest of the mooring, a cable would then be led from the housing to the rest of the instruments. For this system, since there is only interest in the binary "raised" or "lowered" position for the antenna, the mass shifting within the housing will have only two positions, either at the top of the housing to create a moment that would keep the antenna submerged, or at the bottom of the housing to cause the antenna to stably stay erect.

Some of the benefits to this design are the lack of external moving parts, a single point of rotation, and a certain robustness by being able to be easily overcompensated in terms of fouling and provide minimal resistance to high levels of force. Firstly, the entire system has only one mechanism, which is the shifting mass. The entire process is then contained within the housing, with only the housing moving about a pivot point, but it is not mechanically linked to that pivot. The pivot, being an axle for rotation, can then be sufficiently greased or prepared for the repeated actions expected over the lifetime of the mooring's deployment. This system holds inherent benefits over the other designs listed.

Compared to the telescoping antenna, which depended on a sufficient seal subject to friction that, if compromised, would flood the electrical systems within, a rigid tilting antenna design provides solid seals and connections throughout, without moving parts in and out of the antenna system's housing. Then, with the counter-mass, the system could be scaled up to compensate for changes to the material properties of the antenna, the expected environmental forces, as well as bio-fouling that could attempt to disrupt the balance. This has its benefits over the previously mentioned tethered free-floating antenna design that could be drastically affected by growth. For the cases of large forcing and surface strikes, the presence of an inherent point of articulation creates a situation where the antenna system can absorb forces to the point where the counter-mass' righting moment can resist, but will succumb if pushed beyond, rather than potentially suffering damage. This, combined with the smaller surface footprint provided by a thin antenna, means that there is less chance of loss due to being hit by surface traffic. Lastly, because of the simplicity of the mechanism required and the lack of outside mechanical requirements, being just an antenna attached to a cylindrical housing, there is greater potential for minimizing costs of production while improving handling on the decks of small vessels be few hands. For these reasons, the tilting antenna design was chosen to be pursued.

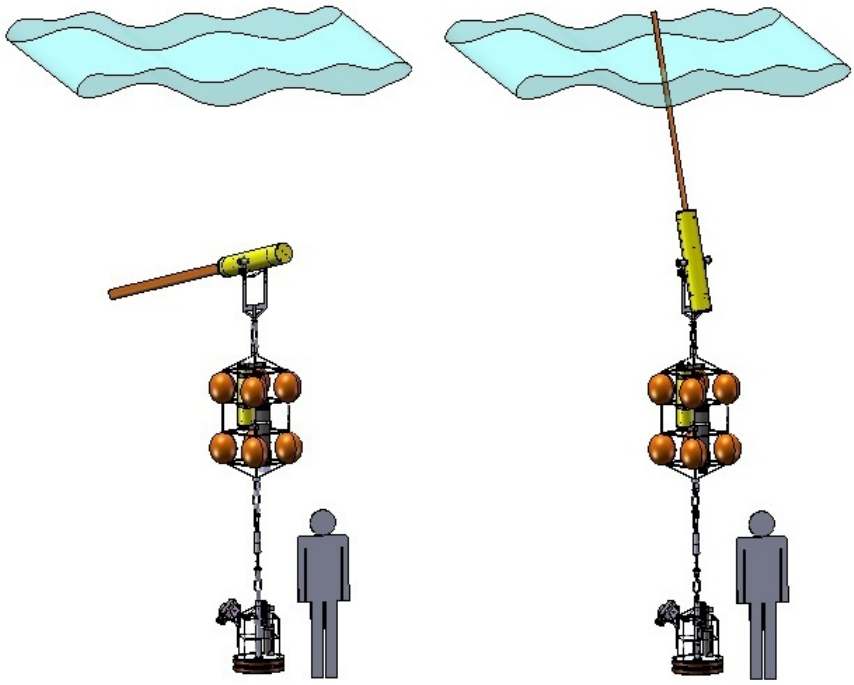

Figure 15: Concept Design of a Tilting Antenna with the Pivot Axis on the Housing. Within, a mass traverses the main housing (illustrated conceptually in Figure 16) to create enough moment to raise and lower the antenna.

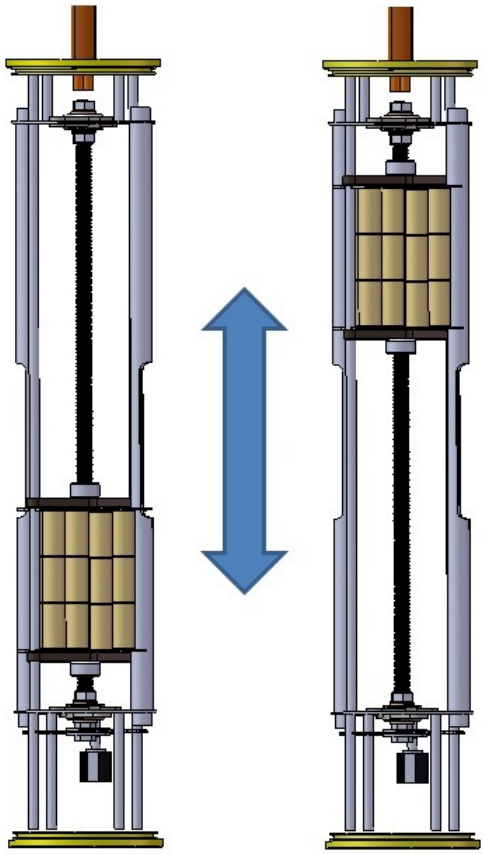

Figure 16: Conceptual Interior of the Tilted Antenna Design, with only the motor, lead screw, and battery pack or weight within, showing the motion of the interior counter-mass. Later designs should minimize the empty space at the ends of the housing to allow the maximum moment to be generated by the counter-mass.

Dynamic Antenna Design

Design Requirement Review

The original requirement is for a method of allowing a shallow water oceanographic mooring, with attached instruments, to provide reliable data telemetry to shore with the added ability to remove any surface footprint at a sufficient depth that any antenna and mooring will be secure from unwarranted human interference surface collisions, while incorporating the necessary aspects to facilitate ease of deployment and recovery operations by a small crew with limited resources.

Design Factors

The overall design is incumbent on the maximizing the available input from a counter-mass within the confines of the housing. The mooring itself needs to be able to be deployed from a smaller boat like a Boston Whaler (which are usually no more than five meters in length) that will not have access to cranes or winches or perhaps even the most basic davits. As such, the system needs to be readily launched by a small crew by hand, necessitating a relatively compact case that can be handled in the confines of a smaller vessel. While it requires the counter-mass to be sufficiently large enough to counter the outside forces, the entire system of antenna and housing must not be so large that two people cannot lift it on a rocking and rolling vessel.

Primary Environmental Considerations

As an element in an oceanographic mooring, and with the housing free to rotate about its pivot axis, the main environmental factors will be due to the inherent mass and buoyancy of the system, horizontal velocity profiles due to currents, and Morison forcing from passing waves. The depth regime is based on the requirement for extremely shallow waters between five to ten meters. This will allow for enough of the system to be under water for smaller vessels to pass over, as previously mentioned, as well as deep enough to prevent passing persons to easily access the entirely submerged mooring. Inversely, the design must have enough vertical clearance from the ocean surface to allow passing waves to not disrupt any communications link.

Overview of Antenna Design

The basic system of the Dynamic Antenna mooring is to have the Dynamic Antenna system as the topmost element, beneath it being any additional flotation, instruments, sensor packages, and housings on a wire tethering the entire mooring to an anchor on the ocean floor. The Dynamic Antenna assembly will consist of a long, thin antenna that will allow for transmitting data and receiving commands from shore that will be attached to the top of a water-tight housing. The housing will consist of a pressure vessel with a pivot axis located either mid-length on the longitudinal axis of the housing or at another point such as the center of gravity of the entire assembly.Within the housing, to facilitate the raising and lowering of the antenna, an electrical motor will drive a lead screw which will translate a sufficient counter-mass that will consist of a combination of batteries to power the motor, antenna, and other electronics in the housing, and appropriate ballast. The ballast is to produce the required mass in the confines of the housing interior. In another, separate housing will be the main electronics boards that will not only control the data telemetry system, but also the rest of the mooring as well, relaying commands to the instruments and equipment below the Dynamic Antenna system. Additional elements, such as physical stops to prevent the antenna from swinging further than desired, actual housing penetrators, and other minutiae are part of the overall system, but can be addressed in further study. Described is the foundation in which a data telemetry antenna can be suitably and reliably brought above the surface and then retracted below the surface within the constraints and considerations listed previously.

Numerical Modeling and Analysis

For the Dynamic Antenna, the most important aspect is the ability to lift the antenna in and out of the water by way of using the weight of the internal counter-mass to induce a moment. Subsequently, the analysis of the kinds of moments that will be imparted on the Dynamic Antenna that will hinder the effectiveness of the counter-mass is necessary. These moments can be categorized into internal moments due to the static mass and buoyancy of the Dynamic Antenna's components without the counter-mass, and external environmental forces such as passing waves and fluid flows stemming from tidal currents. The foundation for this analysis is described in this section.

Center of Mass and Buoyancy

The first step in calculating the static forces and moments acting on the Dynamic Antenna system is to located the centers of mass and buoyancy. The center of mass will be a constant that will be based on the properties of the housing and the antenna that is independent of the quantity of the system being submerged. What will allow one to examine the effect that submersion has will be locating the center of buoyancy, which is effectively the center of the submerged volume. The location of these respective centers will determine the moment arm that the forces of weight and buoyancy act with in relation to the center of rotation for the Dynamic Antenna. For the sake of simplicity in calculation, it will be assumed that the housing internals: machinery, electronics, and fasteners, will be incorporated into the mass of the housing itself, rather than considering the individual components' centers of mass. The counter-mass will be assumed to be a single block of a uniform shape to give a relative notion of the masses required to have the Dynamic Antenna react in the desired manner. For a set submerged volume and mass for the housing and antenna, respectively (m_h, m_a, V_{sh}, V_{sa}) they will have their own respective centers of mass and buoyancy (as C_{mh}, C_{ah}, C_{vsh}, and C_{vsa} in Figure 17) . Since both will be uniform cylinders, one can take them to be at the geometric center. Taking the base of the housing to be the datum surface, one can calculate the centers of mass and buoyancy relative to that datum (with L_{mh},L_{ma}, L_{vh}, L_{va} being the respective centers of mass and volume to the datum point):

$$L_{cm} = \frac{m_h L_{mh} + m_a L_{ma}}{m_h + m_a}, \tag{1}$$

$$L_{cB} = \frac{V_{sh} L_{vh} + V_{sa} L_{va}}{V_{sh} + V_{sa}}. \tag{2}$$

$$\tag{3}$$

Resultantly, one can take the moment arm to be the distance from the center of mass or buoyancy to the center of rotation. This will allow for the moment convention of counter-clockwise rotation being positive moment and clockwise, negative by adhering to the convention of downwards vertical forcing being a negative value. The illustration in Figure 17 shows the theoretical locations of the centers of mass and buoyancy, the actual location will be highly dependent on the physical properties and dimensions of the housing and antenna.

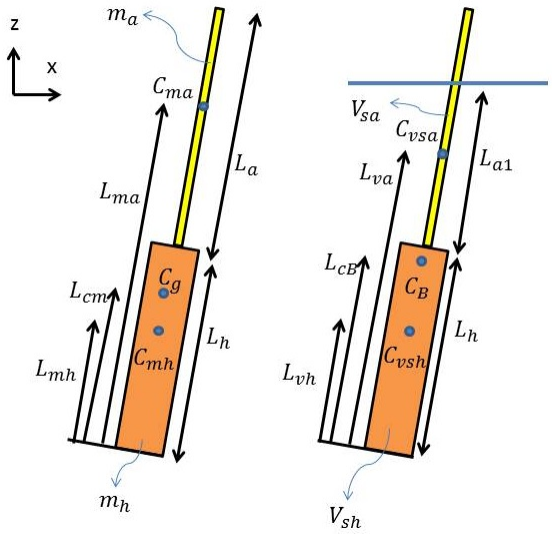

Figure 17: Drawing of the location of the centers of mass and buoyancy for each component (C_{ma}, C_{mh}, C_{vsa}, C_{vsh}) and the entire system (C_g, C_B) which are dependent on the mass and submerged volumes of the components (m_h, m_a, V_{sh}, V_{sa}) and the respective lengths from the bottom of the housing (acting as the datum) to these centers (L_{mh}, L_{ma}, L_{vh}, L_{va}).

Net Static Force and Moment

For finding the resultant static moment imparted on the Dynamic Antenna system for a range of rotation, the equations for force and moment become dependent on the angle γ which is the angle generated between the vertical plane and the angle of the reclined antenna. This angle affects the effective force due to weight and buoyancy by changing the line of action and breaks the forces into effective components that will act perpendicular to the line of action and create a moment. The static forces generated come from the mass of the entire assembly and the buoyancy force generated by the displaced water. The immersion fluid is taken to be seawater at $20°C$. The mass and weight of the Dynamic Antenna assembly is formed as follows where ρ_h and rho_a are the respective material densities, V_h and V_a are the material volumes, and g is the acceleration due to gravity (negative in the coordinate system):

$$m_h = \rho_h V_h, \tag{4}$$

$$m_a = \rho_a V_a, \tag{5}$$

$$m_{ha} = m_h + m_a, \tag{6}$$

$$F_g = -m_{ha} g \sin(\gamma). \tag{7}$$

While for the buoyancy force, that is taken from the total submerged volume only. For that, L_{sh} is taken to be the volume of the entire housing, while the submerged volume of the antenna is taken to be dependent on the depth at which the assembly is set. To that end, the determining datum for the depth is marked at the center of rotation, with the length of the housing split between the lower portion L_{h1} and the upper portion closer to the antenna being L_{h2} (as shown in Figure 18). It is important to note, here, that the later value of $\%L_h$ as listed in Tables 1 - 7, equates to the percentage of the housing's length, measured from the bottom, to the center of rotation. Likewise, the overall depth d is then split between the length below d_1 and above d_2 the center of rotation for the assembly. To find the effective length and volume of the antenna below the surface L_{a1}, one can utilize the angle of recline, the depth to the center of rotation and the length of the housing from that center to the antenna:

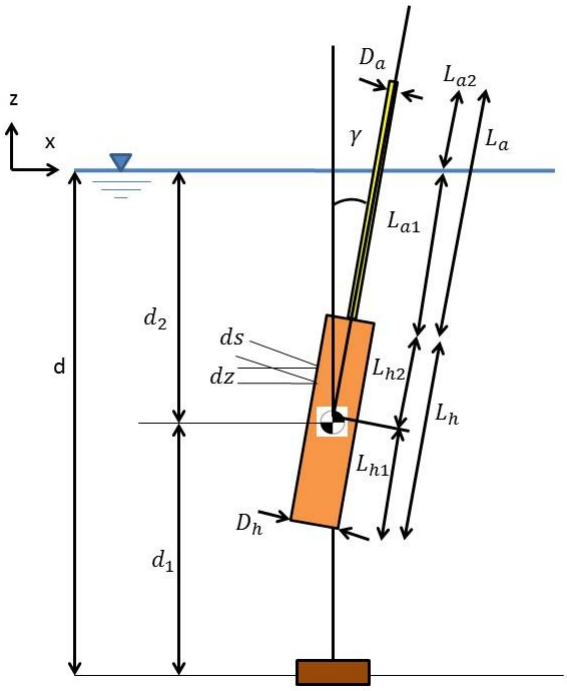

Figure 18: Illustration of the major dimensions for the Dynamic Antenna in relation to the depth as well as to the location of the axis of rotation. The lengths of the housing (L_h) and antenna (L_a) are split between the location of the pivot and the surface, respectively (L_{h1}, L_{h2}, L_{a1}, L_{a2}). These values are combined with the diameters (D_a, D_h). Also shown are the components of the depth that is also split at the pivot point (d, d_1, d_2). For the integration of the hydrodynamic forces along the length of the Dynamic Antenna, the velocity at at the specific depth (dz) will be combined with the area of the unit length (ds). All subsequent moment calculations will be made reflecting the change in angle (γ).

$$L_{h1} = (\%L_h)L_h, \tag{8}$$

$$L_{a1} = \frac{d_2}{cos(\gamma)} - L_{h2}, \tag{9}$$

$$V_{sa} = \frac{D_a^2}{4} L_{a1}. \tag{10}$$

The total buoyant force can be calculated (bearing in mind that it is a positive vertical force):

$$V_{sh} = \frac{D_h^2}{4} L_h, \tag{11}$$

$$V_{sa} = \frac{D_a^2}{4} L_{a1}, \tag{12}$$

$$F_B = (V_{sh} + V_{sa}) \rho_{sw} g \sin(\gamma). \tag{13}$$

The wet weight of the assembly can be calculated from subtracting the buoyant force from the weight, but for the calculation of moments, it is more useful to keep them in their respective values. The resultant moments due to the static mass and buoyancy of the antenna and housing assembly can then be formulated with the previously mentioned equations for the center of mass and buoyancy:

$$L_{cg} = \frac{m_h L_{mh} + m_a L_{ma}}{m_h + m_a}, \tag{14}$$

$$L_{cB} = \frac{V_{sh} L_{vh} + V_{sa} L_{va}}{V_{sh} + V_{sa}}. \tag{15}$$

$$L_{MG} = L_{cm} - L_{h1}, \tag{16}$$

$$L_{MB} = L_{cb} - L_{h1}, \tag{17}$$

$$M_B = B_B L_{MB}, \tag{18}$$

$$M_g = m_{ha} L_{MG}. \tag{19}$$

$$\tag{20}$$

With L_{Mb} and L_{Mm} as the resultant moment arms, the static moments generated from the weight and the buoyancy of the system can be calculated for all angles γ as evident below (Figure 19).

External Forcing from Waves and Currents

After establishing the inherent moments within the system, attention can now be brought on the outside factors affecting the deployed antenna system. These will consist of wave action and ocean currents. With the different environmental factors acting on the entirety of the system, it is important to outline some other details of the assembly that will be important, particularly the

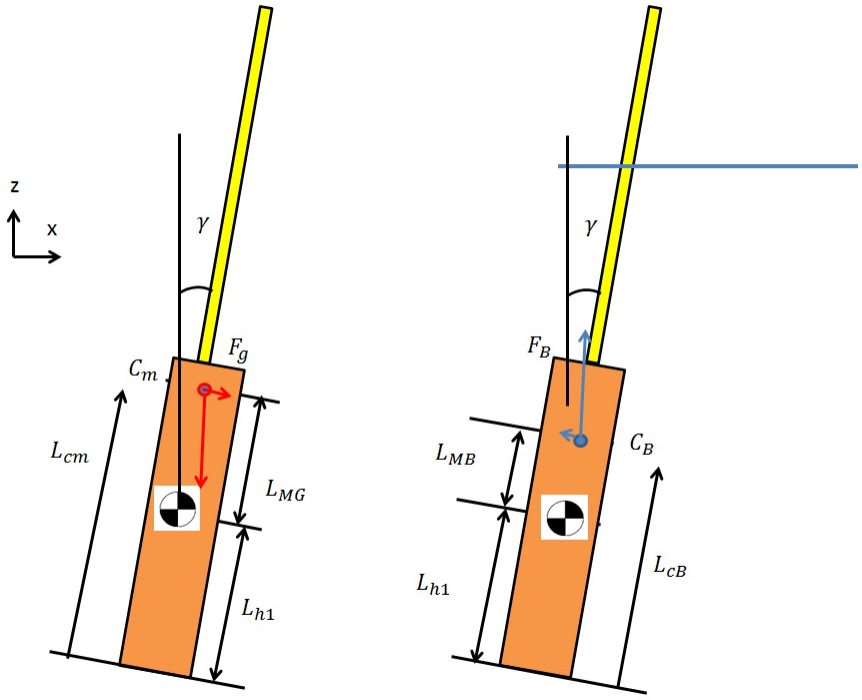

Figure 19: Illustration of the internal forces acting on the Dynamic Antenna, where the vertical force of weight and buoyancy contribute a component of force to the moment about the pivot. The force from gravity and buoyancy (F_g, F_B) have a component that acts along the line of action based on the angle (γ) of recline with the moment arm being taken from the centers of mass and buoyancy to the pivot point (L_{MG}, L_{MB}).

center of area. It is at the center of area that the sum total of these forces will be acting upon and thus the moment arm will be from said center of area to the center of rotation. To formulate the center of area, one simply requires the centroid and the area moment of inertia for the projected area of the entire assembly, since the wave and current forces will be imparting moment along the entire length of the assembly (White, 2008). For the centroid, one can locate it by first breaking it into separate rectangular areas and then relating the respective centroids to an origin on the projected area:

$$L_A = \frac{\sum A_i L_i}{\sum A_i}. \tag{21}$$

(22)

It is at this center of area that sum total hydrodynamic forcing will occur and thus the

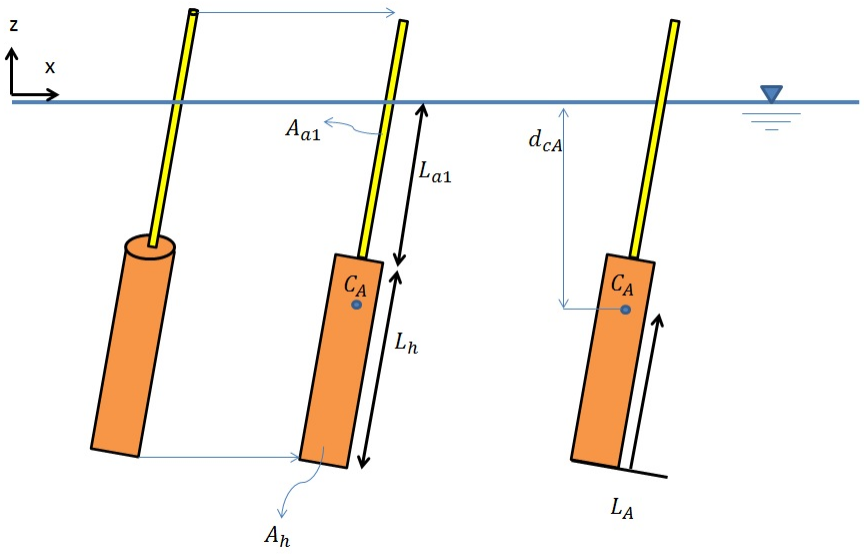

Figure 20: Illustration of the theoretical location of the center of area (C_A, L_A), which is dependent on the submerged area (A_{a1}, A_h).

moment arm is the distance between the axis of rotation and this point.

Current Force

Flow-Stream Principle

No matter the strength of the antenna mechanism to keep it upright, there will be some forcing that will cause unwanted tilt to the antenna. As a result, there needs to be a look at the effect such angles have on the process of drag on a long body. There is a very definitive influence on the drag effects on a cylinder based on the angle of recline γ which is the angle from the vertical the cylinder is rotated (Figure 21) (Hoerner, 1965). The changes are on the velocity pressure forces that act on a normal vector, so apart from the traditional drag from a vertical cylinder that is along the axis of flow (C_d), there are modifications to the lift (C_l) and the drag acting normal to the axis of the cylinder (C_n), all of these drag coefficients are the modifications from the standard coefficient, C_D, for flow normal to the cylinder. These, then, are defined as:

$$C_n = C_D(\cos^2\gamma), \tag{23}$$

$$C_d = C_D(\cos^3\gamma), \tag{24}$$

$$C_l = C_D(\sin\gamma\cos^2\gamma), \tag{25}$$

$$D_{(ndl)} = C_{(ndl)}\frac{\rho}{2}U^2A_p. \tag{26}$$

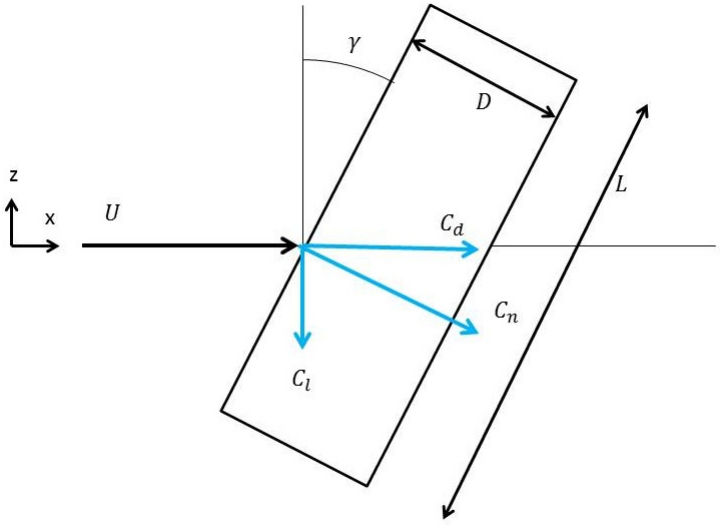

Figure 21: Illustration of the Cross-Flow Principle showing the shift in axes of the drag coefficients (C_d, C_n, C_l) across a cylinder with a length and diameter set at an angle (γ) exposed to some fluid flow (U).

With these coefficients in hand, one can find the changes in the drag force for all angles. Also, since the main goal is to design an effective method to resist overturning of the antenna, the most useful drag component is that that acts normal to the antenna length. This will be useful to compare against the effective moment generated by the counter-mass through different angles of rotation.

Moment due to Current

For a stated current profile that could be uniform or vary with depth, the fluid flow imparts a force on the antenna and housing which then creates a moment. One can calculate the total force acting on the assembly, combining the total force acting on the housing and on the submerged

antenna for some fluid flow U:

$$F_{Dh} = \int_h \frac{1}{2} C_n \rho_{sw} U^2 A_h, \tag{27}$$

$$F_{Da} = \int_a \frac{1}{2} C_n \rho_{sw} U^2 A_{a1} = \int_a \frac{1}{2} C_n \rho_{sw} U^2 (L_{a1} D_a), \tag{28}$$

$$F_{Dha} = F_{Dh} + F_{da}, \tag{29}$$

$$M_c = F_{Dha}(L_A - L_{h1}). \tag{30}$$

$$\tag{31}$$

Then, with the total force, one can simply calculate the moment generated by acting the force - which is the normal force already - on a moment arm equal to the distance between the center of area to the center of rotation. This is for cases for only a fluid flow acting on the assembly (Figure 22). Later on, the current flow will be incorporated with the wave forces to create a total environmental impact.

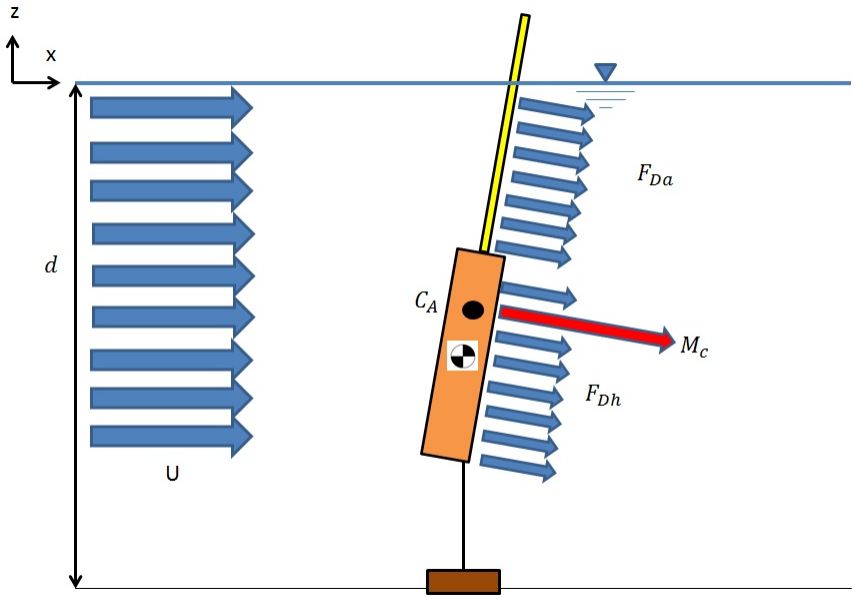

Figure 22: Illustration of the theoretical hydrodynamic force and moment (M_c, shown in red to signify a moment that sinks the antenna) due to a uniform horizontal velocity current U producing a force on the antenna and housing (F_{Da}, F_{Dh}) acting at the center of area.

Wave Forcing: Morison Equation

Since the depth regime for the Dynamic Antenna system is set to be relatively shallow, waves are an important factor to consider in terms of the total force and moment acting on the system that would cause it to overturn. Thus, the examination follows of the effect that waves will have on the system, involving changing the submerged volume and creating force and moment. For the purposes of this project it will be considered that the waves will be surface gravity waves (as shown in Figure 23).

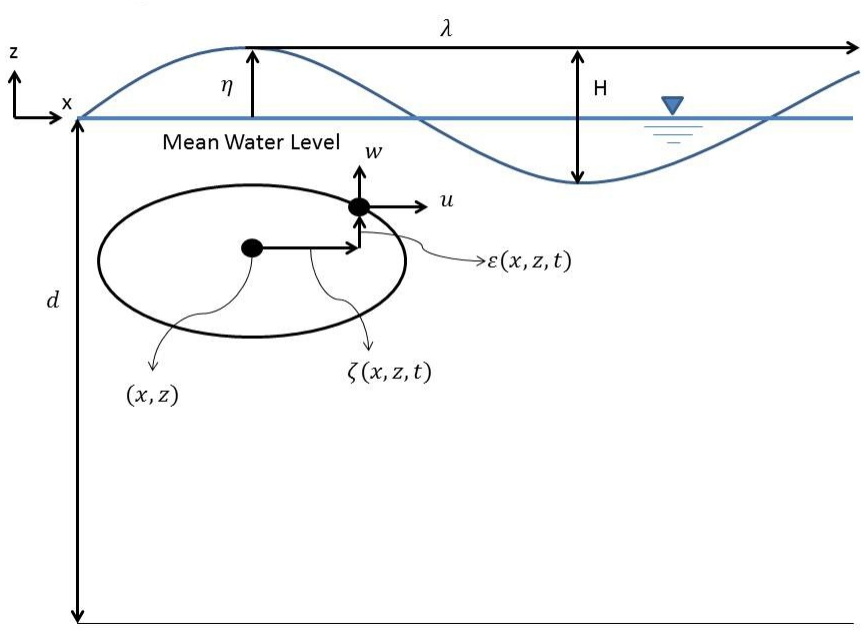

Figure 23: Illustration of the aspects of surface gravity waves with some surface profile (η) due to the period and wave height (H) and wavelength (λ) and depth (d) that creates the orbital path of the water particles (ζ, ε) with their own orbital velocity (u, w).

To that end, determining the force imparted by wave forcing, and eventually including current values, will use the Morison Equation for hydrodynamic forcing in oscillating flows (Sorenson, 2006):

$$F_w(x,z,t) = F_D + F_I. \tag{32}$$

$$F(x,z,t) = \frac{1}{2} C_d \rho_{sw} A_p u_w \left|u_w\right| + \int_A p_x dA + \kappa \rho_{sw} V_s a_x. \tag{33}$$

The wave force is dependent on two terms: the drag force and the inertial force. The first is the hydrodynamic drag force that comes from the fluid velocity u_w imparting friction and normal pressure to the object with some drag coefficient C_D over a projected cross sectional area A_p. It is important to note that while the most common form is simply u^2, since the direction of the flow changes over time, maintaining the proper value (either a positive flow or negative flow) is essential, hence the velocity multiplied by its absolute value (Equations 46 and 47). For the accelerating flow, there must be a pressure gradient and the second term is evident of that, where the pressure, p_x integrated over the cross-sectional area representing the accelerating fluid gradient over the object. The third portion is the representation of the "added mass" term, where the acceleration of the body essentially required to shift a body of fluid that is equal to the submerged displacement of the object. As such, the third term is the product of the fluid density, the submerged volume, the wave particle acceleration, and the dimensionless coefficient κ that represents the ratio of the acceleration of the hypothetical mass to the true fluid acceleration (Equations 50 - 57). Often times for simple cylinders, this dimensionless κ value is about equal to one (Sorensen, 2006).

Wave Kinematics

Surface gravity waves can be characterized for coastal engineering purposes most often from the wave heights,

$$\lambda = \frac{gT^2}{2\pi} \tanh\left(\frac{2\pi d}{\lambda}\right). \tag{34}$$

From the wavelength, the wavenumber k can be calculated. Combining the wavenumber with the angular frequency σ, the free-surface wave profile can be construed for the given wave amplitude H. Additionally, the particle orbits can be calculated for a mean position in the water column over time (x, z, t).

$$k = \frac{2\pi}{\lambda}, \tag{35}$$

$$\sigma = \frac{2pi}{T}, \tag{36}$$

$$\eta = \frac{H}{2}\cos(kx - \sigma t) = \frac{H}{2}\cos(2\pi(\frac{x}{L} - tT), \tag{37}$$

$$\zeta = -\frac{H}{2}\left[\frac{\cosh(k(d+z))}{\sinh(kd)}\right]\cos(kx - \sigma t), \tag{38}$$

$$\varepsilon = \frac{H}{2}\left[\frac{\sinh(k(d+z))}{\sinh(kd)}\right]\cos(kx - \sigma t). \tag{39}$$

$$u = \frac{\pi H}{T}\left[\frac{\cosh(k(d+z))}{\sinh(kd)}\right]\cos(kx - \sigma t), \tag{40}$$

$$w = \frac{\pi H}{T}\left[\frac{\sinh(k(d+z))}{\sinh(kd)}\right]\cos(kx - \sigma t), \tag{41}$$

$$a_x = \frac{2\pi^2 H}{T^2}\left[\frac{\cosh(k(d+z))}{\sinh(kd)}\right]\sin(kx - \sigma t), \tag{42}$$

$$a_z = -\frac{2\pi^2 H}{T^2}\left[\frac{\sinh(k(d+z))}{\sinh(kd)}\right]\cos(kx - \sigma t), \tag{43}$$

$$\tag{44}$$

Wave Force Due to Particle Velocity

Taking the wave fluid particle velocity (Equations 41 and 42), one can find the nominal drag force over a uniform cylinder by integrating along its length. For the two different components, the antenna and the housing, the drag force is taken to be following along the length of each component, measured from the free surface (as illustrated by dz and ds in Figure 18) . Subsequently, the drag coefficient, based on the previously mentioned cross-flow principle, will be that of C_n (Equation 24) since that normal component to the drag force is the most important in terms of finding the moment about the center of rotation. Upon integrating the total force acting on both the housing and the antenna can be elucidated:

$$F_{WDh} = \int_h \frac{1}{2} C_n \rho_{sw} u \left|u\right| D_h ds, \tag{45}$$

$$F_{WDa} = \int_a \frac{1}{2} C_n \rho_{sw} u \left|u\right| D_a ds, \tag{46}$$

$$F_{WDha} = F_{WDh} + F_{Wda}, \tag{47}$$

$$M_{WDha} = F_{WDha}(L_A - L_{h1}). \tag{48}$$

Wave Force Due to Inertia and Added Mass

To determine the total inertial force from the pressure gradient and the force required to accelerated the displaced fluid mass, the pressure term can be considered as the force required to accelerate a volume of fluid matching that of the object, V_s at the rate of a_x. This is similar to the added mass term, which is representative of the displaced fluid mass that is being moved by the object, and so the two can be combined into the single term for the inertial force with the added mass coefficient C_m.

$$F_I = \int_A p_x dA, \tag{49}$$

$$\int_A p_x dA = \rho_{sw} V_s a_x, \tag{50}$$

$$F_{am} = \kappa \rho_{sw} V_s a_x, \tag{51}$$

$$F = \int_A p_x dA + \kappa \rho_{sw} V_s a_x, \tag{52}$$

$$F = (1 + \kappa) \rho_{sw} V_s a_x, \tag{53}$$

$$(1 + \kappa) = C_m, \tag{54}$$

$$V_s = V_{sh} + V_{sa}, \tag{55}$$

$$F_I = C_m \rho_{sw} V_s a_x. \tag{56}$$

Keulegan-Carpenter Number

However, there are conditions in which to examine the components of the Morison forcing, particularly if one examines with the maximum force on the structure. In particular, taking the maximum horizontal velocity for the maximum drag force precludes that there is a minimal accel-

eration, and vice versa. As such, to determine the required parameter for the maximum forcing on the Dynamic Antenna, one must ascertain - from the wave conditions and the submerged body, which aspect will be more dominant, either the drag force due to velocity, or the inertial force due to acceleration. To this end, a common non-dimensional number, the Keulegan-Carpenter number, is used (Sorensen, 2006). By relating the maximum underwater wave particle velocity to the period and the characteristic length of the body (for the Dynamic Antenna, the diameter of the antenna and housing, respectively) one can find which force aspect is dominant.

$$u_{max} = \frac{\pi H}{T}\left[\frac{\cosh(k(d+z))}{\sinh(kd)}\right], \tag{57}$$

$$KC = \frac{u_{max}T}{D_{a/h}}. \tag{58}$$

For an illustration of the value of the non-dimensional KC number, please refer to Graphs 25 through 33 in the appendix. It will illustrate that the inertial forces dominate only in the most benign of wave conditions, while the drag force from the antenna dominates that regime for the example design.

Total Wave Moment

It is a simple operation to have that total hydrodynamic loading acting on the center of area, with the total force acting about the center of rotation, inducing a moment (Figure 24). Here, the moment arm is, again, taken to be the distance from the bottom of the housing to the center of area minus the distance from the bottom to the center of rotation:

$$M_W = (F_{WDha} + F_I)(L_A - L_{h1}). \tag{59}$$

As stated above, this will be subsequently modified to reflect the dominance and predilection for using either the maximum drag force or the maximum inertial force based in part on the Keulegan-Carpenter number.

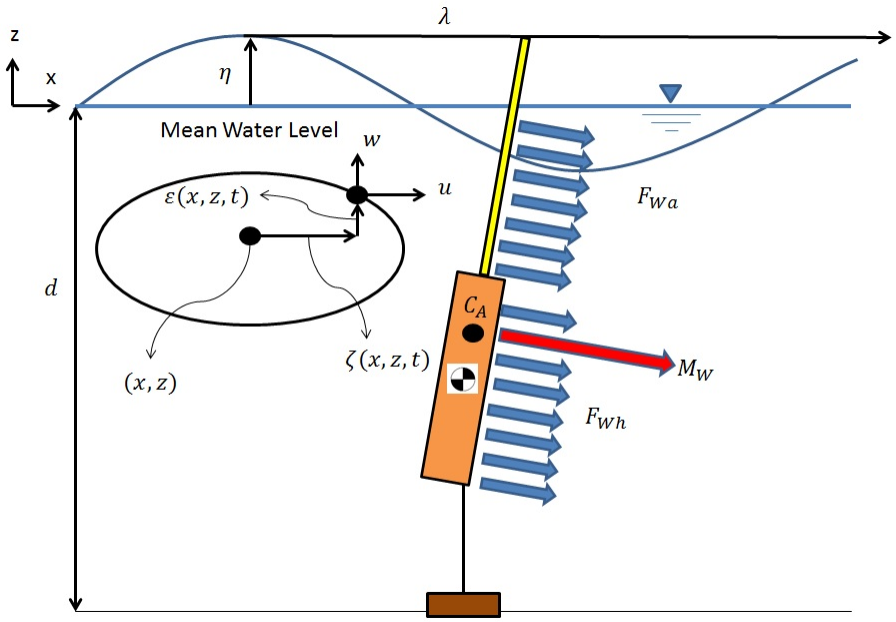

Figure 24: Illustration of the wave-induced moment (M_W) due to the force on the antenna and housing from the fluid particle orbital velocity (F_{Wa}, F_{Wh}).

Counter Mass

As part of the design of the Dynamic Antenna System, a counter-mass has to be utilized to maintain the antenna in an erect position to allow data telemetry. The resultant counter-mass, therefore, must be chosen based on the range of overturning moments it must counteract (Figure 26). A summation of the moments due to static and hydrodynamic forces yields the total moment:

$$M_t = M_B + M_g + M_W + M_c. \tag{60}$$

To calculate the ideal mass required, one has to take the moment arm to be at the theoretical centroid of the counter-mass as well as compensate for the fact that the weight of the mass is a vector with the required calculated counter-force as a component. Taking the shape of the counter-mass as a simple cylinder with a height, equal to the inner diameter of the main housing (the diameter D_h minus the thickness of the housing walls, Th_h), one can locate the mass' centroid, the resultant moment arm, and the weight necessary to counter the total moment acting on the antenna and housing:

$$L_m = \frac{1}{2}(D_h - 2Th_h) + Th_h, \tag{61}$$

$$F_m = \frac{M_t}{L_m}, \tag{62}$$

$$W_m = \frac{F_m}{g \sin(\gamma)}. \tag{63}$$

However, the goal is not to find the ideal counter-mass that would create an equilibrium condition, but to provide an additional safety factor that will provide the necessary force. Being limited, though, by the form factor of the housing as well as the operational requirements stated previously, the counter-mass must be suitably reduced. It is the comparison of the different moments imparting on the Dynamic Antenna system with an arbitrary mass that will be shown, as it will help represent the limitations upon an example system.

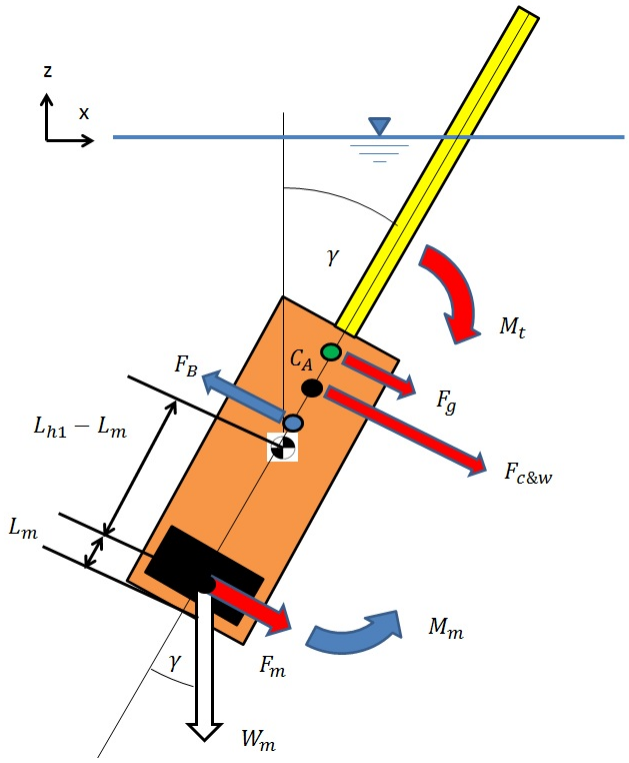

Figure 25: Illustration of all forces (F_B, F_g, $F_{c\&W}$) with total induced moments (M_t) with the required countering moment (M_m), force (F_m), and weight (W_m) of the counter-mass for the given moment arm, considering that the centroid for the counter-mass is offset from the end by the thickness of the housing (L_m). It is important to note that the counter-mass will become more effective with increased angle.

Results

In this section, the calculations of the different configurations for the Dynamic Antenna housing and antenna subjected to different environmental conditions are presented. The analysis will be two-dimensional, with the orientation of the rotation of the antenna to be in line with the X-Axis. The MATLab programming used to calculate the values listed in the graphs below can be found in the appendix.

Environmental Parameters

For this study, the main focus will be on the Dynamic Antenna system as it is presented for ocean deployments where it would be subject to surface forcing from waves and currents. As such, the range of parameters affecting the system will be concerning the depth, the wave profiles, and whichever ocean current velocity is felt appropriate.

Depth Range

For the mooring, the target depth range is from six to ten meters depth. This covers the ideal ranges necessary for extreme shallow water regimes. For moorings intended to go deeper, this would add additional weight due to longer lines and more instruments, which would necessitate a larger flotation element in addition to the main Dynamic Antenna housing. This would then increase the anchor necessary to hold all of those elements to the ocean floor, creating a larger problem of capacity and boat handling than is within the design parameters of this system. Also, as the wave effect decreases with depth - as will be demonstrated below - the ten meter depth limit is a suitable value to examine the limits of the system. At the other end of the spectrum, keeping the minimum depth of five meters is suitable for the reason of providing enough overhead water clearance when the system is retracted so that it is safe from overhead traffic while still providing enough depth below for the attachment of instruments and sensors. While it is possible to decrease the overall dimensions to satisfy depth regimes as shallow as three meters or even two meters depth, the areas where this configuration would be of value, such as inner, sheltered lagoons, would have lower environmental forcing than is the focus of this report. Future studies can be calculated for extremely shallow waters below five meters for use in such tide-pool areas or in rivers and estuaries that may face a steady fluid flow.

Current Flow Regime

With each area of interest under differing conditions in regards to steady fluid flow, it is difficult to specifically and categorically provide a range of current values with an absolutely maximum, as some areas with large tidal changes have high current values upwards of one meters per second, which is in stark contrast to the more benign states of areas offshore which are subject more to wave effects than currents (Broenkow, et. al., 2005). Despite this, it is still important to examine the effects of a uniform flow across the Dynamic Antenna system. What will be of interest is the changes to the amount of drag force that is acting to overturn the antenna as more of it is submerged. With the center of area being usually below the center of mass, the drag could act to keep the antenna up, depending on the location of the pivot axis, which is investigated further below. As such, taking a cue from the tidal currents recorded at the mouth of the Elkhorn Slough, a range of tidal current values up to one meter per second are utilized as the foundation for the analysis (Broenkow, et. al., 2005).

Wave Profiles

Designing an antenna with the intent of extending and retracting in a turbulent zone such as the surf would require a very active and robust system that would belie the core nature of an efficient, reliable, and cost effective solution. As such, the wave profiles, for this study, will be based on the range of wave data collected at the Scripps Institution of Oceanography (SIO) pier in La Jolla, CA as part of the CDIP network (Graph 2). It is a wave sensor that is attached to the piling of the pier. The mean water level has been recorded at eight meters, but for the sake of examination, the range will then be expanded to cover the maximum (ten meters depth) as well as the lower end (in this case, six meters depth) for even distribution.

Taking the significant wave heights (H_s), peak and average period (Ts and Ta) from the CDIP data for the time of February 9th to the 13th, which provides a better example of the conditions (rather than the extreme case on the 14th of February), which will then, when combined with the relation set by Sorensen, (Equation 42), for the matching wavelength for a set period and depth, the other properties of the wave profile can be ascertained.

Graph 2: A Sample of wave data collected at the SIO Pier CDIP Station, showing the range of wave period and height used for analysis of wave forcing. CDIP

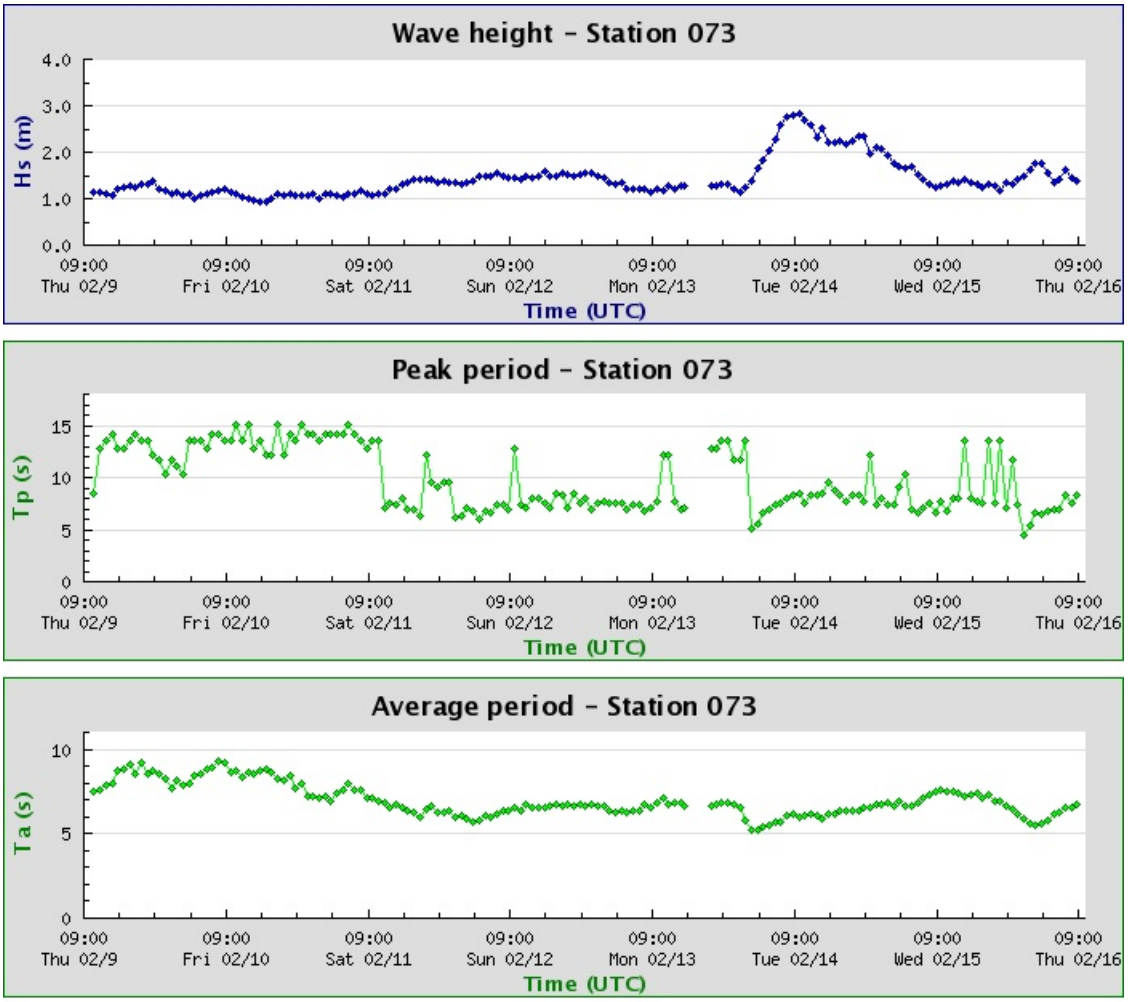

Assumptions

For these parameters, several aspects of the analysis had to be constrained, lest the volume of independent variables overwhelm the scope of this study. For this study, to examine the maximum possible forcing due to waves, the maximum velocity and acceleration due to waves will be taken in the positive X-Direction, as that will create the most overturning moment on the antenna and the housing, which is the most interesting consideration for the design. However, as per the Keulegan-Carpenter number defined above (and illustrated in the appendix), the wave regimes across the housing and the antenna will illustrate the greater importance on the drag force and, thus, the maximum wave particle velocity. The current will be uniform across the span of the antenna and the housing (as shown in Figure 22). Also, the depth of the center of rotation will be set as a constant (three meters depth) which will affect the overall influence of the moments, but is figured to be acceptable, as this depth constant is reflective of the desired clearance from the surface for the antenna when it is fully submerged. For the mass distribution in the antenna and the housing, it will be a uniform distribution, to simplify the calculations. Also, for the calculations of the counter moment, a 20 kilogram (44 lbs.) weight is used. This is a reasonably sized weight for an item designed to fit within the housing as well as a weight for lifting by one person.

For the antenna and housing dimensional parameters, the overall shape is regulated to simple cylinders and their requisite drag coefficients and added mass coefficients. Also, the lengths of the respective components are set at one meter for the housing and four meters for the antenna as arbitrary lengths. The housing size is guided by the constraints of handling and also for a base size to build off of. Similarly, for the antenna, it is borne out of the initial constraint of keeping the system submerged at a depth of three meters, out of the way of passing boats. With the depth of the center of rotation at three meters, a sufficiently long antenna is necessary for spanning that depth as well as having enough length to keep the telemetering tip above passing waves. Additionally, for the housing, the thickness of the walls are set with the housing's thickness of $0.0254m$ nominally. This is a reasonable thickness for most any material as a pressure vessel operating at the shallow depths of this mooring system.

Effects of Changing Environmental Parameters

Alterations to the wave profile parameters produce differing results that are based in part on their relation to the equations that govern the forces acting on the submerged structures. As

illustrated below, the wave moment decreases with increasing depth but increases with increasing period and the wave height, as this relates to the velocity. This comparison was made with configurations 1 through 27, where the individual parameters of significant wave height, wave period, depth, are varied (Table 1). These factors impart their own force on a single configuration of the antenna, as listed below, and the moments are shown. These results are to illustrate and compare the magnitude of influence that the environmental factors of waves have on the total moment. An important element to note is that, as the entire assembly is rotating, and presenting a more streamlined profile to the fluid flow, so as the system rotates, it presents a smaller profile, reducing overall drag.

As for the change in currents, the effect of increasing current is, as to be expected, increasing in overall force and moment on the system as more of the antenna is exposed to the fluid flow. However, as the entire system is submerged, it will be shown that the further rotation decreases the area in the flow until the system is completely horizontal, imparting no moment (Config 77,80,83; Graph 14).

Table 1: Configurations 1 - 31 Properties for Dynamic Antenna and Housing and Environment Parameters of Depth, Wave Height, Wave Period, and Current flow.

Configuration	d [m]	d_2 [m]	T [s]	H [m]	L_h [m]	D_h [m]	$\rho_h[kg/m^3]$	Th_h [m]	$\%L_h$	L_a [m]	D_a [m]	$\rho_a[kg/m^3]$	U [m/s]
config1	6	3	5	0.4	1	0.2302	1025	0.0127	50	4	0.0254	1025	0
config2	8	3	5	0.4	1	0.2302	1025	0.0127	50	4	0.0254	1025	0
config3	10	3	5	0.4	1	0.2302	1025	0.0127	50	4	0.0254	1025	0
config4	6	3	10	0.4	1	0.2302	1025	0.0127	50	4	0.0254	1025	0
config5	8	3	10	0.4	1	0.2302	1025	0.0127	50	4	0.0254	1025	0
config6	10	3	10	0.4	1	0.2302	1025	0.0127	50	4	0.0254	1025	0
config7	6	3	15	0.4	1	0.2302	1025	0.0127	50	4	0.0254	1025	0
config8	8	3	15	0.4	1	0.2302	1025	0.0127	50	4	0.0254	1025	0
config9	10	3	15	0.4	1	0.2302	1025	0.0127	50	4	0.0254	1025	0
config10	6	3	5	0.8	1	0.2302	1025	0.0127	50	4	0.0254	1025	0
config11	8	3	5	0.8	1	0.2302	1025	0.0127	50	4	0.0254	1025	0
config12	10	3	5	0.8	1	0.2302	1025	0.0127	50	4	0.0254	1025	0
config13	6	3	10	0.8	1	0.2302	1025	0.0127	50	4	0.0254	1025	0
config14	8	3	10	0.8	1	0.2302	1025	0.0127	50	4	0.0254	1025	0
config15	10	3	10	0.8	1	0.2302	1025	0.0127	50	4	0.0254	1025	0
config16	6	3	15	0.8	1	0.2302	1025	0.0127	50	4	0.0254	1025	0
config17	8	3	15	0.8	1	0.2302	1025	0.0127	50	4	0.0254	1025	0
config18	10	3	15	0.8	1	0.2302	1025	0.0127	50	4	0.0254	1025	0
config19	6	3	5	1.2	1	0.2302	1025	0.0127	50	4	0.0254	1025	0
config20	8	3	5	1.2	1	0.2302	1025	0.0127	50	4	0.0254	1025	0
config21	10	3	5	1.2	1	0.2302	1025	0.0127	50	4	0.0254	1025	0
config22	6	3	10	1.2	1	0.2302	1025	0.0127	50	4	0.0254	1025	0
config23	8	3	10	1.2	1	0.2302	1025	0.0127	50	4	0.0254	1025	0
config24	10	3	10	1.2	1	0.2302	1025	0.0127	50	4	0.0254	1025	0
config25	6	3	15	1.2	1	0.2302	1025	0.0127	50	4	0.0254	1025	0
config26	8	3	15	1.2	1	0.2302	1025	0.0127	50	4	0.0254	1025	0
config27	10	3	15	1.2	1	0.2302	1025	0.0127	50	4	0.0254	1025	0

Graph 3: Depth influence on wave moment for Configuration 1 - 3, illustrating the overall increase in moment due to decreasing depth.

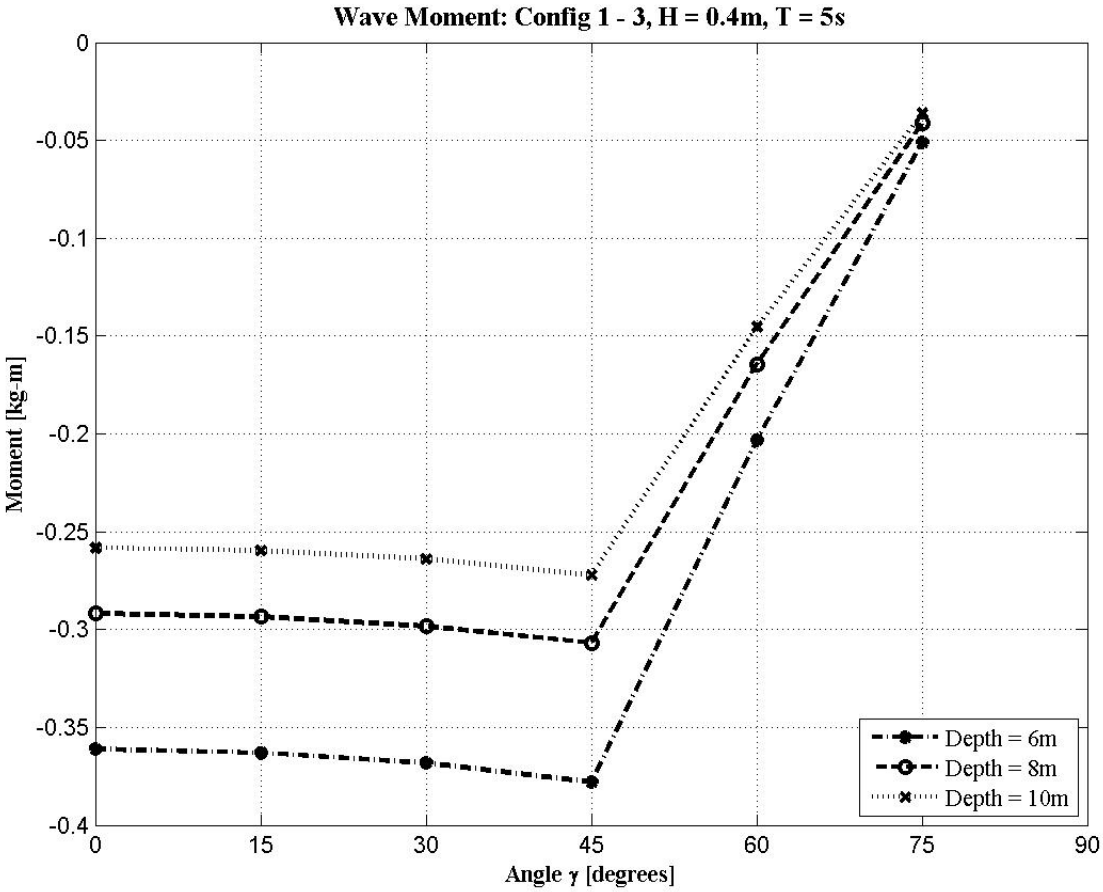

In Graph 3, one can see the influence that the depth plays on the severity of the moment imparted an a uniform structure (as outlined in Table 1) for the different wave profiles. For deeper depths, the overall moment is decreased on the system, but not to a large extent, only by a few tenths of a kilogram-meter. As can be understood, with the increasing reclined angle of the antenna, with more surface exposed, to the flow stream, the waves create more moment. Changing the period of the wave profile alters the overall forcing intensity by increasing the wave moment for longer periods. As indicated below, for the given wave height and depth, longer period waves result in higher forcing and, thus, moment (Graph 4).

Graph 4: Wave period influence on wave moment for Configuration 2, 5, and 8, illustrating the effect of extending the wave period on creating a higher maximum forcing.

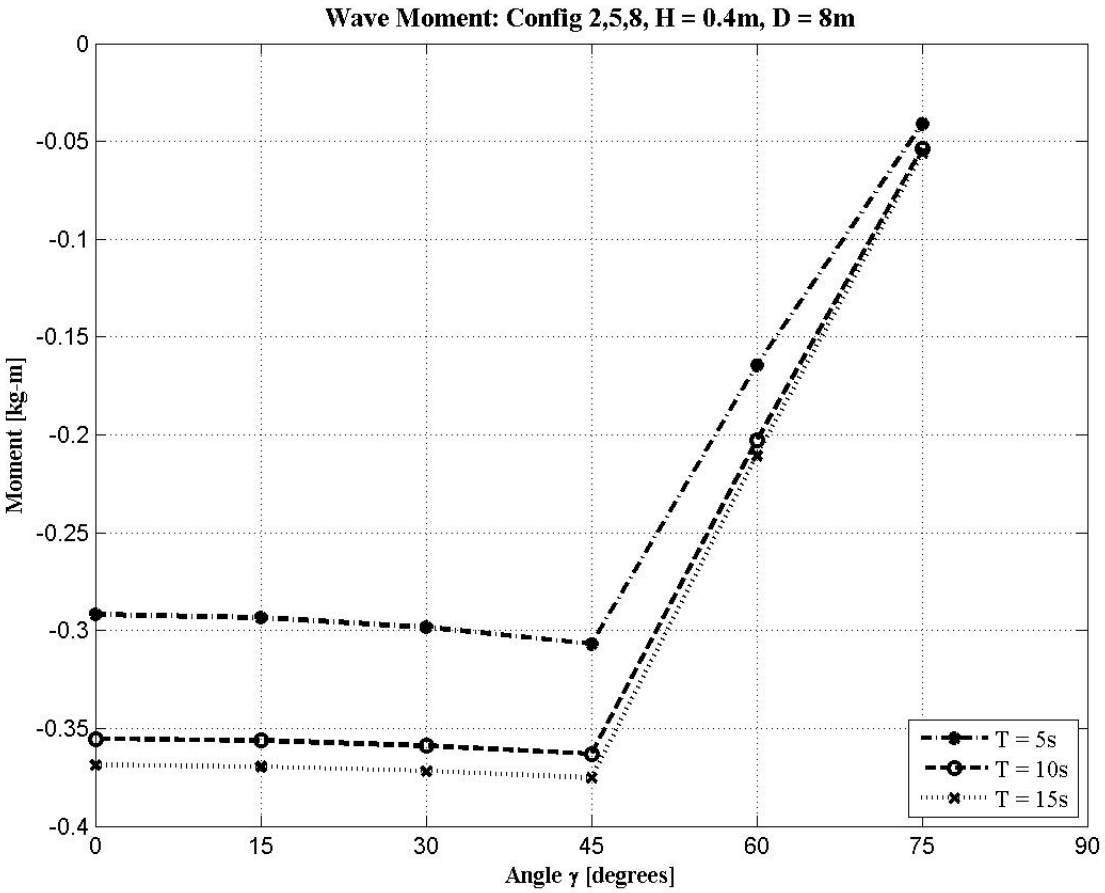

As can be expected, for changes in the significant wave height, the larger waves, which carry more energy, result in higher moments acting on the antenna and the housing (Graph 5). It is the hope that for any design to be successful, overcoming the challenge of high waves with low periods in shallow waters need to be addressed. The driving factor for wave moment will be the wave height. Another consideration that will be addressed later is that, for these wave-induced moments, it is vital that the antenna be able to keep its tip above the crest of these waves, so the comparison between wave height, moment, and vertical tip clearance will discussed.

Graph 5: Wave height influence on wave moment For Configuration 5, 14, and 23, illustrating the significant contribution that increasing wave height has on the force produced.

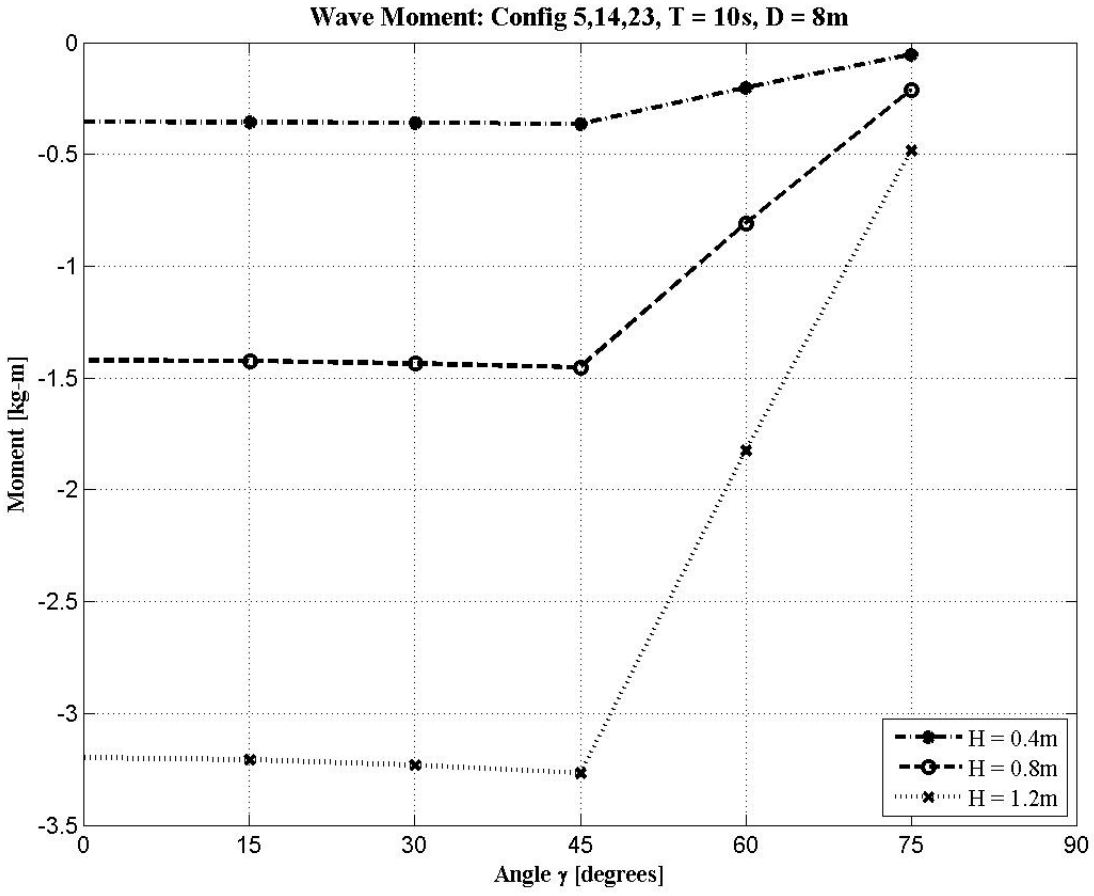

Dimension Parameters

The only aspect of the design that is within the ability to change is the dimension and properties of the housing and then antenna. It is with these elements optimized that the Dynamic Antenna system should be able to perform the tasks asked of it, either to erect the antenna for telemetry or to sink it for protection. Each major aspect of the system: the main housing where the shifting mass, motor, and controller systems will be held in, and the antenna itself, serving as the structural support to whichever means of transmission is required, must have distinct compromises towards the design. Each component must strike a balance between its size due to the hydrodynamic forces imparting on its surface, its overall mass, and its buoyancy. These three areas will be factors that determine the other aspects of the design, such as the location of the pivot axis. While these are considered, the system is constrained by the requirements of providing a long enough antenna to breach the surface through waves, and for a housing to provide sufficient buoyancy to keep itself up, if not the rest of the mooring. Ideally, the housing and antenna are to provide a minimum of additional force to the system, as every portion of the counter-mass ought to be used for opposing environmental forcing. It will be shown that the ideal manner in which this is to be achieved is to have the pivot point placed at point where the housing imparts no net moment, while the antenna is designed to provide little to no moment when submerged.

Varying Housing Dimensions and Properties

With the housing being the largest component in terms of mass and volume which can contribute to the total buoyancy of the submerged mooring, understand the influence that the change on buoyancy as well as the effective area of the housing for the environmental fluid drag is essential. For larger antennas, the mass of these items can impart additional unwanted and uncontrolled forcing on the system leading to overturning to sink or raising. The same can be said if the structure was made to be buoyant. However, since the system is incumbent on pivot axis maintaining proper orientation relative to the rest of the mooring - the pivot structure is not pushed over, which would cause the entire antenna system to be further rotated - a reasonable amount of flotation is needed, let alone for the sake of the mooring to function properly. As such, the displacement and, subsequently, the wet weight, need to be set a value that would maximize the buoyant potential of the housing to provide for the mooring, but minimize its impact on the operations of the Dynamic Antenna. This leads, then, into the desired location of the pivot axis.

The placement of the axis of rotation on the housing is essential to the successful operation of the Dynamic Antenna. By placing it too high on the housing, it provides immense moment to raise the antenna, but little to no assistance in the opposite direction. The same is said for placing the axis of rotation too low on the housing. What compounds the problem is the influence of the housing's buoyancy. With the housing having an ideally large displacement, the buoyant force acting at the submerged structure's center of volume means that it has the potential to overcome any inputs from the counter-mass, even if the whole weight of the counter-mass is acting on as long a moment arm as possible based on the pivot location. With the mass of the housing set at a minimum to maximize available bouyancy, and as the pressure vessel is not required for extreme depths, there is no obvious counter to the moment generated by the buoyancy. With the pivot placed incorrectly, the mass of the housing, coupled with the buoyancy force, results in a very stable system that is very resistant to overturning by any means, natural or artificial, which conflicts with the objective of the design in the first place.

To illustrate the effect that these changes to dimensions and properties of the housing and antenna has on the overall nature of the Dynamic Antenna system by way of moments due to static forcing as well as dynamic loads, the diameter is varied (with the overall length set as one meter since it is at the outer range of handy sizes on a small boat while giving the maximum potential moment arm)(Table 2, Graph 6 - 8) . Also, the position of the pivot axis has been investigated along the housing, hoping to illustrate the differences in influence (Table 3, Graph 9 - 11). Lastly, the density, and thus the mass, of the housing is varied to be either heavier than seawater, more buoyant than seawater, and neutrally buoyant (Table 4, Graph 12).

Varying Antenna Dimensions and Properties

The antenna, being the longest aspect of the system, is subject to further elucidation on the requirements set by it. One requirement of the system is that it has enough length to sufficiently submerge the rest of the mooring. However, due to the passing of waves, the antenna must be long enough to provide enough vertical clearance above the surface for passing waves to not impede data transmission. Should the antenna be too short, traveling waves would crest over the tip, hampering transmissions and causing intermittent connections. While the length of the antenna, then, would be considered to be as long as possible. What prevents this is that the longer the antenna is, the longer and more effective the moment generated, either by a positively buoyant submerged antenna or a heavy implement. Both options create that additional moment that will compromise the effectiveness

of the counter-mass. In that same vein of thought, the length and diameter of the antenna creates an issue due to the fluid drag that an energetic environment acts on the antenna. Thusly, examining the effects of differing diameters and mass properties is a vital aspect of the analysis.

Comparison Between Varying Housing and Antenna Properties

Based on the results from taking the different diameters for the antenna and the housing (Configurations 28 - 31), the change in the amount of hydrodynamic drag due to currents and moments varies much greater due to the change in the diameter of the antenna. The larger housing has a much larger diameter than that of the antenna, but, as the system rotates, additional surface area is presented with a longer moment arm, showing a greater influence from the antenna. Another area of influence is the total static moment. Compared to the volume of the antenna, the volume of the housing, in terms of material and of overall displacement, is much greater, but, in terms of moment, the antenna begins to contribute further, resulting in its importance. Therefore, in considering the dimensions of the system, the antenna can be given measures of freedom, allowing the structure to be built a to a point of maximum structural rigidity and resilience. The housing, though, must be limited by the general requirement of being easily handled on a small boat. With a naturally long antenna needed for surface clearance, it would be necessary to minimize the bulkiness of longest component: the antenna.

Table 2: Configurations 28 - 31 properties for the Dynamic Antenna and Environment, with the variations in antenna and housing diameter with other properties constant.

Configuration	d [m]	d_2 [m]	T [s]	H [m]	L_h [m]	D_h [m]	$\rho_h[kg/m^3]$	Th_h [m]	$\%L_h$	L_a [m]	D_a [m]	$\rho_a[kg/m^3]$	U [m/s]
config28	8	3	15	0.8	1	0.2302	1025	0.0127	50	4	0.0127	1025	0.3
config29	8	3	15	0.8	1	0.2302	1025	0.0254	50	4	0.0127	1025	0.3
config30	8	3	15	0.8	1	0.2540	1025	0.0127	50	4	0.0127	1025	0.3
config31	8	3	15	0.8	1	0.2540	1025	0.0254	50	4	0.0127	1025	0.3

Graph 6: Diameter influence on current moment For Configurations 28 - 31, showing how the increasing diameter of the antenna is the discerning factor in increasing the moment due to current.

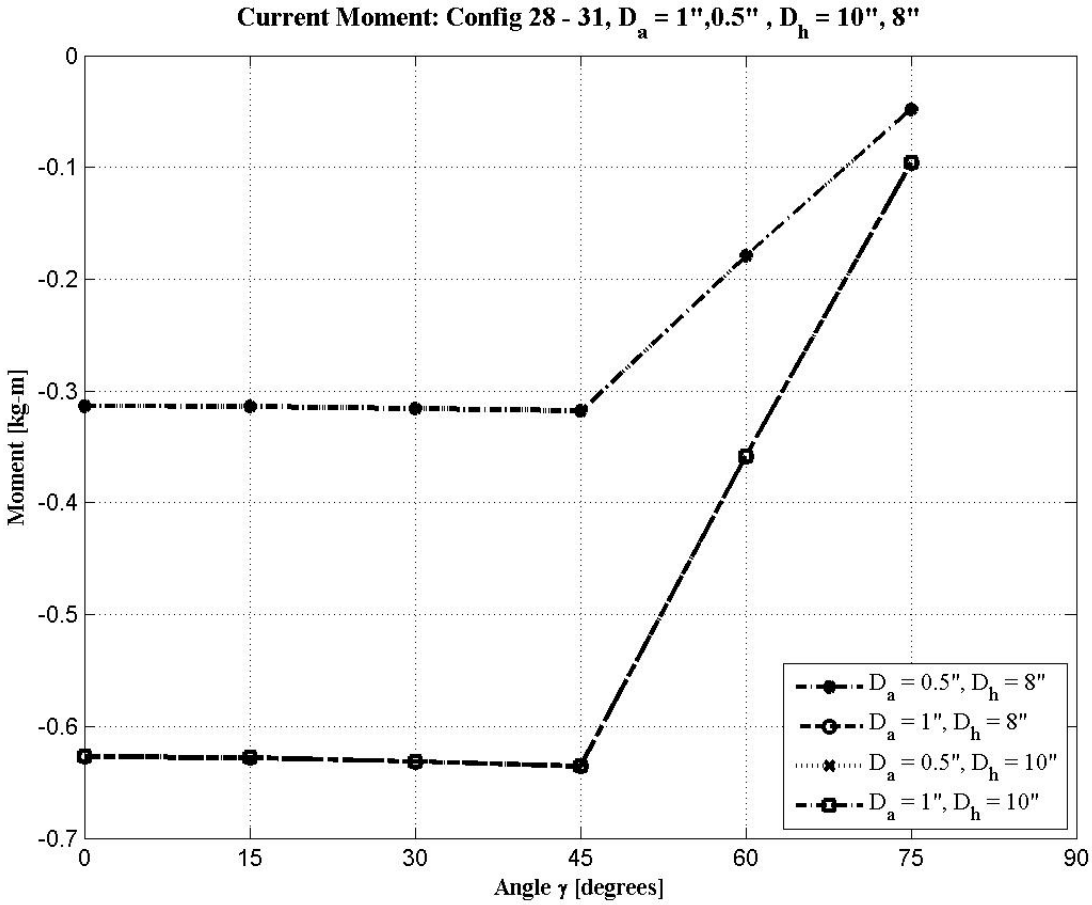

The graph above shows how the influence of the dimensional properties of the antenna can drastically influence the moment acting on the entire system. The moment induced from the change in housing dimensions matter much less than the extra drag induced from a wider antenna (Graph 6 and 7). Of important note is that with the rotating antenna, the further streamlining is offset by the increasing frontal area from the antenna. As a result, the moment is steady until the entire antenna becomes submerged (at about 45 degrees), where the Dynamic Antenna reduces the area exposed to the flow.

For the slim, 0.0127 meter-wide (0.5 inch) antenna, the drag is reduced (the upper line in Graph 6). This same influence can be seen in terms of the wave moments, where the wider antenna dimension is the determining factor in the increase in the moment throughout all angles. However,

the inverse issue with potentially having a decreasing antenna diameter would be the reduction in potential structural strength of a thin antenna. With the proper materials, though, or an improved streamlined shape, this drag induced moment can be reduced. The benefit to having a slimmer housing and antenna is obvious.

In terms of the static moments imparted by the housing and antenna's combined moment due to mass and buoyancy, a particular effect is shown where the static moment is governed by the properties of the antenna rather than the housing (Graph 8). As shown, it is the antenna that produces the larger moment. This must stem from the fact that the antenna, while smaller in volume than the housing, has a much longer moment arm, thus contributing more to the overall effect.

Graph 7: Diameter influence on Wave Moment For Configurations 28 - 31, showing similar influence from a wider antenna on the overall moment.

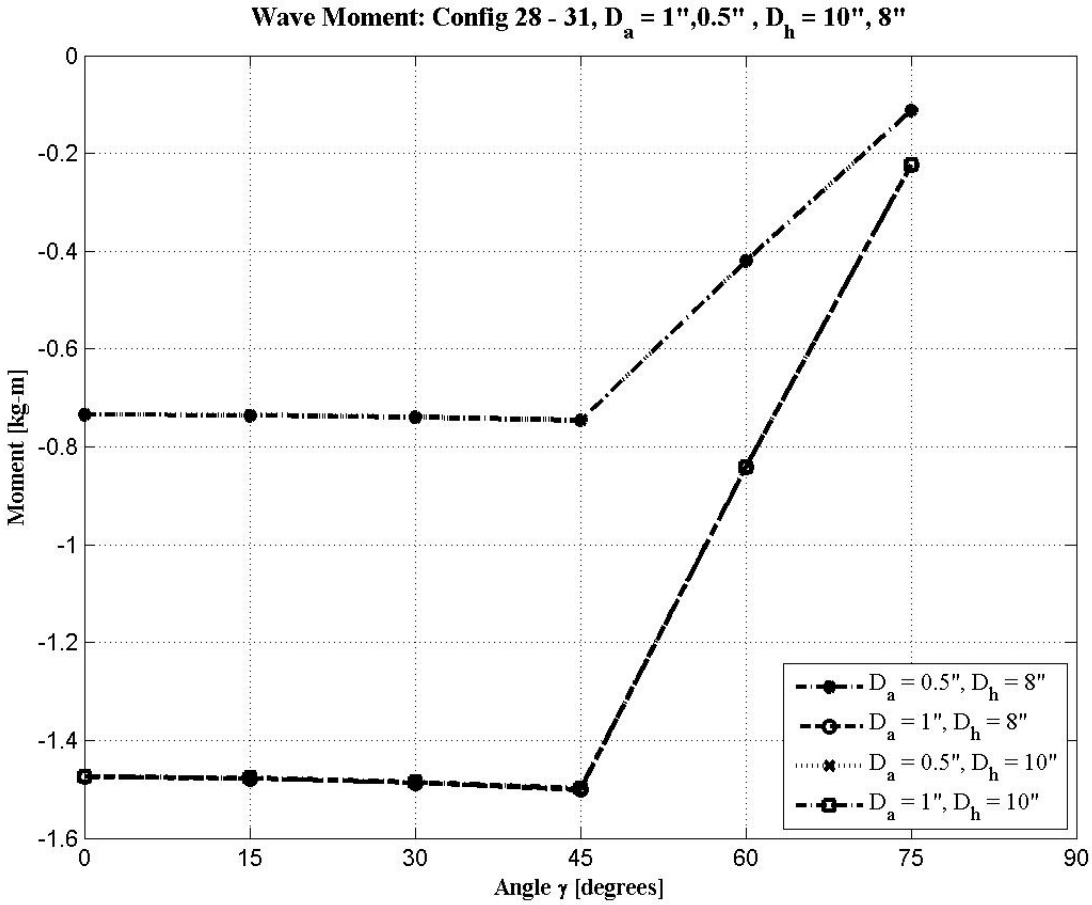

Graph 8: Diameter influence on static moment For Configurations 28 - 31, showing the influence of a wider antenna that, as it sinks further, contributes more on a longer arm to the total moment.

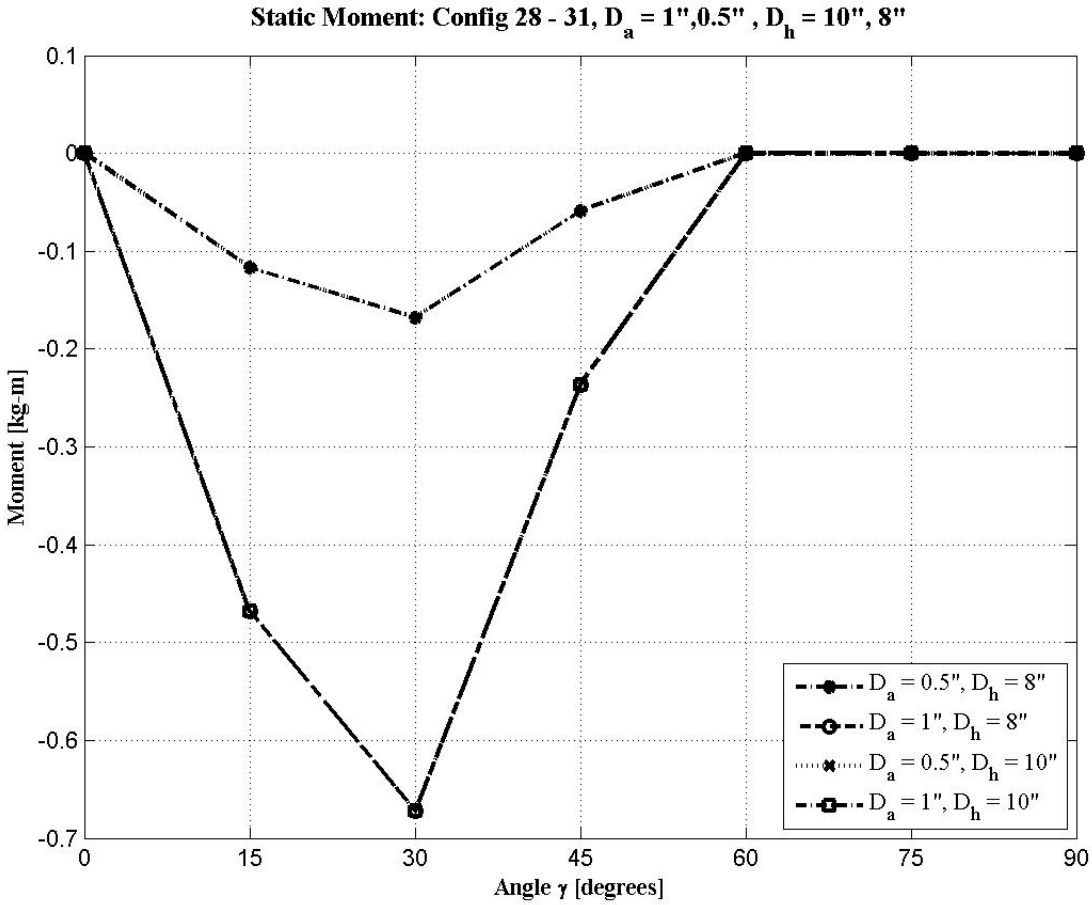

Another property that has the most obvious influences on the overall moment on the system is the actual location of the axis of rotation (Configurations 32 - 41, Table 3). In terms of the environmental factors, placing the pivot higher would provide the ideal conditions where the center of area would be below this axis and therefore the waves and currents in the water would assist in keeping the system upright (Graph 9 and 10). Inversely, the lower the pivot point, the more pronounced the hydrodynamic moment is on overturning the antenna. However, the matter that is most pressing regarding the location of the pivot on the assembly is in terms of the static moment generated by the wet weight of the system. As illustrated in Figure 36, the inherent buoyancy of the housing produces a large moment that can exacerbate the balance of the Dynamic Antenna. For conditions with a higher placed pivot, there will obviously be generated a disproportionate amount of negative moment as the buoyant housing seeks to overturn itself. While this is beneficial for sinking the antenna, it would create an additional moment that the counter-weight would have to overcome. The same can be said for conditions with low set pivots. The buoyancy of the housing would help to keep the overall system more than stable in a variety of environmental conditions, but this, then creates issue when the system attempts to sink. It is the dynamic nature of the system that necessitates neither extreme to be used, as that would, inherently, create an opposing moment that would detract any force from the counter-mass to resist outside influences. In the Graph 11, it would appear that the static moment for the condition where the axis of rotation is in the geometric center of the housing produces zero moment, but, indiscernible, there is a small amount of moment being generated due to the antenna above the surface. Thus, as indicated in the graphs, keeping the center of rotation close to the center of the main contributor to buoyancy , the housing, would minimize static moment on the antenna through its range of motion.

Table 3: Configurations 32 - 41 Properties for Dynamic Antenna and Environment, with the variations in the location of the housing pivot point.

Configuration	d [m]	d_2 [m]	T [s]	H [m]	L_h [m]	D_h [m]	$\rho_h[kg/m^3]$	Th_h [m]	$\%L_h$	L_a [m]	D_a [m]	$\rho_a[kg/m^3]$	U [m/s]
config32	8	3	15	0.8	1	0.2302	1025	0.0254	10	4	0.0127	1025	0.3
config33	8	3	15	0.8	1	0.2302	1025	0.0254	25	4	0.0127	1025	0.3
config34	8	3	15	0.8	1	0.2302	1025	0.0254	50	4	0.0127	1025	0.3
config35	8	3	15	0.8	1	0.2302	1025	0.0254	75	4	0.0127	1025	0.3
config36	8	3	15	0.8	1	0.2302	1025	0.0254	90	4	0.0127	1025	0.3
config37	8	3	15	0.8	1	0.2302	1025	0.0254	10	4	0.0127	1070	0.3
config38	8	3	15	0.8	1	0.2302	1025	0.0254	25	4	0.0127	1070	0.3
config39	8	3	15	0.8	1	0.2302	1025	0.0254	50	4	0.0127	1070	0.3
config40	8	3	15	0.8	1	0.2302	1025	0.0254	75	4	0.0127	1070	0.3
config41	8	3	15	0.8	1	0.2302	1025	0.0254	90	4	0.0127	1070	0.3

Graph 9: Effects of Changing the Pivot Location on Wave Moment For Configurations 32 - 36. With the pivot point closer to the center of area, the moment is reduced.

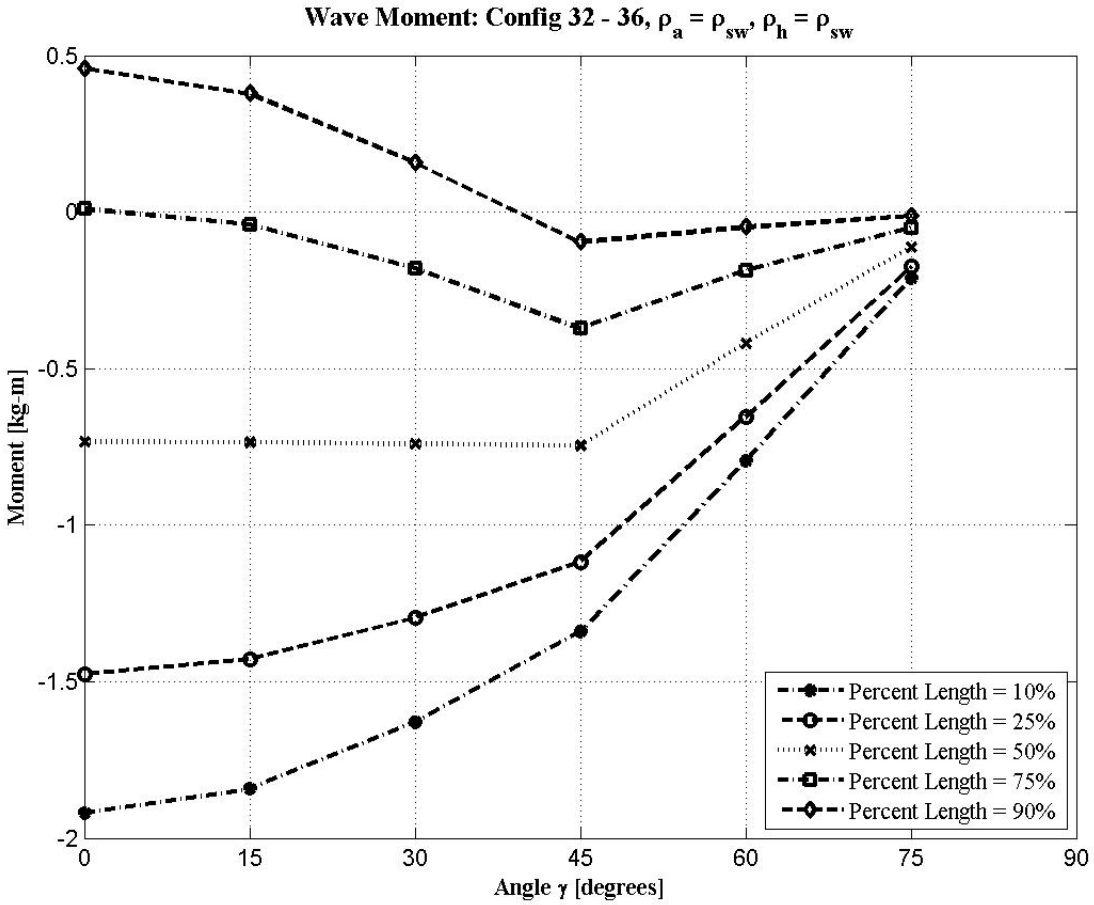

Graph 10: Effects of Changing the Pivot Location on Current Moment For Configurations 32 -36. With the pivot closer to the center of area, the moment is reduced.

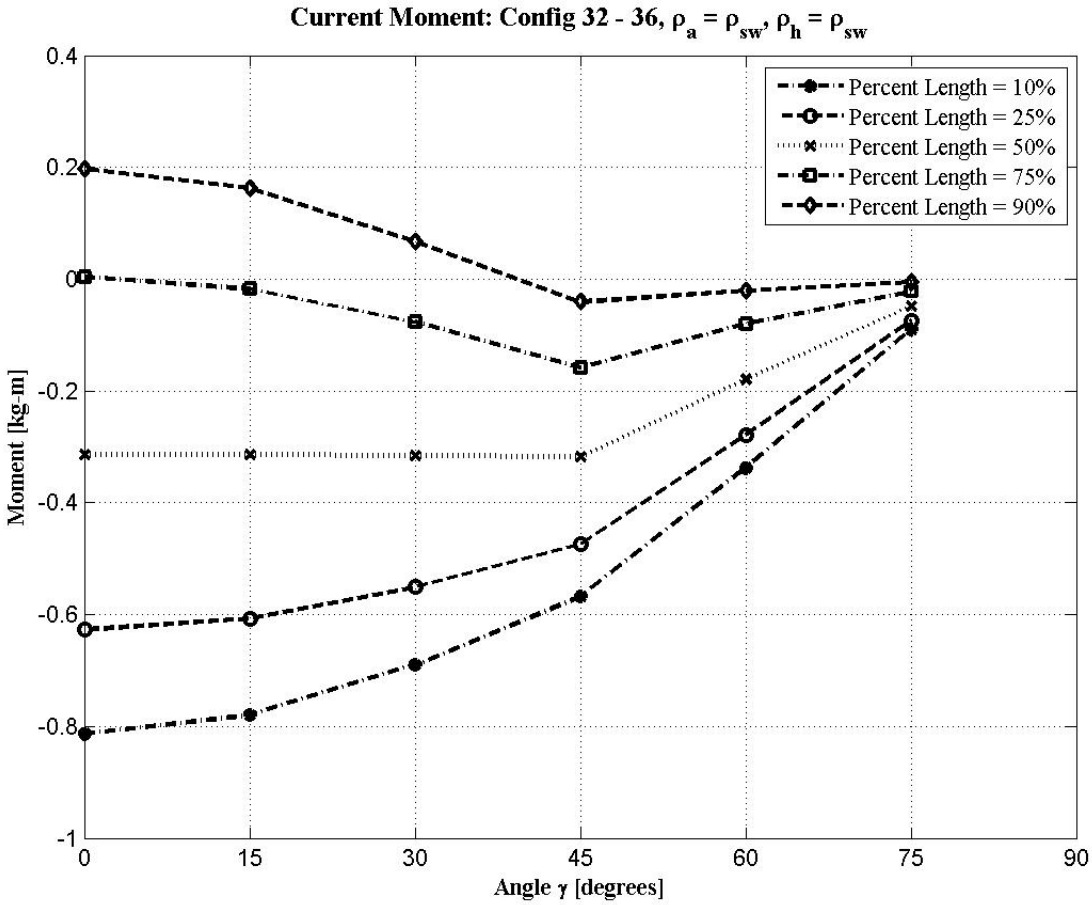

Graph 11: Effects of Changing the Pivot Location on Static Moment for Configurations 32 - 36. Reducing the static moment by placing the pivot at 50% length is ideal.

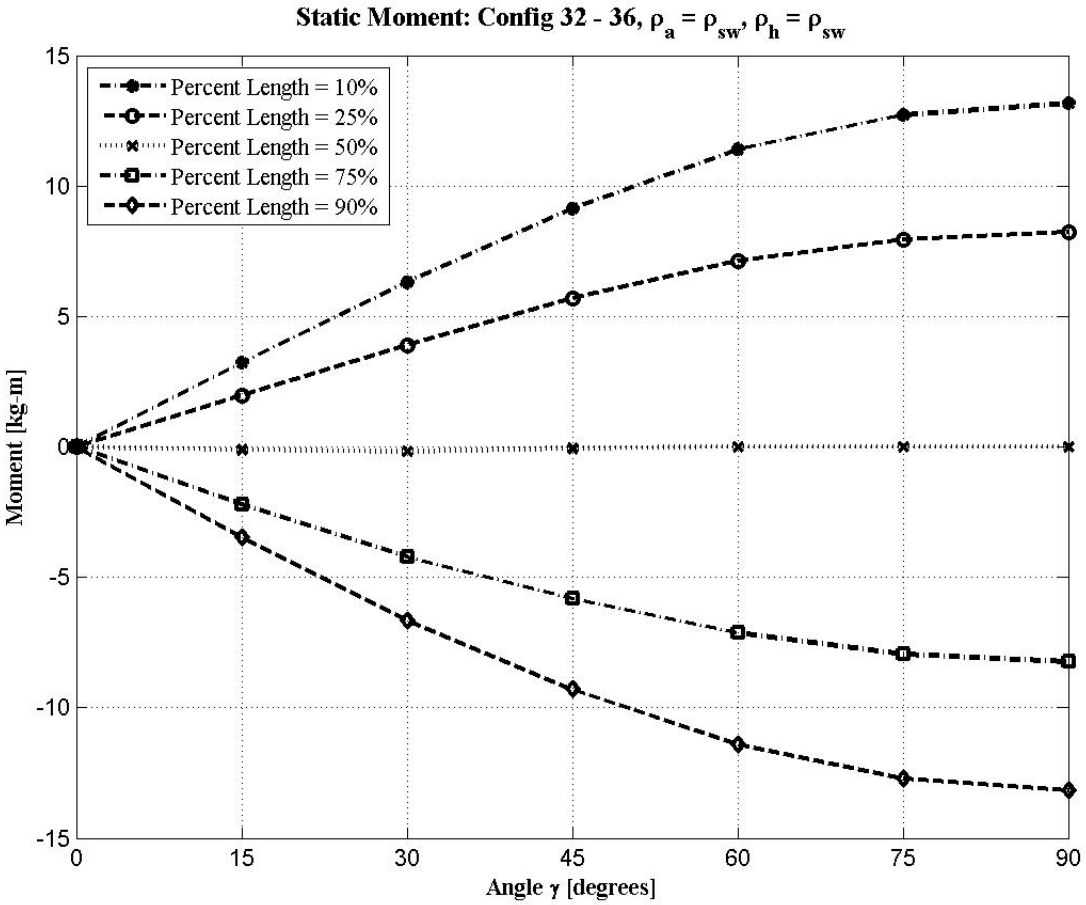

With an understanding of the location of the pivot point, the other aspect influencing the static moment other than the buoyancy of the vessel, namely the masses of the components, bear investigation. To that end, the different configurations of a Dynamic Antenna with different densities is shown in Table 4. As shown below (Graph 12), for the conditions where either the antenna or the housing is neutrally buoyant, denser than seawater, or more buoyant, the major difference comes from the properties of the antenna. Minimizing its influence - as it has the longest moment arm - is of importance to the overall design of the Dynamic Antenna. With a neutrally buoyant antenna, the effect of its weight becomes reduced the more of it becomes submerged, which is helpful for conditions where rising waves knock the system over. To maximize the efficiency of the counter-mass, the reduction of internal moment is vital. For the full listing of configurations that cover this

variance, please refer to the appendix (Table 6 and 7).

Table 4: Configurations 33, 38, 43, 48, 53, 58, 63, 68, and 73 Properties for Dynamic Antenna and Environment, with variations on the densities of the housing and antenna.

Configuration	d [m]	d_2 [m]	T [s]	H [m]	L_h [m]	D_h [m]	$\rho_h[kg/m^3]$	Th_h [m]	$\%L_h$	L_a [m]	D_a [m]	$\rho_a[kg/m^3]$	U [m/s]
config33	8	3	15	0.8	1	0.2302	1025	0.0254	25	4	0.0127	1025	0.3
config38	8	3	15	0.8	1	0.2302	1025	0.0254	25	4	0.0127	1070	0.3
config43	8	3	15	0.8	1	0.2302	1025	0.0254	25	4	0.0127	1000	0.3
config48	8	3	15	0.8	1	0.2302	1070	0.0254	25	4	0.0127	1025	0.3
config53	8	3	15	0.8	1	0.2302	1000	0.0254	25	4	0.0127	1025	0.3
config58	8	3	15	0.8	1	0.2302	1070	0.0254	25	4	0.0127	1070	0.3
config63	8	3	15	0.8	1	0.2302	1000	0.0254	25	4	0.0127	1000	0.3
config68	8	3	15	0.8	1	0.2302	1070	0.0254	25	4	0.0127	1000	0.3
config73	8	3	15	0.8	1	0.2302	1000	0.0254	25	4	0.0127	1070	0.3

Graph 12: Effects of Changing the Antenna and Housing Densities on Static Moment with the pivot placed at 25% of housing length For Configurations noted.

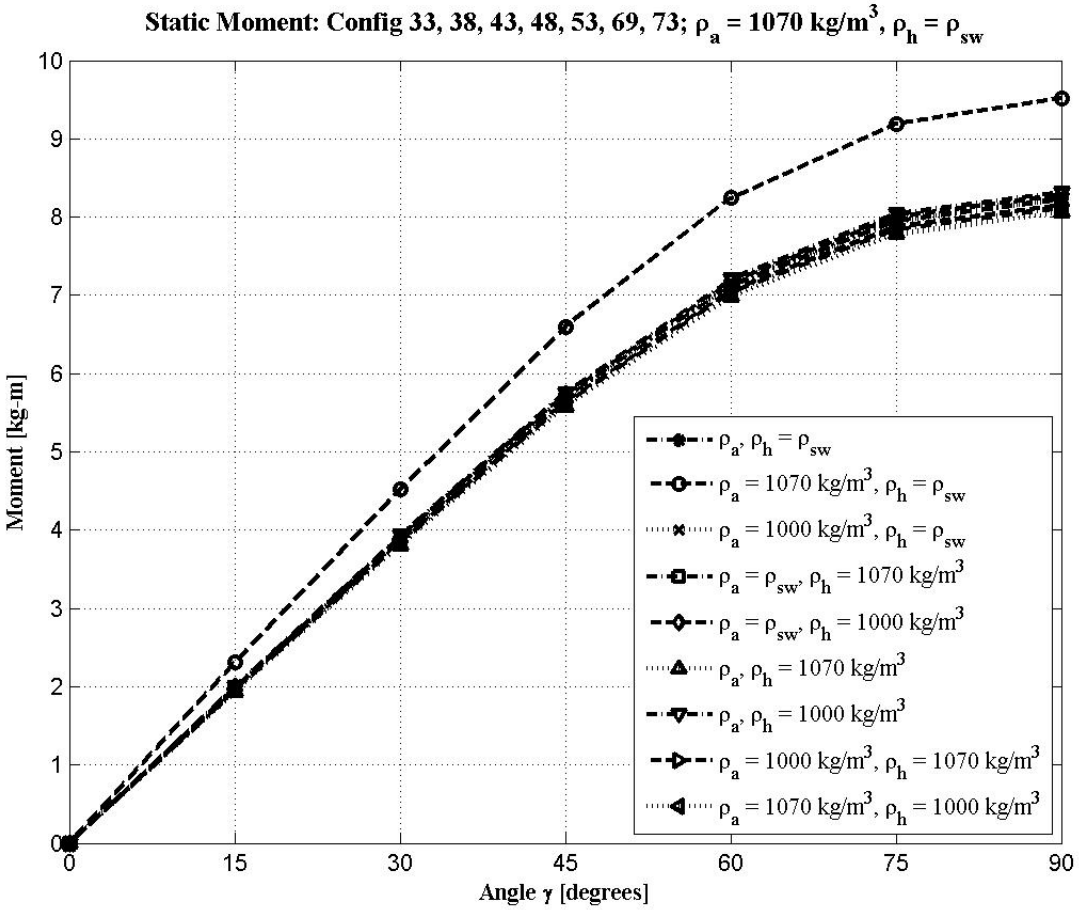

Example Configuration

Based on the results from the different configurations, a general consideration for the components and properties to the Dynamic Antenna System begins to take shape. In this example case, aspects that would detract from the design as well as those that would be beneficial were chosen to create an Dynamic Antenna design. For the antenna, reducing the drag is important, but not as much as insuring that there is enough strength in the structure to support the static and dynamic loading, not to mention the potential strikes that may occur. As such, keeping the diameter on the outside figure of one inch is the considered choice. Additionally, for the antenna, designing it to be neutrally buoyant offers the benefit of minimizing any additional force either due to the weight of the antenna or buoyant force. This leaves the maximum potential moment to keep the antenna submerged or raise it. In total, a long, thin, neutrally buoyant antenna coupled with a thin-walled, larger diameter housing with the pivot at its center of mass provides the a good estimated balance between potential structural strength, volume, and force on the entire system's operation while compromising on the resultant moment bound to occur due to waves and current flows (Graphs 14 - 17). In this section of the analysis, the counter-weight used is a 20 kilogram mass and the total static moment as well as available moment for raising and lowering the antenna is shown (Graph 13). These configurations (Table 5), then, can be applied to the different environmental conditions to examine its responses (Graphs 19 - 24) when coupled with the counter-mass described above.

Table 5: Configurations 77 - 103 Properties for Dynamic Antenna and Environment of an example housing and antenna under different environmental conditions.

Configuration	d [m]	d_2 [m]	T [s]	H [m]	L_h [m]	D_h [m]	$\rho_h[kg/m^3]$	Th_h [m]	$\%L_h$	L_a [m]	D_a [m]	$\rho_a[kg/m^3]$	U [m/s]
config77	8	3	5	0.4	1	0.2302	1040	0.0254	50	4	0.0254	1025	0
config78	8	3	10	0.4	1	0.2302	1040	0.0254	50	4	0.0254	1025	0
config79	8	3	15	0.4	1	0.2302	1040	0.0254	50	4	0.0254	1025	0
config80	8	3	5	0.4	1	0.2302	1040	0.0254	50	4	0.0254	1025	0.5
config81	8	3	10	0.4	1	0.2302	1040	0.0254	50	4	0.0254	1025	0.5
config82	8	3	15	0.4	1	0.2302	1040	0.0254	50	4	0.0254	1025	0.5
config83	8	3	5	0.4	1	0.2302	1040	0.0254	50	4	0.0254	1025	1
config84	8	3	10	0.4	1	0.2302	1040	0.0254	50	4	0.0254	1025	1
config85	8	3	15	0.4	1	0.2302	1040	0.0254	50	4	0.0254	1025	1
config86	8	3	5	0.8	1	0.2302	1040	0.0254	50	4	0.0254	1025	0
config87	8	3	10	0.8	1	0.2302	1040	0.0254	50	4	0.0254	1025	0
config88	8	3	15	0.8	1	0.2302	1040	0.0254	50	4	0.0254	1025	0
config89	8	3	5	0.8	1	0.2302	1040	0.0254	50	4	0.0254	1025	0.5
config90	8	3	10	0.8	1	0.2302	1040	0.0254	50	4	0.0254	1025	0.5
config91	8	3	15	0.8	1	0.2302	1040	0.0254	50	4	0.0254	1025	0.5
config92	8	3	5	0.8	1	0.2302	1040	0.0254	50	4	0.0254	1025	1
config93	8	3	10	0.8	1	0.2302	1040	0.0254	50	4	0.0254	1025	1
config94	8	3	15	0.8	1	0.2302	1040	0.0254	50	4	0.0254	1025	1
config95	8	3	5	1.2	1	0.2302	1040	0.0254	50	4	0.0254	1025	0
config96	8	3	10	1.2	1	0.2302	1040	0.0254	50	4	0.0254	1025	0
config97	8	3	15	1.2	1	0.2302	1040	0.0254	50	4	0.0254	1025	0
config98	8	3	5	1.2	1	0.2302	1040	0.0254	50	4	0.0254	1025	0.5
config99	8	3	10	1.2	1	0.2302	1040	0.0254	50	4	0.0254	1025	0.5
config100	8	3	15	1.2	1	0.2302	1040	0.0254	50	4	0.0254	1025	0.5
config101	8	3	5	1.2	1	0.2302	1040	0.0254	50	4	0.0254	1025	1
config102	8	3	10	1.2	1	0.2302	1040	0.0254	50	4	0.0254	1025	1
config103	8	3	15	1.2	1	0.2302	1040	0.0254	50	4	0.0254	1025	1

Graph 13: Static (with no counter-mass) and total available raising and sinking moment with the counter-mass for the example Dynamic Antenna for configurations 77 - 103 with 20kg counter-mass.

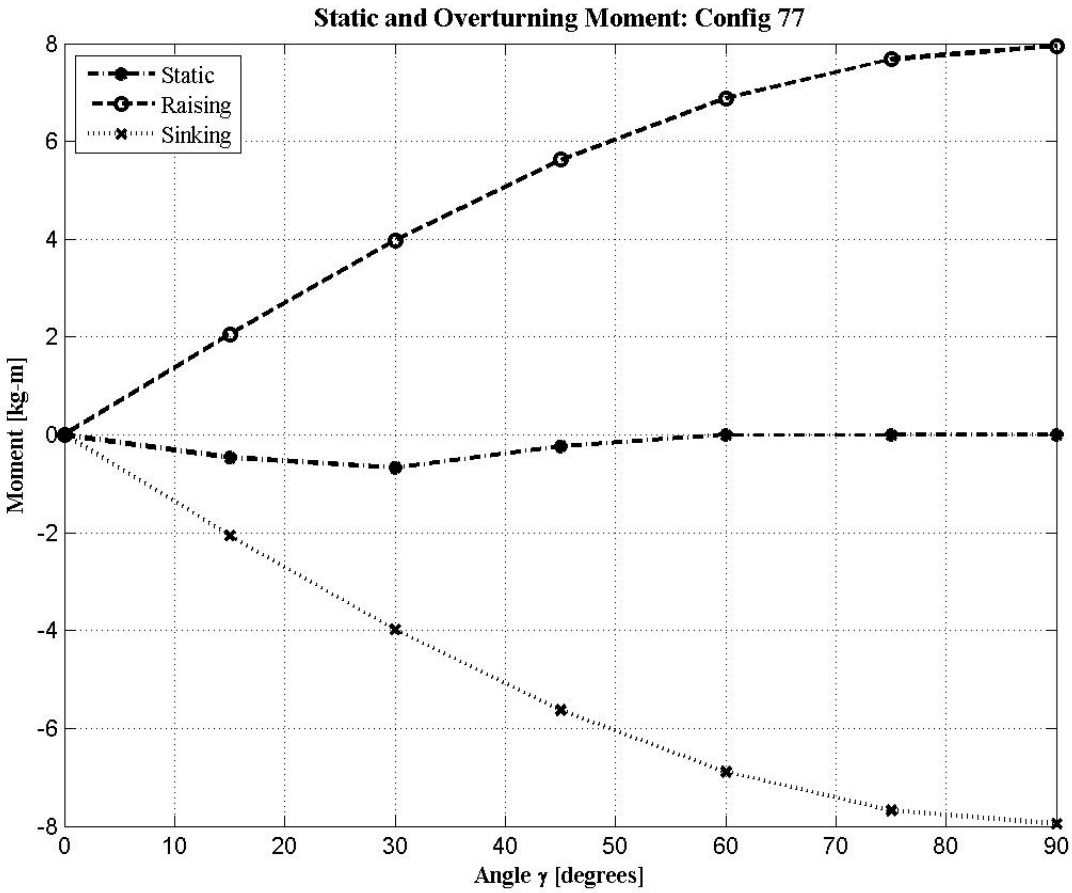

Graph 14: Graph of just the current moment profiles on example configuration 77, 80, and 83 that will be applied for all configurations within 77 - 103.

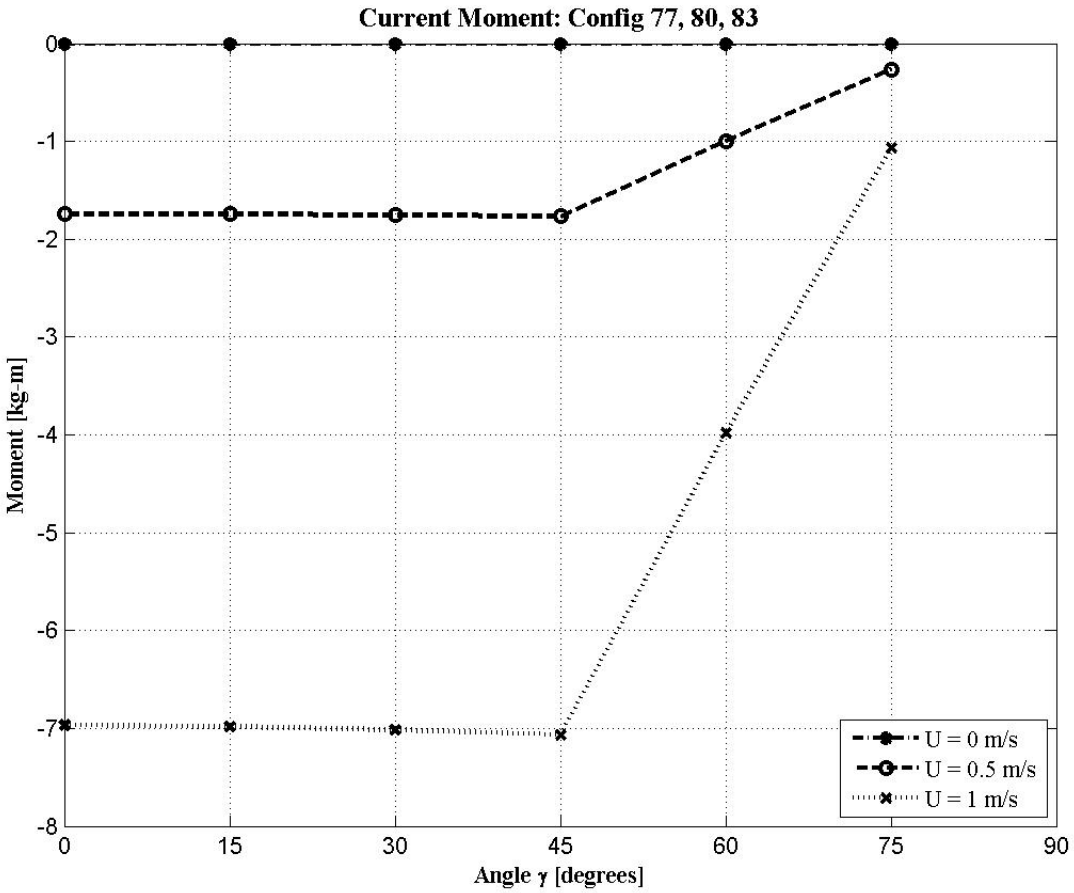

Graph 15: Wave Moment for a Wave Height of 0.4m with varying period with a depth of 8m on an Example Dynamic Antenna For Configurations 77 - 79.

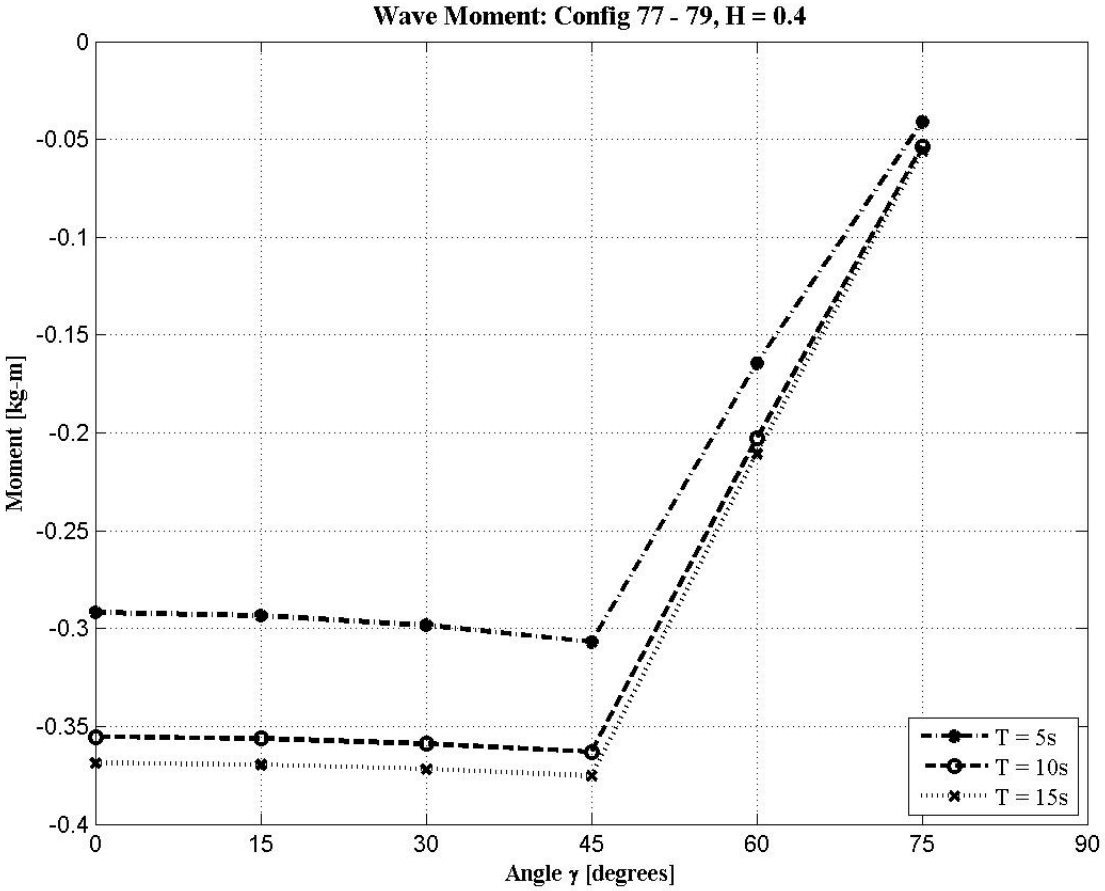

Graph 16: Wave Moment for a Wave Height of 0.8m with varying period with a depth of 8m on an Example Dynamic Antenna for Configurations 86 - 88.

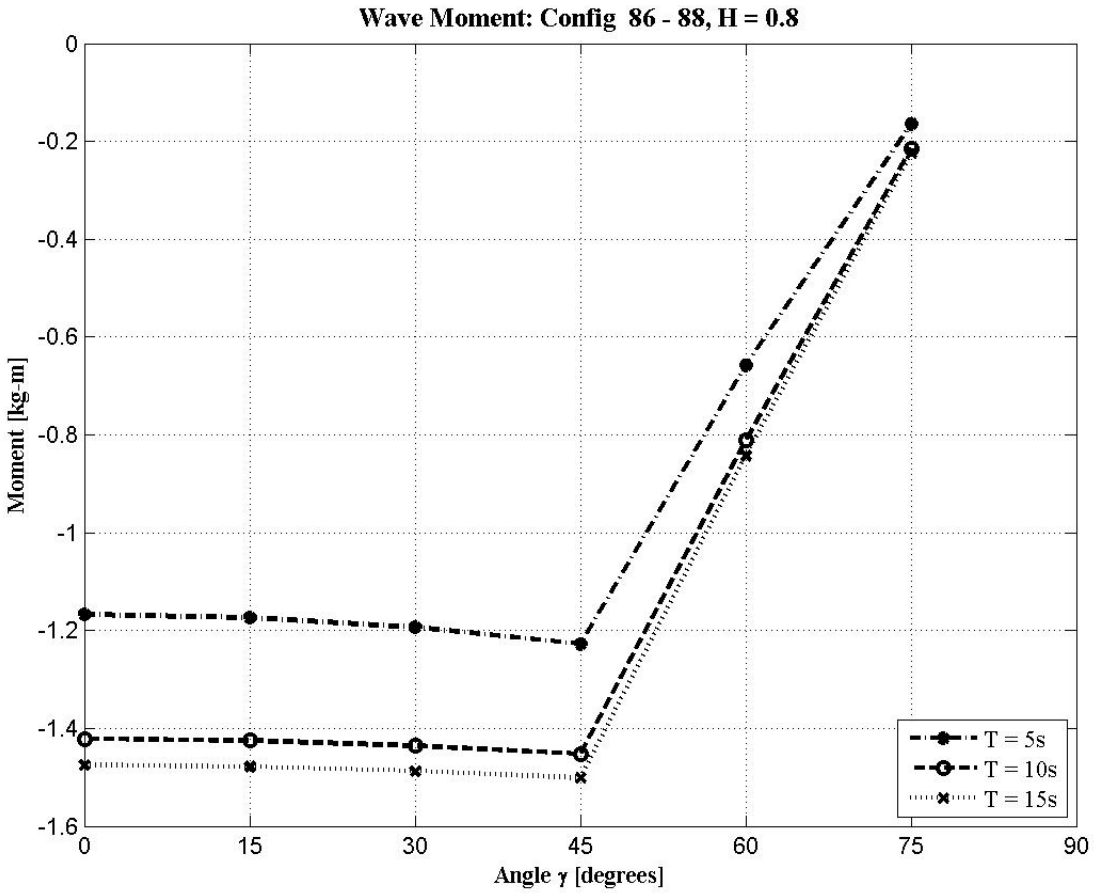

Graph 17: Wave Moment for a Wave Height of 1.2m with varying period with a depth of 8m on an Example Dynamic Antenna For Configurations 95 - 97.

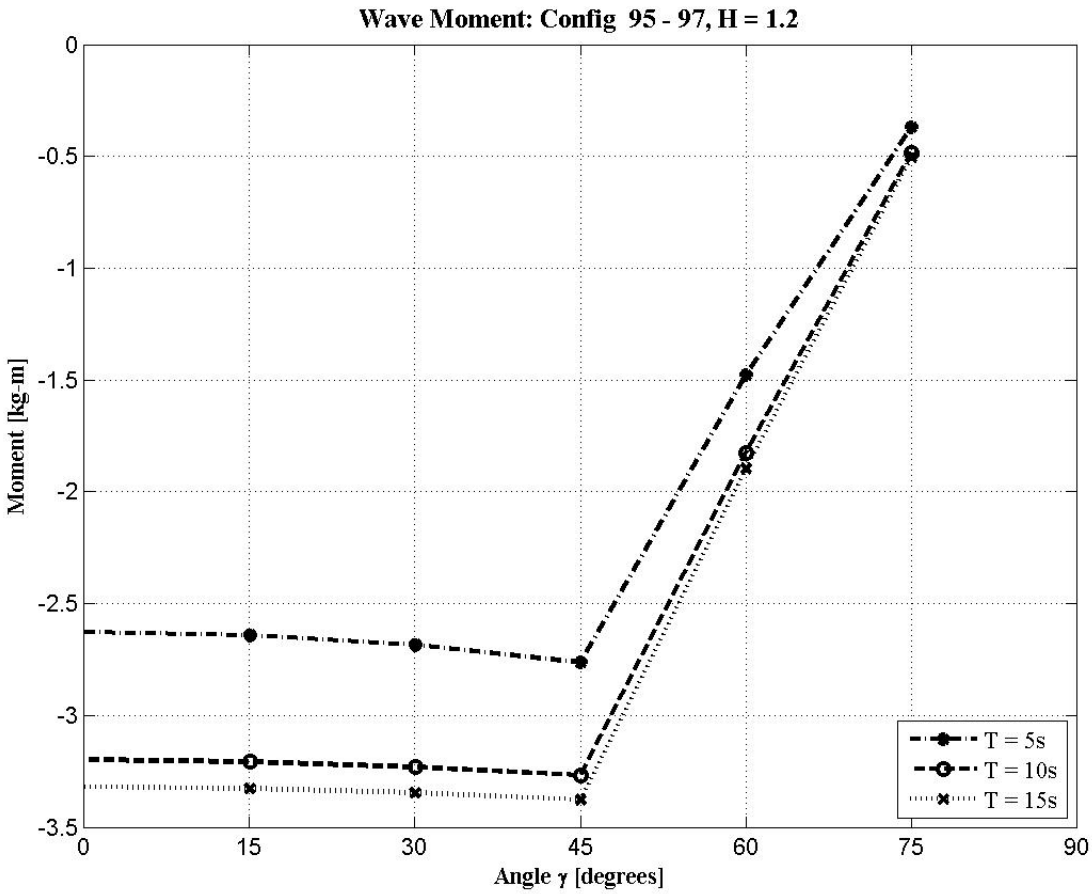

With the constant depth for this example simulation, the maximum moment generated is with the longest period and the largest wave heights (Graph 17). Adding the moment due to currents (Graph 14), produces large moments to be overcome. With these large moments, it is imperative to examine the conditions for successfully raising the antenna. For the given environmental conditions and moments, the antenna is to be in static equilibrium when the net raising moment is zero due to the counter-mass for the given configuration (illustrated in Graphs 19, 21, and 23). At these angles, the counter-weight negates the total moments on the antenna. At this angle, one will be able to observe if the antenna will have enough effective length to be above the passing wave, which an effective amplitude of half the wave height above the mean water level. The figure below shows the window with which to have the antenna effectively above the surface as it rotates (Graph 18).

Graph 18: Dynamic Antenna Tip Height Above Mean Water Level For Configurations 77 - 103

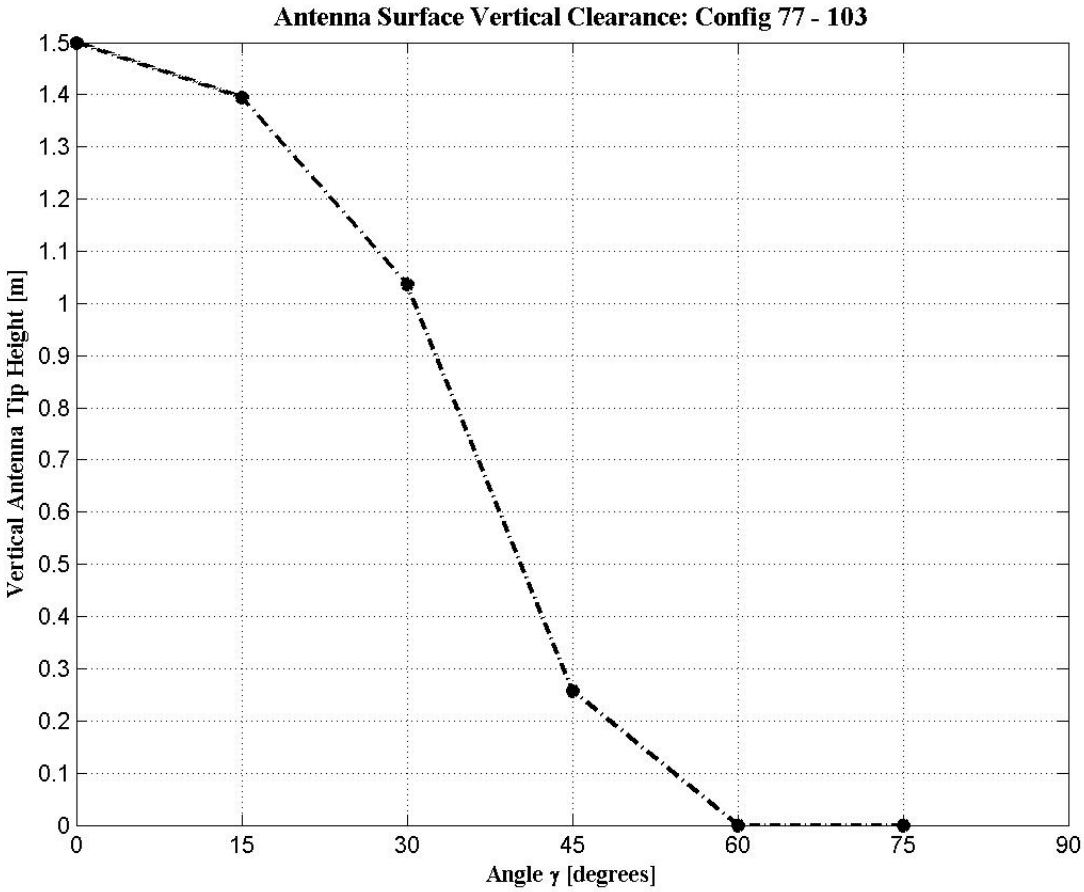

Graph 19: Graph of net raising moment for Configurations 77 - 85 with H = 0.4m, showing that at currents of 0 and 0.5 m/s have equilibrium angles of less than 10 degrees and 20 degrees.

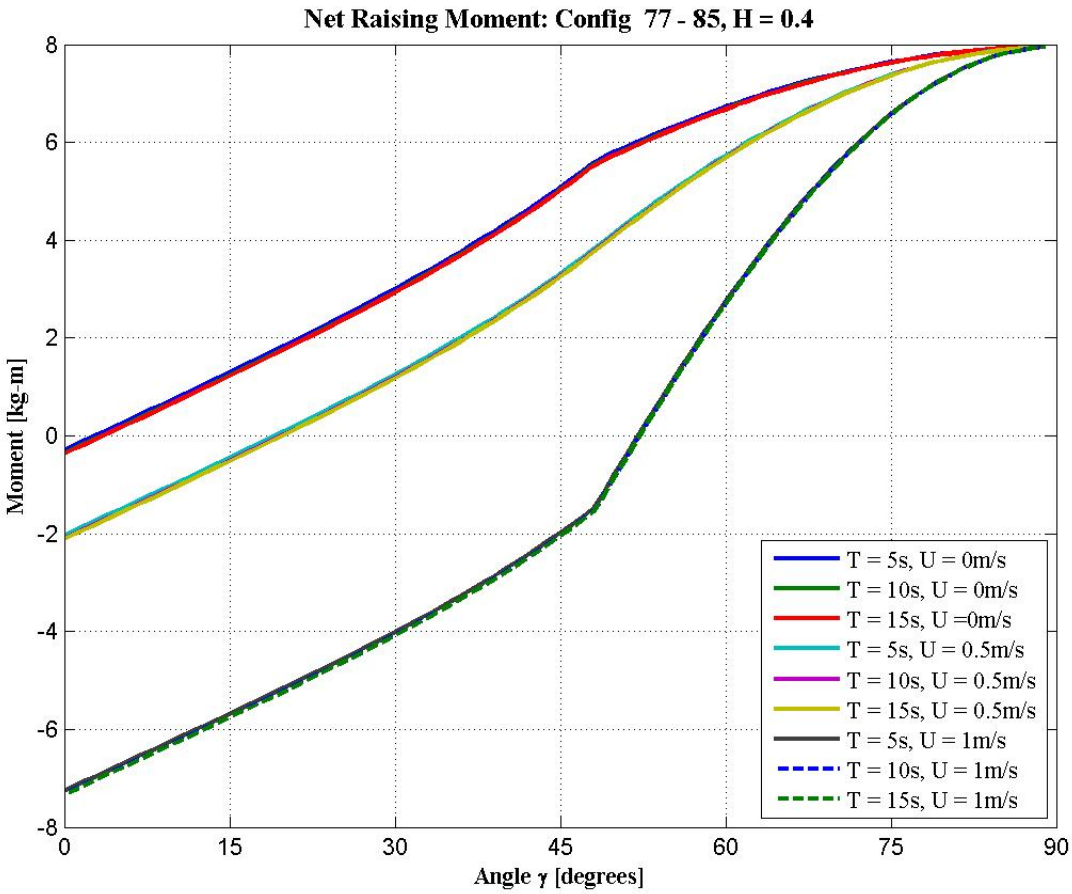

In Graph 19, one can notice that the moment due to current forcing dominates the total moment, causing the equilibrium angle to be pushed further over with the larger current fluid velocity. For the lower current flows, the angle of equilibrium is set so that the antenna is still erect with at least a meter of clearance above the mean water level with the 0.2 meter amplitude waves. As for the net sinking moment (Graph 20), it is apparent that the environment contributes to the easy overturning of the antenna to hide it, as it will continue to do so for the other environmental conditions (Graphs 22 and 24).

Graph 20: Graph of net sinking moment for Configurations 77 - 85 with H = 0.4m, showing the tendency to overturn due to the environmental forces.

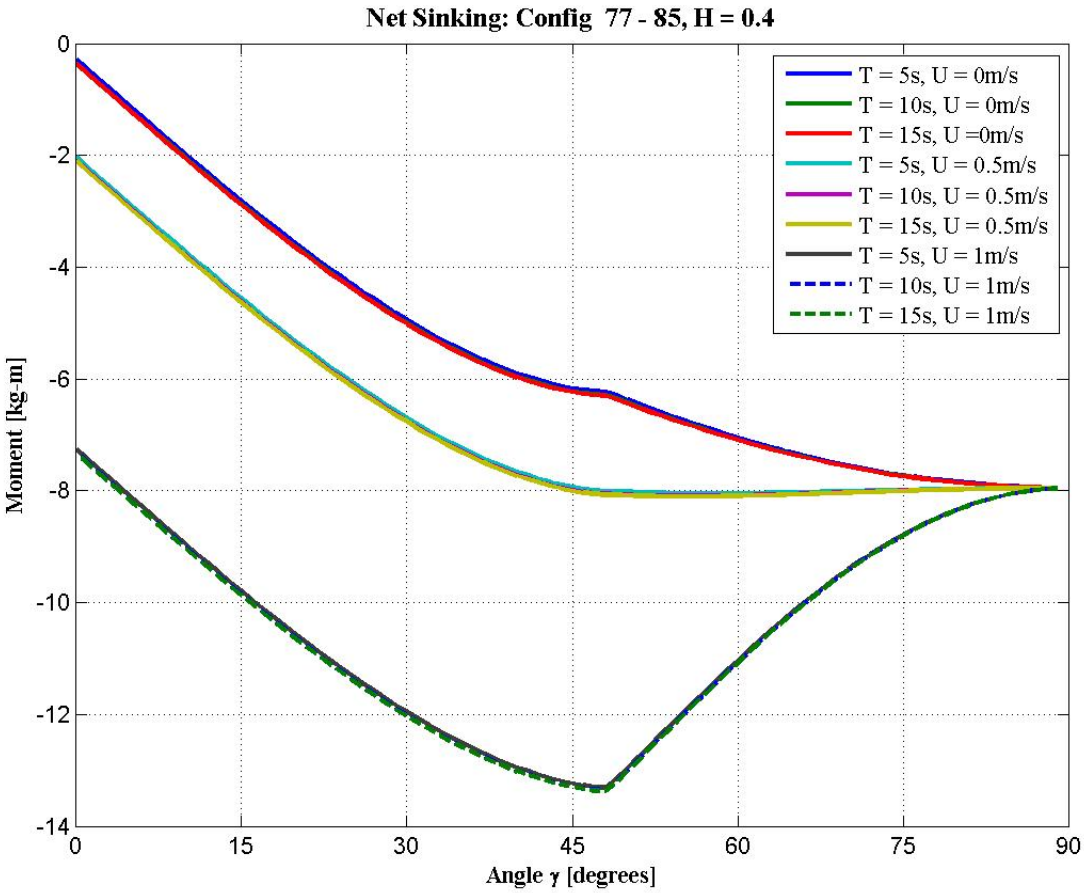

Graph 21: Net Raising Moment For Configurations 86 - 94 with H = 0.8m, showing that at 0 and 0.5 m/s of current, the equilibrium angle is still at 15 and 30 degrees, allowing antenna clearance.

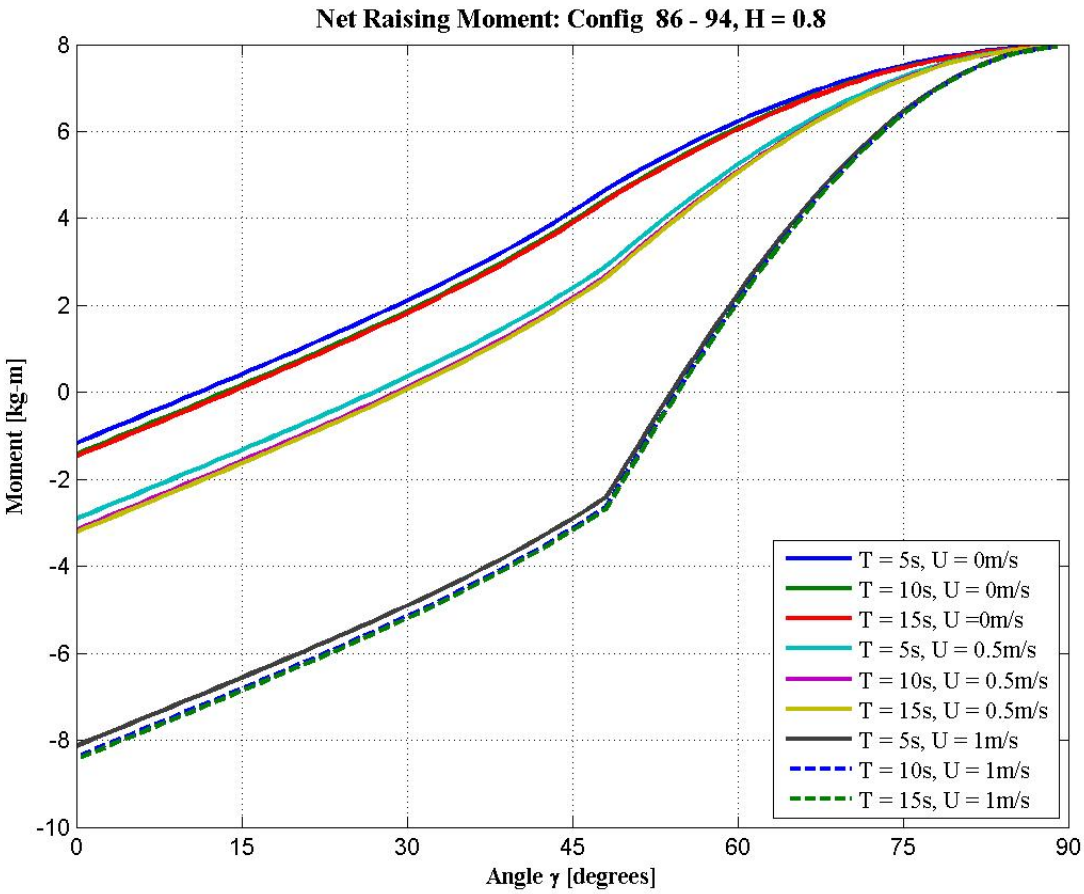

In Graph 21, one can notice that the total moment has been further reduced. Continuing to illustrate the overwhelming influence of the fast fluid flows from the current, the high speed flow has now pushed the equilibrium angle much further, with the lower velocities set at angles between 15 and 30 degrees, where the minimum clearance is roughly one meter. This amount of clearance is still viable, as the 0.4 meter amplitude provides for 0.6 meters of clearance for data telemetry over the wave crest.

Graph 22: Net Sinking Moment For Configurations 86 - 94 with H = 0.8m, showing the tendency to overturn due to the environmental forces.

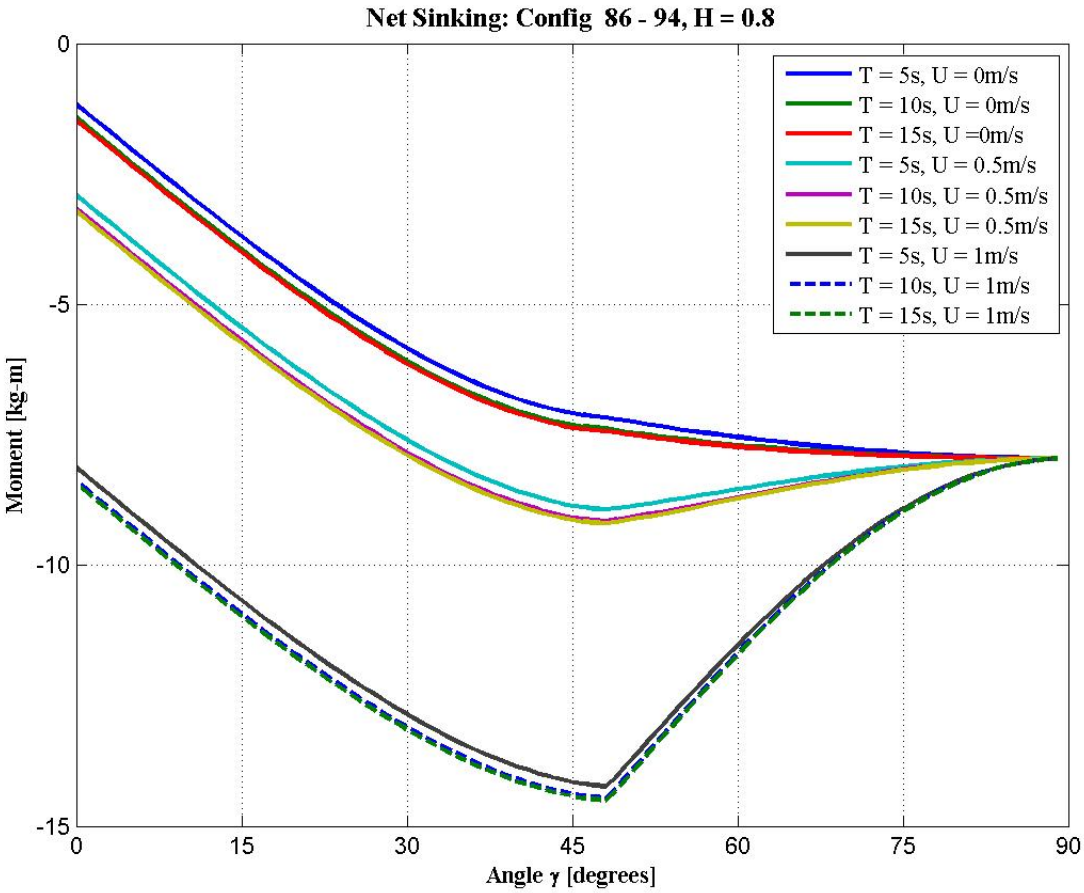

Graph 23: Net Raising Moment For Configurations 95 - 103 with H = 1.2m, showing that the high waves prevent all cases except that without a current to have clearance for the antenna.

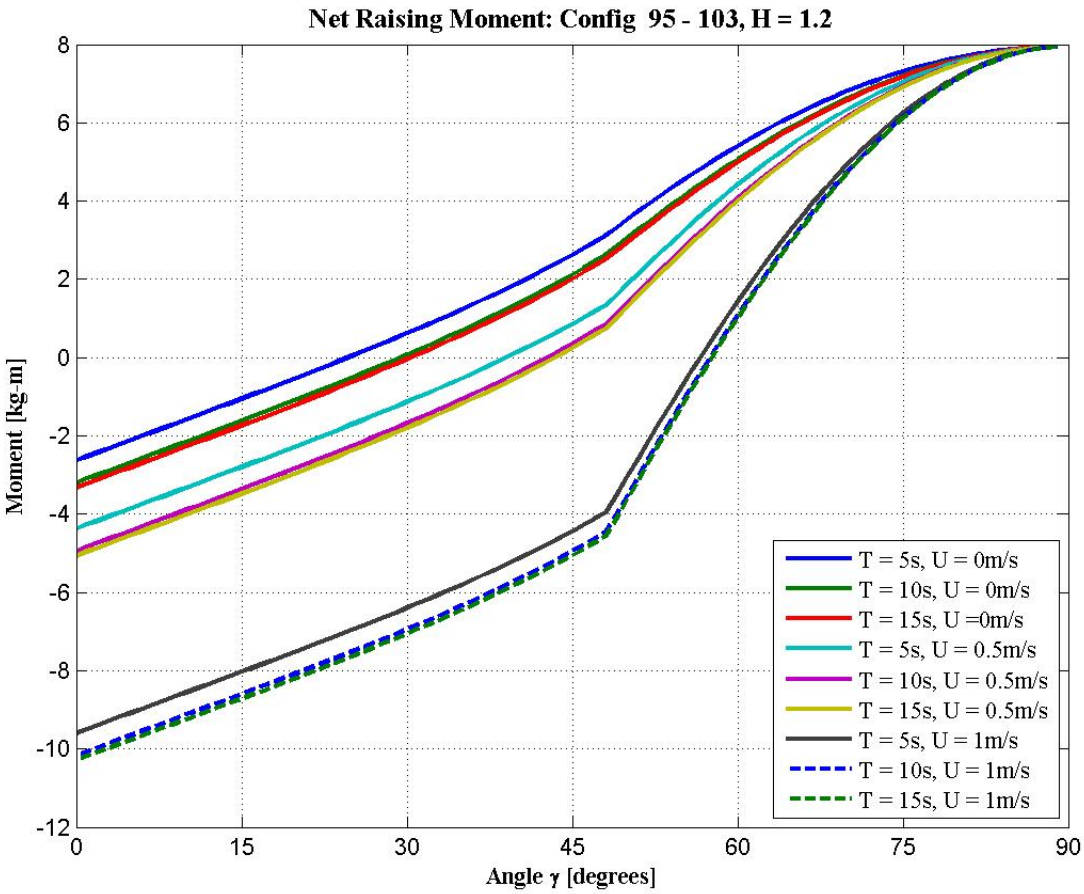

As one can imagine, with the increased wave heights that provide significant changes to the wave-induced moment, there is little to no clearance for the antenna for conditions without any current flow, as the equilibrium angles are all pushed well beyond the points before (Graph 23) to the point where the antenna will not be able to clear the wave crest. This illustrates the potentially devastating environmental conditions can have on the ability of the antenna to provide a stable and reliable telemetry connection. Obviously, measures would have to be taken to allow the system to handle these more severe conditions.

Graph 24: Net Sinking Moment For Configurations 95 - 103 with H = 1.2m, showing the tendency to overturn due to the environmental forces.

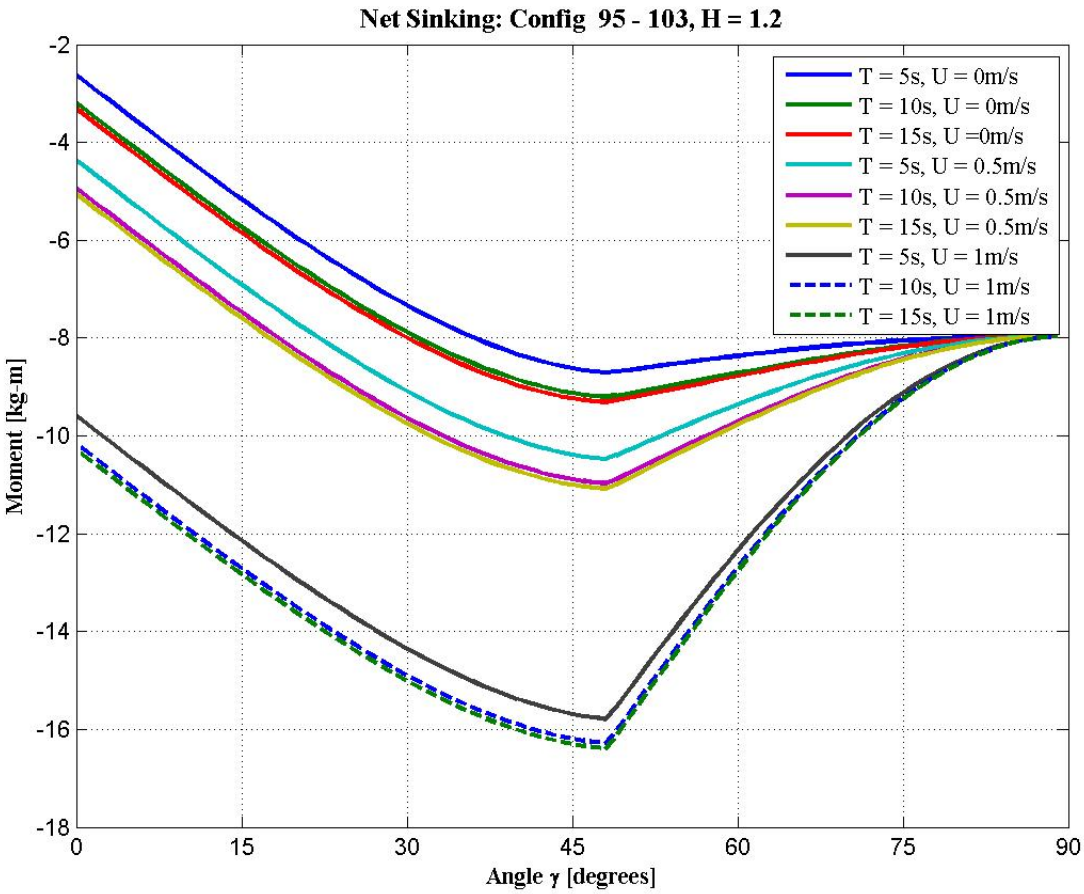

For conditions less than the most extreme, the antenna is able to reach equilibrium with a fair amount of clearance from submersion (Graphs 19 and 21). However, for the more severe conditions due to waves and currents, the amount of clearance continued to degenerate, resulting in the antenna being most swamped by wave crests for the majority of the environments (Graph 23).

Obviously, the current plays a large part in the increase in overall moment on the system, as shown in the lesser conditions (Figure 19 and 21), the doubled increase in velocity between 0.5 and 1 meters per second developed a significant increase in moment. Also of note, is that for higher angles, where there is a net positive moment, showing that the mass, when at its full extension, produces more moment than the elements can deliver, meaning that the system can overcome the forces to raise the antenna to the equilibrium point.

As indicated from the graphs examining the static available sinking moment (Graph 13), it can be surmised that for the counter-weight to have any effect, the Dynamic Antenna would need to initially be set at some angle to produce some initial negative moment to facilitate sinking the antenna. With the design of the upright,the Dynamic Antenna can be held in place at an angle that will prevent the system from being completely upright - and therefore removing any influence from the counter-mass - as well as far over enough to provide the necessary overturning moment to sink the antenna. As for the vertical clearance of the antenna for the wave conditions, bearing in mind the actual amplitude (i.e. the change in surface height due to waves) is one half of the Wave Height listed as H, one can compare where the net raising moment values reach static equilibrium (i.e. equal to zero) to the graph regarding vertical clearance of the antenna above the surface as a function of angle γ to see that the design can keep itself upright through only the worst of environmental conditions. Often, these conditions are brought about by extremely high currents and short period waves with high wave heights. Efforts can be made to reduce these factors in preventing antenna clearance by minimizing the drag on the structure, as is evident of the major role the current flow has in producing overturning moment.

Discussion

Based on the results shown above, system can be built to withstand a variety of different environmental conditions for the example configuration (Graphs 19 - 24). For conditions of high energy, such as large waves and high current, it is within the reasonable realm of possibility to configure a design that would be able to withstand, while erect, the majority of environmental parameters as show in the graphs (Graphs 19, 21, and 23) as well as suitably keep the system submerged (Graphs 20, 22, 24). Within reasonable limits, the antenna should be able to maintain a signal when on the surface in many wave conditions and current profiles. Also, with the stated counter-mass, it can reasonably perform its duties while still being within the bounds of the strength of two people. With this as a baseline, one can reasonably presume that an increase in the counter-weight will only improve this performance.

Further Analysis

With the initial calculations done for the moment due to the maximum horizontal environmental forces acting on the Dynamic Antenna system, the next logical step is to create a method to analyze how the system will react to both currents and waves over time, showing the dynamic position and orientation of the antenna as a wave passes through the mooring from the cyclic forcing. Garnering this idea of the reaction of the system to the orbital and periodic nature of the fluid velocities due to waves, one can better optimize the system through either reducing the length of the antenna or extending it. As the current analysis has always been done using the maximum velocity of the wave particles, examining the forces from both the drag and inertial components over time will allow one to examine the reaction of the antenna to the exchange between the two. Also, a time-series analysis could prove beneficial to the potential lift to the antenna. However, with the shallow depth, any uplifting or other vertical forcing will be minimal.

Otherwise, the next evolution in the design from the current standpoint is to reduce the hydrodynamic drag that is the most prevalent cause for hampering operations with the reduction in static moment following. Previous studies have been conducted to reduce turbulent wake utilizing splitter plates behind cylinders, which would be ideal for the antenna (Park, 1998). A splitter plate would be a simpler add-on to the construction as well as a means of strengthening the antenna without adding too much mass (Anderson, 1997). As for the housing, since it is in the beneficial position of not passing in and out of the water regularly, the focus can be more on pure streamlining

itself. Using the basic cylindrical housing, additional shaped buoyant pieces can be attached to reduce drag, but also increase available flotation to the mooring. With an ideal shape reducing the overall external forces on the Dynamic Antenna that would affect the rotationanal angle, decreasing the internal static moment with the choice of materials can be investigated as well.

Design Considerations

With an understanding of the kind of loads anticipated, materials testing can be introduced to find the best materials for the application as well as mechanisms to reduce stress loading. Extremely large forces, ones far too large for the system to resist, will cause the antenna will simply pivot itself, thereby adding some measure of robustness. An additional lateral rotation point on the mooring could allow the entire Dynamic Antenna to rotate into these extreme forces like a weather vane, decreasing overall drag and stress on the system. By ultimately being compliant to extreme conditions, the Dynamic Antenna allows the system to be built to less stringent rigors and to lesser heights of strength. Additional factors play into the strength required of the antenna. One intent was to use the antenna for recovery operations. Essentially lifting the entire mooring by the antenna until a line can be tied to a more robust element, the antenna, then must be placed under further scrutiny to find the best material and structural design for the intent of supporting potentially a hundred or so kilograms of equipment.

Working outside of the housing and the antenna, the structure that is supposed to support the antenna should be designed to allow the resting points for the antenna either raised or lowered provide stops to keep the angle of the antenna from reaching completely vertical or too far beyond the horizontal, respectively. Also, the structure's stops must be set to have the angle of the raised antenna be far over enough to match the previous moment calculations where the counter-mass begins to become effective in overturning.

Additionally, while it does not pertain to the design itself, investigation into more effective anti-fouling measures and practices would be ideal to increase the longevity of the mooring in waters that are right in nutrient and fauna and flora that could mar the veracity of the system over time.

Something that should warrant analysis is the resistance of the Dynamic Antenna system to side forcing, not so much for moments where it would push the antenna down, but rather rotating about the vertical axis. The notion behind this is that, should wave profiles or current vectors come obliquely to the Dynamic Antenna, the system could allow itself to pivot into the wave front to

provide the minimal resistance.

After the examination of ideal configurations for the Dynamic Antenna itself, integrating that into the rest of the mooring design is needed. From this analysis, additional parameters such as overall flotation, anchor weights, instrument capacity, and reaction to the same environmental parameters can provide the optimal configuration.

Conclusion

The shallow water regime is a difficult area to design a sensing platform for. It is subjected to not only the forces incumbent from the whipping of waves, but the vagaries of passing unscrupulous persons. The pull between the needs of science for real-time data versus the realities of establishing moorings near populated areas limits the current applications and designs to areas sheltered from interference or placing the requisite instruments far out of the immediate reach of both thief and researcher. The challenge stands to create a method and mechanism to allow a monitoring station out in these waters to have the capability for transmitting data and receiving communications from shore in a timely manner, while reducing the chances for damage to be taken at the surface from vandalism and impacts. While there are several potential designs that would, theoretically, provide that capability, the demands of the ocean environment highlight their faults. A design that has a rigid antenna attached to a housing that pivots about an axis, with a mass that is translated within the housing to shift the center of mass to rotate both the antenna and housing together to raise and lower the antenna has the marks to be an effective layout.

The environment close to shore presents a tumultuous area to place an instrument, subject to the waves and other forces at the surface that translates through the water column. Based on the depth, period, and wave height, the waves forcing can range from benign to malevolent. For a horizontal water velocity profile stemming from a tidal current, the forces were as to be expected, with the increasing velocity creating substantially increased forcing. These forces, themselves, changed on the dimensions of the housing and antenna, who imparted their own torque due to the mass and displacement of the system. All of these factors generated a moment on the Dynamic Antenna based on the position of the pivot axis on the housing, with the optimum position being the center of the housing, as it would reduce the influence from the weight of the system itself.

From the analysis of an example configuration, it was evident that, while it wouldn't be able to keep itself erect under the harshest conditions, it would still be able to stay up in less than benign situations. For smaller wave heights, the Dynamic Antenna would be able to have enough clearance for the lower ends of the current flows. However, for the higher wave heights, the combined forces between them were able to swamp the antenna. Through additional optimization analysis in terms of reducing the drag of the antenna and housing, and the overall mass of the components not part of the main counter-weight, the Dynamic Antenna can then be integrated with an optimized mooring design featuring the instruments and electronics for data gathering and

transmission. With this additional investigation, a new tool for supplying essential information for the improved investigation of one of the more difficult, yet vital, parts of the vast seas.

Appendix

Supplementary Tables

The following tables (Tables 6 and 7) contain the complete list of variations used for the analysis regarding the changes in density of the housing and the antenna for differing locations of the pivot on the longitudinal axis of the housing based on the term $\%L_h$. As the focus was on the static moment with changes in density, only, the remaining parameters regarding the waves, currents, depth, as well as the dimensions of the antenna and housing, themselves, remain constant.

Table 6: Configurations 32 - 56 Properties for Dynamic Antenna and Environment, with variations on the densities of the housing and antenna and pivot point location

Configuration	d [m]	d_2 [m]	T [s]	H [m]	L_h [m]	D_h [m]	$\rho_h[kg/m^3]$	Th_h [m]	$\%L_h$	L_a [m]	D_a [m]	$\rho_a[kg/m^3]$	U [m/s]
config32	8	3	15	0.8	1	0.2302	1025	0.0254	10	4	0.0127	1025	0.3
config33	8	3	15	0.8	1	0.2302	1025	0.0254	25	4	0.0127	1025	0.3
config34	8	3	15	0.8	1	0.2302	1025	0.0254	50	4	0.0127	1025	0.3
config35	8	3	15	0.8	1	0.2302	1025	0.0254	75	4	0.0127	1025	0.3
config36	8	3	15	0.8	1	0.2302	1025	0.0254	90	4	0.0127	1025	0.3
config37	8	3	15	0.8	1	0.2302	1025	0.0254	10	4	0.0127	1070	0.3
config38	8	3	15	0.8	1	0.2302	1025	0.0254	25	4	0.0127	1070	0.3
config39	8	3	15	0.8	1	0.2302	1025	0.0254	50	4	0.0127	1070	0.3
config40	8	3	15	0.8	1	0.2302	1025	0.0254	75	4	0.0127	1070	0.3
config41	8	3	15	0.8	1	0.2302	1025	0.0254	90	4	0.0127	1070	0.3
config42	8	3	15	0.8	1	0.2302	1025	0.0254	10	4	0.0127	1000	0.3
config43	8	3	15	0.8	1	0.2302	1025	0.0254	25	4	0.0127	1000	0.3
config44	8	3	15	0.8	1	0.2302	1025	0.0254	50	4	0.0127	1000	0.3
config45	8	3	15	0.8	1	0.2302	1025	0.0254	75	4	0.0127	1000	0.3
config46	8	3	15	0.8	1	0.2302	1025	0.0254	90	4	0.0127	1000	0.3
config47	8	3	15	0.8	1	0.2302	1070	0.0254	10	4	0.0127	1025	0.3
config48	8	3	15	0.8	1	0.2302	1070	0.0254	25	4	0.0127	1025	0.3
config49	8	3	15	0.8	1	0.2302	1070	0.0254	50	4	0.0127	1025	0.3
config50	8	3	15	0.8	1	0.2302	1070	0.0254	75	4	0.0127	1025	0.3
config51	8	3	15	0.8	1	0.2302	1070	0.0254	90	4	0.0127	1025	0.3
config52	8	3	15	0.8	1	0.2302	1000	0.0254	10	4	0.0127	1025	0.3
config53	8	3	15	0.8	1	0.2302	1000	0.0254	25	4	0.0127	1025	0.3
config54	8	3	15	0.8	1	0.2302	1000	0.0254	50	4	0.0127	1025	0.3
config55	8	3	15	0.8	1	0.2302	1000	0.0254	75	4	0.0127	1025	0.3
config56	8	3	15	0.8	1	0.2302	1000	0.0254	90	4	0.0127	1025	0.3

Table 7: Configurations 57 - 76 Properties for Dynamic Antenna and Environment, with variations on the densities of the housing and antenna and pivot point location

Configuration	d [m]	d_2 [m]	T [s]	H [m]	L_h [m]	D_h [m]	$\rho_h[kg/m^3]$	Th_h [m]	$\%L_h$	L_a [m]	D_a [m]	$\rho_a[kg/m^3]$	U [m/s]
config57	8	3	15	0.8	1	0.2302	1070	0.0254	10	4	0.0127	1070	0.3
config58	8	3	15	0.8	1	0.2302	1070	0.0254	25	4	0.0127	1070	0.3
config59	8	3	15	0.8	1	0.2302	1070	0.0254	50	4	0.0127	1070	0.3
config60	8	3	15	0.8	1	0.2302	1070	0.0254	75	4	0.0127	1070	0.3
config61	8	3	15	0.8	1	0.2302	1070	0.0254	90	4	0.0127	1070	0.3
config62	8	3	15	0.8	1	0.2302	1000	0.0254	10	4	0.0127	1000	0.3
config63	8	3	15	0.8	1	0.2302	1000	0.0254	25	4	0.0127	1000	0.3
config64	8	3	15	0.8	1	0.2302	1000	0.0254	50	4	0.0127	1000	0.3
config65	8	3	15	0.8	1	0.2302	1000	0.0254	75	4	0.0127	1000	0.3
config66	8	3	15	0.8	1	0.2302	1000	0.0254	90	4	0.0127	1000	0.3
config67	8	3	15	0.8	1	0.2302	1070	0.0254	10	4	0.0127	1000	0.3
config68	8	3	15	0.8	1	0.2302	1070	0.0254	25	4	0.0127	1000	0.3
config69	8	3	15	0.8	1	0.2302	1070	0.0254	50	4	0.0127	1000	0.3
config70	8	3	15	0.8	1	0.2302	1070	0.0254	75	4	0.0127	1000	0.3
config71	8	3	15	0.8	1	0.2302	1070	0.0254	90	4	0.0127	1000	0.3
config72	8	3	15	0.8	1	0.2302	1000	0.0254	10	4	0.0127	1070	0.3
config73	8	3	15	0.8	1	0.2302	1000	0.0254	25	4	0.0127	1070	0.3
config74	8	3	15	0.8	1	0.2302	1000	0.0254	50	4	0.0127	1070	0.3
config75	8	3	15	0.8	1	0.2302	1000	0.0254	75	4	0.0127	1070	0.3
config76	8	3	15	0.8	1	0.2302	1000	0.0254	90	4	0.0127	1070	0.3

Supplementary Graphs

This section will provide graphs illustrating the reasoning behind taking the maximum velocity and, thus, the drag force component of the Morison Wave forcing only. Graphs 25 through 33 illustrate the previous assertion where the Keulegan-Carpenter number KC is greater than 25 for a predominantly drag-force condition, while for values less than 5, the Inertial force takes precedent. Since none of the values decrease below 5 for any unit length of the housing or the antenna, it will be taken that the drag force is proportionally greater than the inertial force, and so the maximum velocity is to be taken. This is further supported by Graph 34 and 35 that show the acceleration and velocity of the wave particles out of phase, meaning that the maximum force must be composed of one or the other, but not both concurrently. Of note for the KC graphs, each line represents the KC for a particular segment of the lower housing, upper housing, or antenna. For the portions of the housing, the velocity is uniform at the center of rotation, with the velocity changing for each unit length further from the axis of rotation. As for the antenna, the change in velocity is minimal closest to the axis of rotation (i.e. at the top of the housing) while greatest at the tip of the antenna.

Graph 25: Keulegan-Carpenter Number through all angles of the Lower Housing for Config101, T = 5s, showing the predominance of Drag Forcing.

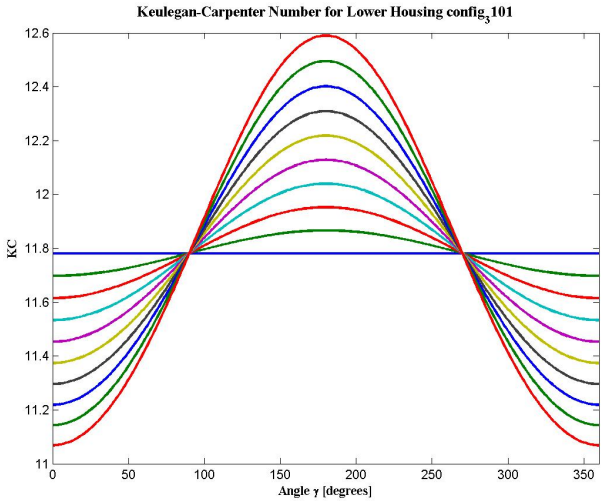

Graph 26: Keulegan-Carpenter Number through all angles of the Upper Housing for Config101, T = 5s, showing the predominance of Drag Forcing.

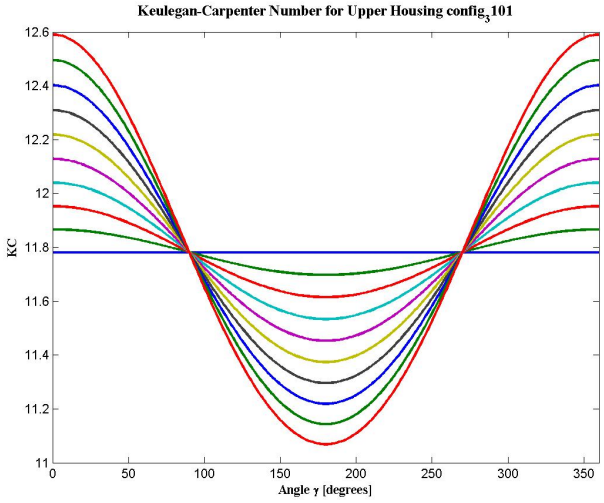

Graph 27: Keulegan-Carpenter Number through all angles of the Antenna for Config101, T = 5s, showing the predominance of Drag Forcing.

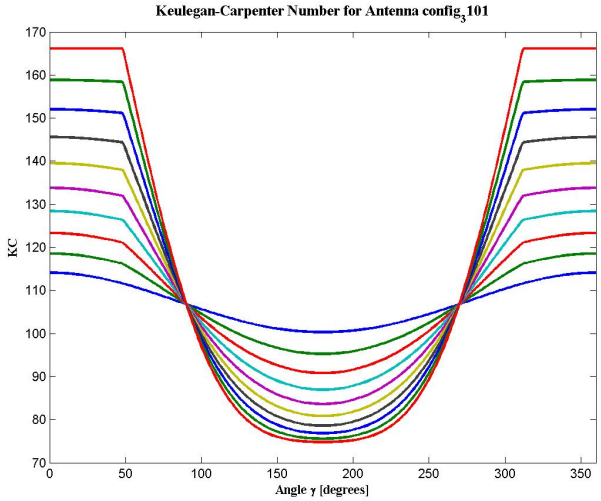

Graph 28: Keulegan-Carpenter Number through all angles of the Lower Housing for Config102, T = 5s, showing the predominance of Drag Forcing.

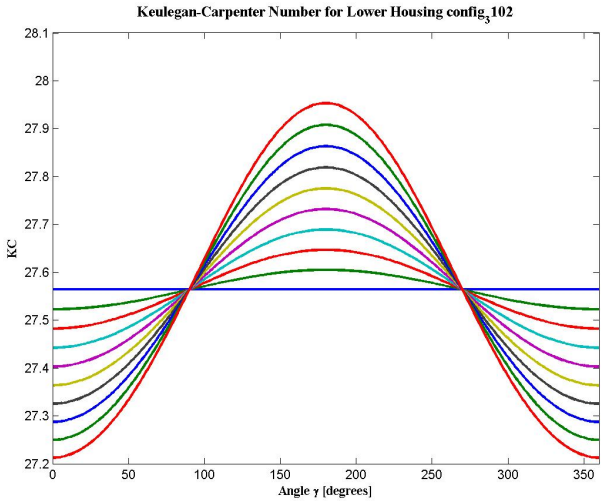

Graph 29: Keulegan-Carpenter Number through all angles of the Upper Housing for Config102, T = 10s, showing the predominance of Drag Forcing.

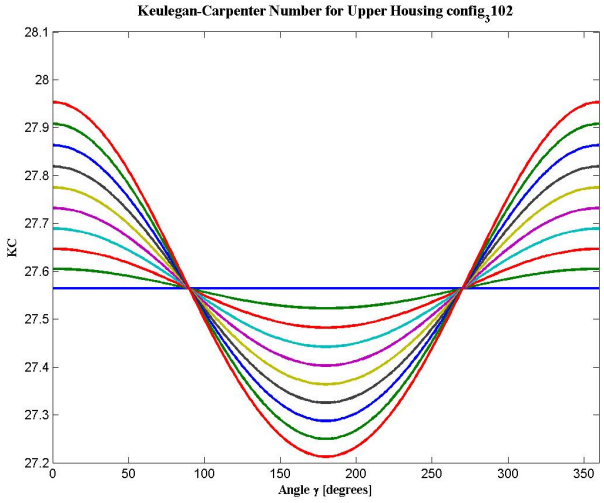

Graph 30: Keulegan-Carpenter Number through all angles of the Antenna for Config102, T = 15s, showing the predominance of Drag Forcing.

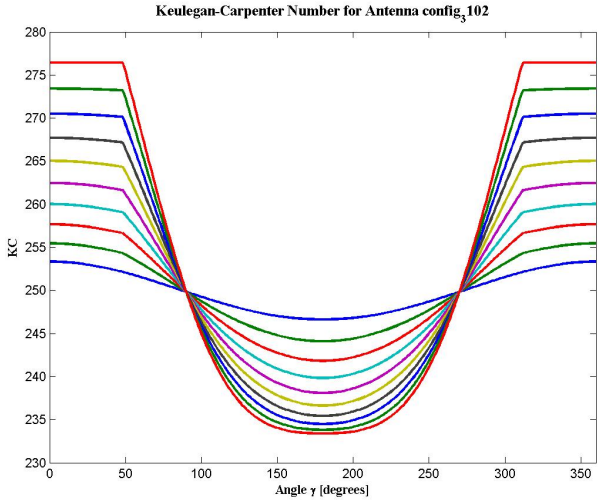

Graph 31: Keulegan-Carpenter Number through all angles of the Lower Housing for Config103, T = 5s, showing the predominance of Drag Forcing.

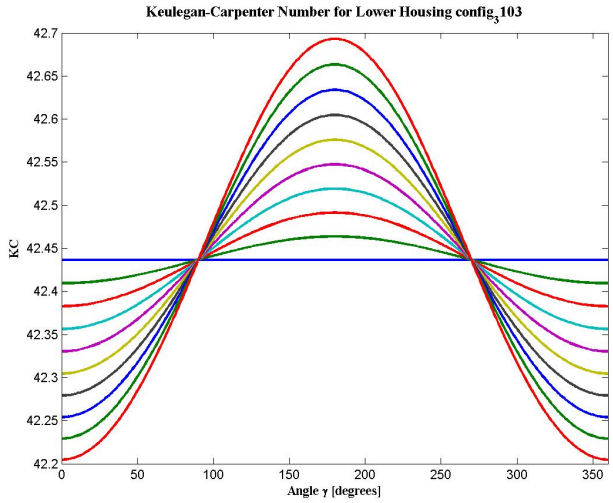

Graph 32: Keulegan-Carpenter Number through all angles of the Upper Housing for Config103, T = 10s, showing the predominance of Drag Forcing.

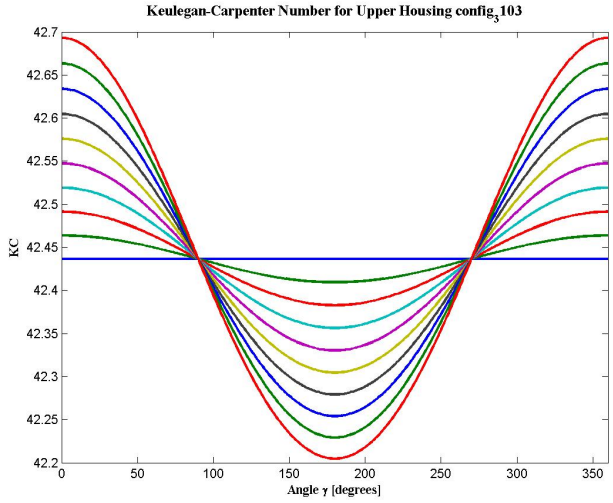

Graph 33: Keulegan-Carpenter Number through all angles of the Antenna for Config103, T = 15s, showing the predominance of Drag Forcing.

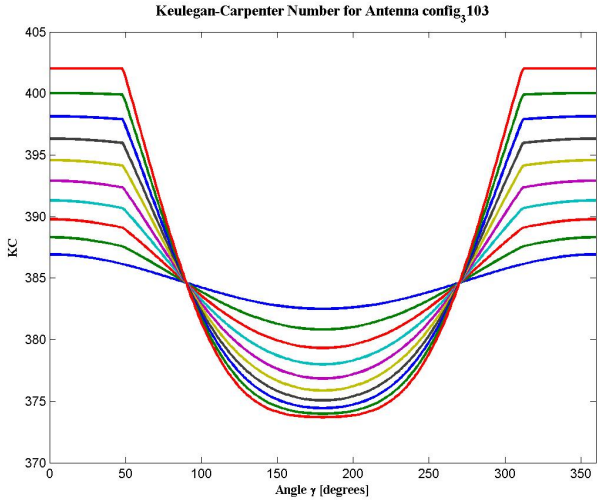

Graph 34: Wave Particle Horizontal Velocity for Configuration 100, showing the similar velocities for all depths expected of shallow depths. H = 1.2, T = 15s.

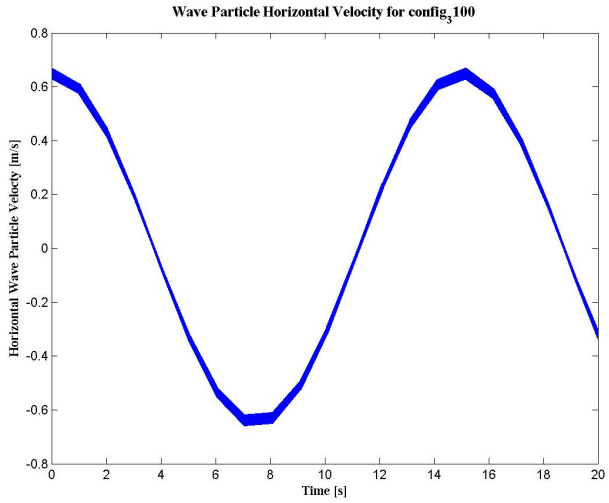

Graph 35: Wave Particle Horizontal Acceleration for Configuration 100, showing the similar acceleration for all depths expected of shallow depths. H = 1.2, T = 15s.

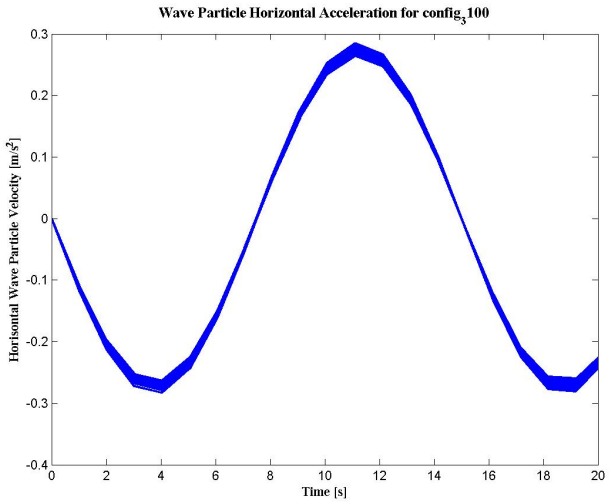

Graphs 34 and 35 illustrate the issue with finding the maximum wave force in regards to taking the maximum acceleration or velocity, as the velocity lags behind the acceleration where the point of maximum velocity is at the point of zero acceleration and vice versa. To determine which aspect to use, the Keulegan-Carpenter number is used.

MATLab Code

```
%% Dynamic Antenna Modeling Analysis
% February 2012

%This script is designed to take any configuration of the Dynamic Antenna
%which will consist of two cylinders incident and concentric. There will be
%several required user imputs such as the properties of the antenna,
%cylinder, and the environment.

%This script's output will be graphical representations of the properties
%of the waves (orbits, surface contour, acceleration, velocity, force, and
%moment incurred in total on the assembly), currents inherent in the water
%(force and moment), as well as the static forces and moments due to the
%properties of the assembly.

%First and foremost, the parameters have to be inputted. There are quite a
%few required parameters

%% Input Parameters

clear all
close all

dd = dir('*.txt');
ff = {dd.name};
clear dd

%% M-file to run dynant_thesis_022012 for all the configurations in the
% folder and save them to their own folders with graphs and .mat files

for ii= 1:length(ff)
   aa = ['config',num2str(ii),'.txt'];

   bb = ['config_3',num2str(ii)];




    %mm = input('Dynant Configuration \n','s');
    mm = aa;
    nheaderlines = 0;
    A = importdata(mm, ';' , nheaderlines);
   mkdir(bb);
    cd (bb)


d = A.data(1);          % Water Depth
d_2 = A.data(2);        % Depth of Axis of Rotation
x_d = A.data(3);        % Horizontal Position of Mooring
z_d = A.data(4);        % Vertical Position of Base of Mooring
rho_sw = A.data(5);     % Density of Seawater
```

```
g = A.data(6);          % Gravitational Acceleration
gam = A.data(7);        % Range of Angle of reclination
t_0 = A.data(8);        % Span of Time t
T = A.data(9);          % Period
H = A.data(10);         % Wave Height (1/2 Amplitude)
L_h = A.data(11);       % Length of Housing
D_h = A.data(12);       % Diameter of Housing
rho_h = A.data(13);     % Density of Housing
Th_h = A.data(14);      % Thickness of Housing Walls
perc_frac = A.data(15); % Percent Distance of Housing to Rotation Axis
L_a = A.data(16);       % Length of Antenna
D_a = A.data(17);       % Diameter of Antenna
rho_a = A.data(18);     % Density of Antenna
Th_a = A.data(19);      % Thickness of Antenna Walls
U = A.data(20);         % Uniform Current Velocity


gamma = 0:gam;
d_1 = d - d_2;
x = x_d;
t = linspace(0,t_0,100);
z = linspace(-d,0,10);

%Finding the Wavelength for a particular period and significant wave height
%based on the Dispersion Equations
%First, create a sampling of wavelengths to estimate across

Lx = linspace(0,1000,10000); %Sample Wavelengths
Ly = (g * T^2) / ( 2 * pi ) * tanh(2 * pi * d ./ Lx);
Lz = Lx - Ly; %Determines the Difference between the Sample and the Result
[rte,index] = min(abs(Lz - 0)); %Index with minimal difference
L = Lx(index);

k = (2*pi)/L; % Wavenumber
ss = (2 * pi)/ T; % Rotational frequency
n = (H/2) .* cos(k*x-ss.*t);
d_n = d+n; % Surface Profile


%Housing Properties
L_h1 = perc_frac * L_h; % Length of Housing Below Rotation
L_h2 = L_h - L_h1;  % Length of Housing Above Rotation
V_h = (D_h / 2)^2 * pi * L_h; %Volume of Entire Housing
m_h = -(V_h - ((D_h - 2 * Th_h)/2)^2 * pi * (L_h - 2*Th_h))*rho_h;
    % Mass of Housing
B_h = rho_sw * V_h; % Displacement of Housing

%Antenna Properties
V_a = (D_a /2)^2 * pi * L_a; % Volume of Entire Antenna
m_a = -(V_a - (((D_a - 2 * Th_a)/2)^2 * pi * (L_a - 2*Th_a)))...
    * rho_a; % Mass of Antenna
B_a = rho_sw * V_a; % Displacement of Antenna
```

```
L_as = (d_2)./cosd(gamma) - L_h2; % Combined Submerged Length for angles
L_as(L_as >= L_a) = L_a;    % When the entire antenna is submerged
L_as(L_as <= 0) = L_a;  % For Angles greater than 90
L_a1 = L_as;    % Submerged Length of Antenna
L_a2 = L_a - L_a1; % Surface Length of Antenna


%Submerged and unsubmerged antenna volume
V_a1 = (L_a1) .* (D_a/2)^2 * pi;
V_a2 = V_a - V_a1;

% Center of Mass, Center of Buoyancy, Center of Gravity
L_cm = ((0.5*L_h * m_h) + (0.5 * L_a + L_h) * m_a) / (m_h + m_a);
L_cb = (0.5*L_h * V_h + (0.5 * L_a + L_h) * V_a1) ./ (V_h + V_a1);

% Net Torque on Submerged Dynamic Antenna System
F_ma = m_a .*sind(gamma);
F_mh = m_h .*sind(gamma);
F_Ba = B_a .*sind(gamma);
F_Bh = B_h .*sind(gamma);
F_m = F_ma + F_mh;
F_B = F_Ba + F_Bh;
T_m = ((m_a + m_h).*sind(gamma)) * (L_cm - L_h1); % Mass
T_B = ((V_a1 + V_h).*rho_sw .* sind(gamma)) .* (L_cb - L_h1); % Buoyancy
M_s = T_m + T_B; % Net Moment



figure;
set(gcf,'DefaultLineLineWidth',2)
plot(gamma, F_ma, ...
    gamma, F_mh, ...
    gamma, F_Ba, ...
    gamma, F_Bh, ...
    gamma, F_m,...
    gamma, F_B)
hh = legend('Antenna Mass Force','Housing Mass Force','Antenna Buoyancy',...
    'Housing Buoyancy','Total Mass Force','Total Buoyancy');
set(hh,'FontSize',10,'FontName','Times New Roman')
title(['Static Force ',bb],'fontsize',12,'fontname','Times New Roman',...
    'fontweight','bold');
xlabel('Angle \gamma [degrees]','FontSize',10,'fontname',...
    'Times New Roman','fontweight','bold');
xlim([0 360]);
ylabel('Force [kg]','FontSize',10,'fontname',...
    'Times New Roman','fontweight','bold');
saveas(gcf, ['Static_Force_',num2str(bb)],'jpg');
close

figure;
set(gcf,'DefaultLineLineWidth',2)
plot(gamma, T_m,...
```

```
    gamma, T_B, ...
    gamma, M_s)
hh = legend('Mass Moment','Buoyancy Moment','Net Moment');
title(['Static Moment ',bb],'fontsize',12,'fontname','Times New Roman',...
    'fontweight','bold');
set(hh,'FontSize',10,'FontName','Times New Roman')
xlabel('Angle \gamma [degrees]','FontSize',10,'fontname',...
    'Times New Roman','fontweight','bold');
xlim([0 360]);
ylabel('Moment [kg-m]','FontSize',10,'fontname',...
    'Times New Roman','fontweight','bold');
saveas(gcf, ['Static_Moment_',num2str(bb)],'jpg');
close

%% Current Drag


c = 1.2; %drag coefficient of a simple cylinder
cn = c * cosd(gamma).^2;
c_d = c * cosd(gamma).^3;
cl = c * sind(gamma) .* cosd(gamma).^2;

N = cn .* (D_a * L_a1 + D_h * L_h) * rho_sw/2;
D = c_d .* (D_a * L_a1 + D_h * L_h) * rho_sw/2;
Lv = cl .* (D_a * L_a1 + D_h * L_h) * rho_sw/2;

%Columns represent the different velocities
%Rows Represent the different Angles
DN = N' * U.^2 / 9.81;
DD = D' * U.^2 / 9.81;
DL = L' * U.^2 / 9.81 ;

% Center of Area
L_ca = ((D_a .* L_a1 .* ((0.5 .* L_a1) + L_h)) + (D_h * L_h * (0.5 * L_h)))...
    ./ ((D_a .* L_a1) + (D_h * L_h)); % Relative to the housing bottom
L_diff = L_ca - L_h1; % Relative to the Axis of Rotation

d_diff = L_diff .* cosd(gamma); % Change in depth to the Center of Area
d_p = d_2 - d_diff; % Depth of the center of area
p_p = rho_sw * g * (d_p);



I_h = (1/12) * D_h * L_h;
I_h = I_h + (D_h * L_h) * (L_ca - 0.5*L_h);
I_a = (1/12) * (D_a * L_a1);
I_a = I_a + (D_a * L_a) * (0.5 * L_a1 + L_h - L_ca);
I_ha = I_h + I_a;
L_p = (I_ha .* cosd(gamma)) ./ ( d_p.* ((D_h * L_h) + (D_a .* L_a1)));
% Distance from the center of rotation to the center of pressure
%L_cp =  L_h1 + L_p; % Center of Pressure, below the Center of Rotation
%L_pi = L_p ./ abs(L_p);
```

```
% L_cpf = (L_cm - L_p - L_h1);
% L_cpi = L_cpf ./ abs(L_cpf);
% L_cp = L_cpf ./ L_cpi;
L_cpi = L_p ./ abs(L_p);
L_cp = (L_h1 - (L_ca - L_p)) ./ L_cpi;
L_cp = L_diff .* -L_cpi; % Only uses center of area
M_c = DN.*L_cp'; % Creates Positive Moment

figure;
plot(gamma, DN,'linewidth',2)
title(['Force due to Uniform Current Drag for ',bb],'fontsize',12,...
    'fontname','Times New Roman','fontweight','bold');
xlabel('Angle \gamma [degrees]','fontsize',10,'fontname',...
    'Times New Roman','fontweight','bold');
xlim([0 360]);
ylabel('Force [kg]','FontSize',10,'fontname',...
    'Times New Roman','fontweight','bold');
saveas(gcf, ['Current_Force_',num2str(bb)],'jpg');
close

figure;
plot(gamma, M_c,'linewidth',2)
title(['Moment due to Uniform Current Drag for ',bb],'fontsize',12,...
    'fontname','Times New Roman','fontweight','bold');
xlim([0 360]);
xlabel('Angle \gamma [degrees]','FontSize',10,'fontname',...
    'Times New Roman','fontweight','bold');
ylabel('Moment [kg-m]','FontSize',10,'fontname',...
    'Times New Roman','fontweight','bold');
saveas(gcf, ['Current_Moment_',num2str(bb)],'jpg');
close

%% Wave Forcing

%Wave Surface Profile
eta = H/2 * sin(k*x - ss*t);
eta_2 = eta + d;

% Solving the dz and dz of the components for the wave forcing
L_hv2 = L_h2 .* cosd(gamma);
z_hv2 = -d_2 + L_hv2; %vertical length above rotation
L_hv1 = L_h1 .* cosd(gamma);
z_hv1 = -d_2 - L_hv1; %vertical length below rotation

L_av = L_a2 .* cosd(gamma); %Surface Vertical Clearance of Antenna
z_as = (L_a1 + L_h2) .*cosd(gamma) - d_2; %Vertical Depth of Submerged tip
%z_as = d_2 + L_as;



for i = 1:length(gamma) % Establishing the dz
    z_dhv1(i,:) = linspace(-d_2,z_hv1(i),10);
```

```
    z_dhv2(i,:) = linspace(-d_2,z_hv2(i),10);
    z_das(i,:) = linspace(z_hv2(i),z_as(i),10);
end


for i = 1:length(gamma);
    AA(i,:) = diff(z_dhv1(i,:))./ cosd(gamma(i));
    BB(i,:) = diff(z_dhv2(i,:))./cosd(gamma(i));
    CC(i,:) = diff(z_das(i,:))./cosd(gamma(i));
end
L_das = CC(:,1); % ds for dz of the Antenna
L_dhv1 = abs(AA(1)); % ds for dz of the lower portion of the housing
L_dhv2 = abs(BB(2)); % ds for dz of upper portion of the housing


%Particle Orbit
figure;

for i = 1:length(z)
    xx(i,:) = -(H/2) * (cosh(k*(z(i) + d)) / sinh(k*d))...
        * sin(k*x_d - ss*t);
    yy(i,:) = z(i) + H/2 * (sinh(k*(z(i) + d)) / sinh(k*d))...
        * cos(k*x_d - ss *t);
    lmao(i) = z(i);
     plot(xx(i,:), yy(i,:),'linewidth',2)
    hold on
    plot(x,z(i),'r.','linewidth',2)
end
title(['Particle Orbit for ',bb],'fontsize',12,'fontname',...
    'Times New Roman','fontweight','bold');
xlabel('Horizontal Position [m]','FontSize',10,'fontname',...
    'Times New Roman','fontweight','bold');
ylabel('Vertical Position [m]','FontSize',10,'fontname',...
    'Times New Roman','fontweight','bold');
% hh = legend(['z = ',num2str(lmao(1))],['z = ',num2str(lmao(2))],...
%     ['z = ',num2str(lmao(3))],['z = ',num2str(lmao(4))],...
%     ['z = ',num2str(lmao(5))],['z = ',num2str(lmao(6))],...
%     ['z = ',num2str(lmao(8))],['z = ',num2str(lmao(8))],...
%     ['z = ',num2str(lmao(9))],['z = ',num2str(lmao(10))]);
% set(hh,'FontSize',10,'FontName','Times New Roman')
saveas(gcf, ['Particle_Orbits_',bb],'jpg');
close

%Particle Velocity
%Determining the velocity profile means taking the cos and sin values to be
%equal to 1 for the maximum horizontal and vertical velocities.

figure;
for i = 1:length(z)
    u(i,:) = (H/2) * ss * cosh(k*(z(i) + H))/sinh(k*d)...
        * cos(k*x_d - ss *t);
    w(i,:) = (H/2) * ss * sinh(k *(z(i)+H))/sinh(k*d)...
```

```
        * sin(k*x_d - ss *t);
      plot(t,u(i,:),'linewidth',2)
    hold on
end
title(['Wave Particle Horizontal Velocity for ',bb],'fontsize',12,...
    'fontname','Times New Roman','fontweight','bold');
xlabel('Time [s]','FontSize',10,'fontname',...
    'Times New Roman','fontweight','bold');
xlim([0 20]);
ylabel('Horizontal Wave Particle Velocty [m/s]','FontSize',10,'fontname',...
    'Times New Roman','fontweight','bold');
saveas(gcf, ['Particle_Velocity_',bb],'jpg');
close


figure;
for i = 1:length(z)
    a_x(i,:) = 2 * (ss^2/2) * (H/2) * cosh(k*(z(i) + d))/sinh(k*d)...
        * sin(k*x_d - ss *t);
    a_y(i,:) = -2 * (H/2) * (ss^2/2)  * sinh(k *(z(i)+d))/sinh(k*d)...
        * cos(k*x_d - ss*t);
     plot(t,a_x(i,:),'linewidth',2);
    hold on
end
title(['Wave Particle Horizontal Acceleration for ',bb],'fontsize',12,...
    'fontname','Times New Roman','fontweight','bold');
xlabel('Time [s]','FontSize',10,'fontname',...
    'Times New Roman','fontweight','bold');
xlim([0 20]);
ylabel('Horisontal Wave Particle Velocity [m/s^2]','FontSize',10,'fontname',...
    'Times New Roman','fontweight','bold');
saveas(gcf, ['Particle_Acceleration_',bb],'jpg');
close

% Based on the iterations of z, the drag force calculated is for each unit
% length. Particle Velocity and accelerationfor each depth at each angle
% for each component.
% Here, the dz vales are set (dz,dgamma)
% Also, for the maximum value, we must take the maximum velocity and
% accerlation


% Lower Portion of Housing (h1)
for i = 1:length(gamma), j = 1:10;
    Cm = 2; %Inertia coefficient
    u_h1(i,:)= (H/2) * ss * cosh(k*(z_dhv1(i,:) + d))./sinh(k*d);
    w_h1(i,:) = (H/2) * ss * sinh(k *(z_dhv1(i,:)+d))./sinh(k*d);
    ax_h1(i,:) = 2 * (ss^2/2) * (H/2) * cosh(k*(z_dhv1(i,:) + d))/sinh(k*d);
    ay_h1(i,:) = -2 * (H/2) * (ss^2/2) * sinh(k *(z_dhv1(i,:)+d))/sinh(k*d);
 %Drag force per unit length
    Du_h1(i,j) = cn(i) * rho_sw/2 * L_dhv1 *  D_h *...
       (u_h1(i,j).*abs(u_h1(i,j)))/9.81;
```

```
%Integrated Force per degree
    %F_Dh1(i) = trapz(Du_h1(i,:));
    F_Dh1(i) = sum(Du_h1(i,:));
% Inertia Force
P_Ih1(i,:) = (Cm * rho_sw * L_dhv1 * ((D_h/2)^2 * pi) * ax_h1(i,:))/9.81;
    %F_Ih1(i) = trapz(P_Ih1(i,:));
    F_Ih1(i) = sum(P_Ih1(i,:));
end
F_wh1 = F_Dh1; %+ F_Ih1;

KC_h1 = (u_h1 * T) / D_h; %Keulegan-Carpenter Number

figure;
set(gcf,'DefaultLineLineWidth',2)
plot(gamma, KC_h1);
title(['Keulegan-Carpenter Number for Lower Housing ',bb] ,'fontsize',12,...
    'fontname',...
    'Times New Roman','fontweight','bold');
xlabel('Angle \gamma [degrees]','FontSize',10,'fontname',...
    'Times New Roman','fontweight','bold');
xlim([0 360]);
ylabel('KC','FontSize',10,'fontname',...
    'Times New Roman','fontweight','bold')
saveas(gcf, ['Keulegan-Carpenter_h1_',num2str(bb)],'jpg');
close

% Upper Portion of Housing (h2)
for i = 1:length(gamma), j = 1:10;
    u_h2(i,:)= (H/2) * ss * cosh(k*(z_dhv2(i,:) + d))./sinh(k*d);
    w_h2(i,:) = (H/2) * ss * sinh(k *(z_dhv2(i,:)+d))./sinh(k*d);
    ax_h2(i,:) = 2 * (ss^2/2) * (H/2) * cosh(k*(z_dhv2(i,:) + d))/sinh(k*d);
    ay_h2(i,:) = -2 * (H/2) * (ss^2/2) * sinh(k *(z_dhv2(i,:)+d))/sinh(k*d);
 %Drag force per unit length
    Du_h2(i,j) = cn(i) * rho_sw/2 * L_dhv2 *  D_h *...
        (u_h2(i,j).*abs(u_h2(i,j)))/9.81;
%Integrated Force per degree
    %F_Dh2(i) = trapz(Du_h2(i,:));
    F_Dh2(i) = sum(Du_h2(i,:));
% Inertia Force
P_Ih2(i,:) = (Cm * rho_sw * L_dhv2 * ((D_h/2)^2 * pi) * ax_h2(i,:))/9.81;
    %F_Ih2(i) = trapz(P_Ih2(i,:));
    F_Ih2(i) = sum(P_Ih2(i,:));
end
F_wh2 = F_Dh2; %+ F_Ih2; % The maximum force on the upper housing for all
                         % angles gamma
KC_h2 = (u_h2 * T)/D_h;
figure;
set(gcf,'DefaultLineLineWidth',2)
plot(gamma, KC_h2);
title(['Keulegan-Carpenter Number for Upper Housing ',bb] ,'fontsize',12,...
    'fontname',...
    'Times New Roman','fontweight','bold');
```

```
xlabel('Angle \gamma [degrees]','FontSize',10,'fontname',...
    'Times New Roman','fontweight','bold');
xlim([0 360]);
ylabel('KC','FontSize',10,'fontname',...
    'Times New Roman','fontweight','bold')
saveas(gcf, ['Keulegan-Carpenter_h2_',num2str(bb)],'jpg');
close
% Antenna
for i = 1:length(gamma), j = 1:10;
    u_a(i,:)= (H/2) * ss * cosh(k*(z_das(i,:) + d))./sinh(k*d);
    w_a(i,:) = (H/2) * ss * sinh(k *(z_das(i,:)+d))./sinh(k*d);
    ax_a(i,:) = 2 * (ss^2/2) * (H/2) * cosh(k*(z_das(i,:) + d))/sinh(k*d);
    ay_a(i,:) = -2 * (H/2) * (ss^2/2) * sinh(k *(z_das(i,:)+d))/sinh(k*d);

 %Drag force per unit length
    Du_a(i,j) = cn(i) * rho_sw/2 * L_das(i) *  D_a *...
        (u_a(i,j).*abs(u_a(i,j)))/9.81;
%Integrated Force per degree
    % F_Da(i) = trapz(Du_a(i,:));
    F_Da(i) = sum(Du_a(i,:));
% Inertia Force
P_Ia(i,:) = (Cm * rho_sw * L_das(i) * (D_a^2/4 * pi) * ax_a(i,:))/9.81;
    %F_Ia(i) = trapz(P_Ia(i,:));
    F_Ia(i) = sum(P_Ia(i,:));
end
F_wa = F_Da; %+ F_Ia; % The maximum force on the antenna for all
                      % angles gamma
KC_a = (u_a * T)/D_a;
figure;
set(gcf,'DefaultLineLineWidth',2)
plot(gamma, KC_a);
title(['Keulegan-Carpenter Number for Antenna ',bb] ,'fontsize',12,...
    'fontname',...
    'Times New Roman','fontweight','bold');
xlabel('Angle \gamma [degrees]','FontSize',10,'fontname',...
    'Times New Roman','fontweight','bold');
xlim([0 360]);
ylabel('KC','FontSize',10,'fontname',...
    'Times New Roman','fontweight','bold')
saveas(gcf, ['Keulegan-Carpenter_a_',num2str(bb)],'jpg');
close

% Combined Forces from all of the different Components
F_w = F_wh2 + F_wa + F_wh1;

figure;
set(gcf,'DefaultLineLineWidth',2)
plot(gamma, F_Dh1, ...
    gamma, F_Ih1, ...
    gamma, F_Dh2, ...
    gamma, F_Ih2, ...
    gamma, F_Da, ...
```

```
    gamma, F_Ia)
title(['Wave Force Components for ',bb] ,'fontsize',12,'fontname',...
    'Times New Roman','fontweight','bold');
hh = legend('Lower Housing Wave Drag','Lower Housing Inertia Force',...
    'Upper Housing Wave Drag','Upper Housing Inertia Force',...
    'Antenna Wave Drag','Antenna Inertia Force');
set(hh,'FontSize',10,'FontName','Times New Roman')
xlabel('Angle \gamma [degrees]','FontSize',10,'fontname',...
    'Times New Roman','fontweight','bold');
xlim([0 360]);
ylabel('Force [kg]','FontSize',10,'fontname',...
    'Times New Roman','fontweight','bold')
saveas(gcf, ['Individual_Wave_Force_',num2str(bb)],'jpg');
close

figure;
set(gcf,'DefaultLineLineWidth',2)
plot(gamma, F_wh1,...
    gamma, F_wh2,...
    gamma, F_wa,...
    gamma, F_w);
hh = legend('Lower Housing','Upper Housing','Antenna','Total');
set(hh,'FontSize',10,'FontName','Times New Roman')
xlabel('Angle \gamma [degrees]','FontSize',10,'fontname',...
    'Times New Roman','fontweight','bold');
xlim([0 360]);
ylabel('Force [kg]','FontSize',10,'fontname',...
    'Times New Roman','fontweight','bold');
title(['Force Due to Waves On Dynamic Antenna Assembly for ',bb]...
    ,'fontsize',12,'fontname','Times New Roman','fontweight','bold');
saveas(gcf, ['Wave_Force_',num2str(bb)],'jpg');
 close

% Moment Calculated from the distance from the center of pressure to the
% center of rotation

M_w = F_w .* L_cp;

figure;
plot(gamma, M_w,'linewidth',2)
title(['Total Wave-Induced Moment for Angles \gamma for ',bb],...
    'fontsize',12,'fontname','Times New Roman','fontweight','bold');
xlabel('Angle \gamma [degrees]','FontSize',10,'fontname',...
    'Times New Roman','fontweight','bold');xlim([0 360]);
ylabel('Moment [kg-m]','FontSize',10,'fontname',...
    'Times New Roman','fontweight','bold')
saveas(gcf, ['Wave_Moment_',num2str(bb)],'jpg');
close

%% Counter Mass Calculation

M_cm = -(M_s + M_w + M_c'); % Total Countering Moment needed
```

```
L_mm = L_h1 - (0.5 * (D_h - 2*Th_h)); % Moment Arm of Mass at bottom
L_mm_s = L_h2 - (0.5 * (D_h - 2*Th_h)); % Moment Arm of Mass at Top
f_m = M_cm / L_mm; %Opposing force necessary
f_m_s = M_cm / L_mm_s;
m_m = f_m ./ sind(gamma) / 9.81; %Mass of the counter

figure;
set(gcf,'DefaultLineLineWidth',2)
plot(gamma, M_s,...
    gamma, M_w, ...
    gamma, M_c, ...
    gamma, -M_cm);
title(['Moments due to Static, Current, and Wave Forces for ',bb]...
    ,'fontsize',12,'fontname','Times New Roman','fontweight','bold');
hh = legend('Static Moment','Current Drag Moment','Wave Forcing Moment',...
    'Total Moment');
set(hh,'FontSize',10,'FontName','Times New Roman');
xlabel('Angle \gamma [degrees]','FontSize',10,'fontname',...
    'Times New Roman','fontweight','bold');xlim([0 360]);
ylabel('Moment [kg-m]','FontSize',10,'fontname',...
    'Times New Roman','fontweight','bold');
saveas(gcf, ['Acting_Moments_',num2str(bb)],'jpg');
close

% The center of mass of the counter-mass is taken to be the centroid of an
% object that is the diameter of the interior of the housing and has the
% length equal to that.

mm = 10;
    %input('Mass \n'); % Inputted Mass Value
M_m = L_mm * (mm .* sind(gamma)); % Raising Moment
M_m_s = -L_mm_s * (mm.*sind(gamma)); % Sinking Moment
M_t = -M_cm + M_m; % Total Raising Moment
M_t_s = -M_cm + M_m_s; % Total Sinking Moment

fs = 2;
    %input('Factor of Safety \n');
m_fs = mm * fs; % Counter Mass with Factor of Safety
M_fs = L_mm * (m_fs .* sind(gamma)); % Safe Raising Moment
M_tfs = -M_cm + M_fs; % Safe Total Moment for Raising
M_fs_s = -L_mm_s * (m_fs .* sind(gamma));  % Safe Sinking Moment
M_tfs_s = -M_cm + M_fs_s; % Safe Total Moment for Sinking
[rte,index] = min(abs(M_tfs_s));
g0 = index;
gam0 = gamma(g0);

M_net = -M_cm;

figure;
set(gcf,'DefaultLineLineWidth',2)
plot(gamma, M_fs,...
    gamma, M_fs_s)
```

```
title(['Safe Moment Generated for Raising/Sinking in ',bb,...
    'with a Counter Mass of ',num2str(m_fs),'kg'],'fontsize',12,...
    'fontname','Times New Roman','fontweight','bold');
hh = legend('Raising Moment','Sinking Moment');
set(hh,'FontSize',10,'FontName','Times New Roman');
xlabel('Angle \gamma [degrees]','FontSize',10,'fontname',...
    'Times New Roman','fontweight','bold');xlim([0 360]);
ylabel('Moment [kg-m]','FontSize',10,'fontname',...
    'Times New Roman','fontweight','bold');
saveas(gcf, ['CounterMass_Moments_',num2str(bb)],'jpg');
close

figure;
set(gcf,'DefaultLineLineWidth',2)
plot(gamma, M_net, ...
    gamma, M_m, ...
    gamma, M_m_s,...
    gamma, M_fs,...
    gamma, M_fs_s, ...
    gamma, M_tfs, ...
    gamma, M_tfs_s);
title(['Moment Generated by Counter Mass for ',bb],'fontsize',12,...
    'fontname','Times New Roman','fontweight','bold')
hh = legend('Forcing Moment','Basic Raising Moment',...
    'Basic Sinking Moment', 'Safe Raising Moment','Safe Sinking Moment',...
    'Total Safe Raising Moment', 'Total Safe Sinking Moment');
set(hh,'FontSize',10,'FontName','Times New Roman');
xlabel('Angle \gamma [degrees]','FontSize',10,'fontname',...
    'Times New Roman','fontweight','bold');xlim([0 360]);
ylabel('Moment [kg-m]','FontSize',10,'fontname',...
    'Times New Roman','fontweight','bold');
saveas(gcf, ['Total_Resultant_Moments_',num2str(bb)],'jpg');
close


figure; plot(gamma, M_s, 'b', ...
    gamma, M_c','k',...
    gamma,M_w, 'g',...
    gamma, M_cm,'c'), hold on
plot(gamma, M_m,'--m')
plot(gamma, M_t,'r.')
plot(gamma, M_t_s,'--r')
plot(gamma, M_fs, 'k.')
plot(gamma, M_tfs,'b.')
plot(gamma, M_tfs_s,'g.')
close


%% Stability

y = D_a./cosd(gamma); % Major Axis Length of Waterline Footprint
V_sub = V_h + V_a1; % Total Submerged volume
```

```
I_O = (pi /4) * (1/2).* y * (1/2 * D_a)^3; % Area Moment of Inertia
L_bar = I_O .* tand(gamma) ./ V_sub; % Shift in Center of Buoyancy
L_cB2 = (0.5*L_h * V_h + (0.5 * L_a1 + L_h) .* V_a1) ./ (V_h + V_a1);
    % Center of Submerged Volume
MG = I_O./V_sub - (L_cm - L_cB2); % Distance from Metacentric Height to
    % Center of Gravity with no Counter-Mass
L_cm2 = ((L_h1 * m_h) + (0.5 * L_a + L_h) * m_a ...
    + m_fs * L_mm) / (m_h + m_a + m_fs); % Center of Mass with Counter
MG2 = I_O./V_sub - (L_cm2 - L_cB2); % New MG



figure;hold on;
plot(gamma,MG,'r','linewidth',2)
plot(gamma, MG2,'b','linewidth',2)
xlabel('Angle \gamma [degrees]','fontsize',10,'fontname',...
    'Times New Roman','fontweight','bold');
xlim([0 360]);
ylabel('MG [m]','FontSize',10,'fontname',...
    'Times New Roman','fontweight','bold')
title(['Stability for ',bb],'fontsize',12,'fontname',...
    'Times New Roman','fontweight','bold');
hh = legend('No Counter Mass','With Counter Mass');
set(hh,'FontSize',10,'FontName','Times New Roman');
saveas(gcf,['Stability ',bb],'jpg');
close

%% Save All Values to a MAT File
saving = ['config',num2str(ii),'.mat'];
save(saving)

% Adding to a larger Matrix of Values for Comparison

    % Changing Dimensions
    d_n_config(ii,:) = d_n; % Surface Profile
    L_a1_config(ii,:) = L_a1; % Submerged Antenna Length
    L_a2_config(ii,:) = L_a2; % Surfaced Antenna Length
    L_av_config(ii,:) = L_av ./ cosd(gamma);
    d_a_config(ii,:) = d + L_av; % Total Height from bottom
    L_cm_config(ii,:) = L_cm;
    L_cp_config(ii,:) = L_cp;
    L_mm_config(ii,:) = L_mm;
    L_mm_s_config(ii,:)= L_mm_s;
    gam0_config(ii) = gam0; % Angle Where Sinking Moment Equals 0


    % Force
    F_ma_config(ii,:) = F_ma;
    F_mh_config(ii,:) = F_mh;
    F_Ba_config(ii,:) = F_Ba;
    F_Bh_config(ii,:) = F_Bh;
    F_m_config(ii,:) = F_m;
```

```
    F_B_config(ii,:) = F_B;
    F_c_config(ii,:) = DN;
    F_Dh1_config(i,:) = F_Dh1;
    F_Ih1_config(i,:) = F_Ih1;
    F_wh1_config(i,:) = F_wh1;
    F_Dh2_config(i,:) = F_Dh2;
    F_Ih2_config(i,:) = F_Ih2;
    F_wh2_config(i,:) = F_wh2;
    F_Da_config(i,:) = F_Da;
    F_Ia_config(i,:) = F_Ia;
    F_wa_config(i,:) = F_wa;
    F_w_config(i,:) = F_w;


    %Moments
    T_m_config(ii,:) = T_m;
    T_B_config(ii,:) = T_B;
    M_cm_config(ii,:) = M_w + M_s + M_c'; % Total Outside Moment
    M_w_config(ii,:) = M_w; % Form matrix of Wave Moment from Each Config
    M_s_config(ii,:) = M_s; % Form matrix of Static Moment
    M_c_config(ii,:) = M_c; % Form matrix of Current Moment
    M_m_config(ii,:) = M_m; % Raising Moment Due to Initial Mass (10kg)
    M_m_s_config(ii,:) = M_m_s; % Sinking Moment Due to Initial Mass (10kg)
    M_fs_config(ii,:) = M_fs; % Safe Raising Moment (f = 2)
    M_fs_s_config(ii,:) = M_fs_s; % Save Sinking Moment (f = 2)
    M_tfs_config(ii,:) = M_tfs; % Total Raising Moment
    M_tfs_s_config(ii,:) = M_tfs_s; % Total Sinking Moment

cd ..



end

saving = 'config_comparison_3.mat';
save(saving)
```

References

1. Adams, Lisa G; Matsumoto, George I. *Investigating Coastal Process and Nitrate Levels in the Elkhorn Slough Using Real-Time Data.* Oceanography, Vol. 20, No. 1, pp. 200 - 204. 2007.

2. Anderson, E. A.; Szewczyk, A. A. *Effects of a Splitter Plate on the Near Wake of a Circular Cylinder in 2 and 3-dimensional Flow Configurations.* Experiments in Fluids, Vol. 23, pp. 161 - 174. 1997.

3. Anthony, K. R. N.; Kline, D. I.; Dove, S.; Hoegh-Guldberg, O. *Ocean Acidification Causes Bleaching and Productivity Loss in Coral Reef Builders.* Proceedings of the National Academy of Sciences,Vol. 105, No. 45, pp. 17442-17446. 2008.

4. Breitburg, Denise. *Effects of Hypoxia, and the Balance Between Hypoxia and Enrichment, on Coastal Fishes and Fisheries.* Estuaries, Vol. 25., No. 4b, pp. 767 - 781. 2002.

5. Broenkow, William W.; Breaker, Lawrence C. *A 30-year History of Tide and Current Measurements in Elkhorn Slough, California.* Moss Landing Marine Laboratories. Moss Landing, CA. 2005.

6. Eakin, C. M.; Lough, J. M.; Heron, S. F. *Climate Variability and Change: Monitoring Data and Evidence for Increased Coral Bleaching Stress. Coral Bleaching*, van Oppen, M. J. H., Lough, J. M. (eds.), Chapter 4, Springer-Verlag Berlin Heidelberg. 2009.

7. Hoerner, Dr.-Ing Sighard F. Fluid-Dynamic Drag, 2nd Edition. Hoerner Fluid Dynamics, 1965

8. Kenyon, Kern E. *Shallow water Gravity Waves: A Note on the Particle Orbits.* Journal of Oceanography, Vol. 52, pp. 353 - 357. 1996.

9. Palumbi, S.R. *The Ecology of Marine Protected Areas.* Marine Community Ecology. Pp. 509 - 530. Bertness, Mark D.; Gaines, Steven; Hay, Mark. Editors. Sinauer Associates Inc. 2001.

10. Park, Woe-Chul; Higuchi, Hiroshi; *Numerical Investigation of Wake Flow Control by a Splitter Plate.* Korean Society of Mechanical Engineers (KSME) International Journal, Vol. 12, No. 1, pp. 123 - 131. 1998.

11. Roemmich, Dean; Johnson, Gregory C.; Riser, Stephen; Davis, Russ, Gilson, John; Owens, W. Brechner; Garzoli, Silvia L.; Schmid, Claudia; Ignaszewiski, Mark. *The Argo Program: Observing the Global Ocean with Profiling Floats.* Oceanography, Vol. 22, No. 2, pp. 34 -43. 2009.

12. Sandin, Stuart A.; Smith, Jennifer E.; DeMartini, Edward E.; Dinsdale, Elisabeth A.; Donner, Simon D.; Friedlander, Alan M.; Konotchick, Talina; Malay, Machel; Maragos, James E.; Obura David; Pantos, Olga; Paulay, Gustav; Richie, Morgan; Rohwer, Forest; Schroeder, Robert E.; Walsh, Sheila; Jackson, Jeremy B. C.; Knowlton, Nancy; Sala, Enric. *Baselines and Degradation of Coral Reefs in the Northern Line Islands.* Public Library of Science One, Vol. 3, Issue 2, pp. 1 - 11. 2008.

13. Teng, Chung-Chu; Cucullu, Stephen; McArthur, Shannon; Kohler, Craig; Burnett, Bill; Bernard, Landry. *Vandalism Experienced by NOAA National Data Buoy Center.* Oceans 2009, Marine Technological Society MTS/IEEE, pp. 1 - 8. 2009.

14. Thorpe, Steve A. *Measurement Techniques, Sensors and Platforms.* Encyclopedia of Ocean Sciences, 2nd Edition. 2009.

15. White, Frank M. Fluid Mechanics. 6th Edition. McGraw-Hill, New York, NY. 2008.

16. Costal Data Information Program. Scripps Institution of Oceanography. CDIP.ucsd.edu.

17. Land/Ocean Biogeochemical Observatory. Monterey Bay Aquarium Research Institute. Mbari.org/lobo/

18. Ocean Time-Series Group. Scripps Institution of Oceanography. Mooring.ucsd.edu

19. Woods Hole Oceanographic Institution. Whoi.edu

Bibliography

1. Boyd, Janice D.; Burnes, Richard; Frye, Daniel E; Peters, Don; Arthur, Richard; Bricker, Bruce. *A Self- Deploying, Depth-Adaptive Coastal Oceanographic Mooring.* Naval Research Laboratory. Report Number: NRL/FR/7332– 98-9681. 1998.

2. Branco, Brett; Torgersen, Thomas; Bean, John R; Grenier, Gary; Arbige, Dennis. *A New Water Column Profiler for Shallow Aquatic Systems.* Liminology and Oceanography: Methods, Vol. 3, pp. 190 - 202. 2005.

3. Dudinzki, Kathleen M.; Brown, Shani J.; Lammers, Marc.; Lucke, Klaus.; Mann, David A.; Simard, Peter.; Wall, Carrie C.; Rasmussen, Marianne Helene; Magnúsdóttir, Edda Elísabet; Tougaard, Jakob; Eriksen, Nina; *Trouble- Shooting Deployment and Recovery Options for Various Stationary Passive Acoustic Monitoring Devisces in Shallow- and Deep-Water Applications.* Acoustical Society of America, Vol. 129, pp. 436 - 448. 2011.

4. Haritos, N. *Introduction to the Analysis and Design of Offshore Structures - An Overview.* Electronic Journal of Structural Engineering. 2007.

5. Harris, Dr. Lee E. Ph.D. P.E. *Stability Analysis for the Submerged Reef Ball Breakwater Proposed for the 'Undisclosed Hotel' Resort, Quintana Roo, Mexico.* Reef Ball Foundation. Athens, GA.

6. Higley, Paul D.; Joyal, Arthur B. *New Mooring Design for a Telemetering Offshore Oceanographic Buoy.* Ocean's '78, pp. 10 - 17. 1978.

7. Hoegh-Guldberh, O.; Mumby, P. J.; Hooten, A. J.; Steneck, R. S.; Greenfield, P.; Gomez, E.; Harvell, C. D.; Sale, P. F.; Edwards A. J.; Caldeira, K.; Knowlton, N.; Eakin, C. M.; Iglesias-Prieto, R.; Muthiga, N.; Bradbury, R. H.; Dubi, A.; Hatziolos, M. E. *Coral Reefs Under Rapid Climate Change and Ocean Acidification.* Science, Vol. 318, pp. 1737 - 1742. 2007.

8. Holmes, Patrick, PhD. A Course in Coastal Defense Systems I, *Chapter 5: Coastal Processes: Waves.* Professional Development Programme: Coastal Infrastructure Design, Construction and Maintenance. Department of Civil Engineering, The University of the West Indies. St. Lucia, West Indies. 2001.

9. Howell, Gary L. *Shallow Water Directional Wave Gages Using Short Baseline Pressure Arrays.* Coastal Engineering, Vol. 35. pp. 85 - 102. 1998.

10. Italiano, Francesco, Editor. *Abstracts Volume: Second International Workshop of Research in Shallow Marine and Fresh Water Ecosystems.* INGV (Istituto Nazionale de Geofissica e Vulcanologia, Sezione de Palermo - Geochemica). Palermo, Italy. 2010.

11. Kenyon, Kern E. *Shallow water Gravity Waves: A Note on the Particle Orbits.* Journal of Oceanography, Vol. 52, pp. 353 - 357. 1996.

12. Knowlton, Nancy; Jackson, Jeremy B. C. *Shifting Baselines, Local Impacts, and Global Change on Coral Reefs.* Public Library of Science: Biology, Vol. 6, Issue 2, pp. 215 - 220. 2008.

13. Kundu, Pijush K.; Cohen, Ira M. Fluid Mechanics. Fourth Edition. Elsivier, Inc. San Diego, Ca. 2008.

14. Navarro, Gabriel; Gutiérrez, Javier; Díez-Minguito, Manuel; Losada, Miguel Angel; Ruiz, Javier. *Temporal and Spatial Variability in the Guadalquivir Estuary: A Challenge for Real-Time Teleme-*

try. Ocean Dynamics, Vol. 61, pp. 753 - 765. 2011.

15. Pandian, P. Kasintha; Emmanuel, Osalusi; Ruscoe, J. P.; Side, J. C.; Harris R. E.; Kerr, S. A.; Bullen, C. R. *An Overview of Recent Technologies on Wave and Current Measurement in Coastal and Marine Applications.* Journal of Oceanographic and Marine Science, Vol. 1, No. 1, pp. 001 - 010. 2010.

16. Schmidt, W.E.; Woodward, B. T.; Millikan, K.S.; Guza, R. T.; Raubenheimer, B.; Elgar, Steve. *A GPS-Tracked Surf Zone Drifter.* Journal of Atmospheric and Oceananic Technology, Vol. 20, pp. 1069 - 1075. 2003.

17. Sumaila, Ussif Rashid; Guénette, Sylvie; Alder, Jackie; Chuenpagdee, Ratana; *Addressing Ecosystem Effects of Fishing Using Marine Protected Areas.* International Council for the Exploration of the Seas Journal of Marine Science, Vol. 57, pp. 752 - 760. 2000.

18. Taft, Brett; Teng, Chung-Chu. *Low Load compliant Mooring History and Status Update.* MTS (Marine Technological Society), 2009.

19. Terro, Mohamad J.; Abdel-Rohman, Mohamed.; *Wave Induced Forces in Offshore Structures Using Linear and Nonlinear Forms of Morison's Equation.* Journal of Vibration and Control, Vol. 13, No. 139., pp. 139 - 157. 2006.

20. Utter, Barbara D.; Denny, Mark W. *Wave-Induced Forces on the Giant Kelp* Macrocystis Pyrifera *(Aghardh): Field Test of a Computational Model.* The Journal of Experimental Biology, Vol. 199, pp. 2645 = 2654. 1996.

21. Williams, Anthony N. *Wave Forces on Inclined Circular Cylinder.* Journal of waterway, Port, Coastal and Ocean Engineering, Vol. 111, No. 5, pp. 910 - 920. 1985.